Hormone-dependence of gene and protein expression in barley aleurone & Characterization of NADPH-dependent thioredoxin reductase/thioredoxin system in barley seeds

Shahpiri, Azar; Finnie, Christine; Svensson, Birte

Publication date:
2008

Document Version
Publisher's PDF, also known as Version of record

Hormone-dependence of gene and protein expression in barley aleurone layer
&
Characterization of NADPH-dependent thioredoxin reductase/thioredoxin system in barley seeds

Ph.D. Thesis

2008

Azar Shahpiri

Enzyme and Protein Chemistry, Department of Systems Biology-DTU

Technical University of Denmark

Supervisors:

Associate Prof. Christine Finnie

Enzyme and Protein Chemistry

Department of Systems Biology-DTU

Technical University of Denmark

Prof. Birte Svensson

Enzyme and Protein Chemistry

Department of Systems Biology-DTU

Technical University of Denmark

Preface

This thesis represents the results of my Ph.D. study carried out at Enzyme and Protein Chemistry (EPC), Department of Systems Biology, Technical University of Denmark (DTU) for the period of February 2005 to February 2008. The project was founded by Danish Agriculture and Veterinary Research Council, the Danish Centre for Advanced Food Studies and Iranian Ministry of Science, Research and Technology.

The work has resulted in the following manuscripts:

Shahpiri A, Svensson B, Finnie C. Hormone-dependence of transcript accumulation, protein synthesis and release from barley aleurone layers. In Prep. (Chapter 2)

Shahpiri A, Svensson B, Finnie C (2008) The NADPH-dependent thioredoxin reductase/thioredoxin system in germinating barley seeds: gene expression, protein profiles and interactions between isoforms of thioredoxin h and thioredoxin reductase. Plant Physiol **146**: 789-799 (Chapter 3 and Appendix 2)

Bønsager BC, **Shahpiri A**, Finnie C, Svensson B. Monitoring enzymes of the ascorbate-glutathione cycle of the barley seed embryo during seedling growth. In Prep. (Appendix 3)

Shahpiri A, Hägglund P, Maeda K, Svensson B, Finnie C. Interaction between thioredoxin h (Trx h) and NADPH-dependent thioredoxin reductase (NTR) from barley studied by site directed mutagenesis. In Prep. (Chapter 4)

Acknowledgements

The Ph.D. study is a journey which takes many years to complete. During this exciting and stimulating, but at times exhausting and difficult journey, I was accompanied by a group of people who supported me in multiple ways and without whom I am sure I would have gotten lost along the way.

I owe a deep depth to my supervisors who supported me throughout the Ph.D. process. I would like to thank my primary supervisor, **Associate Professor Christine Finnie** for being a rich source of scientific inspiration and enthusiasm, for excellent technical help, nice discussions, and her support, which always came at exactly the right time. Her contribution to this thesis, however, does not only encompass her role as an academic supervisor, but include her ongoing friendship, care and support on a personal level without which this journey may never have been completed. My second supervisor, **Professor Birte Svensson** who gave me the opportunity to carry out my Ph.D. study at EPC. I am very grateful for her optimism and inspiration throughout the study, her support and nice advices when needed.

My special thanks go to **Per Hägglund** and **Kenji Maeda** for the very fruitful and stimulating discussions we had and with their help with proof-reading chapter 4 and making their valuable and helpful comments. **Birgit Christine Bønsager** is sincerely thanked for her assistance with preparing embryo samples and her contribution to the ascorbate peroxidase related experiments (Appendix 3). I am also very grateful to **Anders Laurell Blom Møller** for translation of the summary of this thesis to Danish.

I would like to thank the technicians: **Mette Christensen**, **Karina Rasmussen**, **Birgit Andersen**, **Anne Blicher**, **Susanne Blume,** and **Inga Jacobsen** for their excellent assistance in the lab.

I would like to thank my former office mates: **Dale Shelton** and **Radovan Hynek** for making every day at work enjoyable.

I would like to thank former and present employees in Building 224 for creating a friendly and kind working environment.

I would like to acknowledge **Professor B. Buchanan** (University of California, Berkeley, USA) for providing rabbit anti-wheat Trx h, **Professor F. J. Cejudo** (University of Sevilla, Sevilla, Spain) for providing rabbit anti-wheat NTR and **Professor J. P. Jacquot** (INRA, Nancy, France) for providing recombinant Arabidopsis NTR.

Last but not least, I would like to give my special thanks to my family in Iran, for their support and encouragement during my Ph.D. while they have been far away for these years…but close. My special thanks go to my husband, **Mohammad** for his endless patience, support, collaborations and scientific discussions.

Summary

The aleurone layer of cereal seeds plays a key role in germination, responding to a gibberellic acid (GA) signal by synthesizing hydrolytic enzymes that are released to the endosperm, before undergoing cell death. The barley (*Hordeum vulgare*) aleurone layer can be separated from the other seed tissues and maintained in culture, allowing the study of GA, abscisic acid (ABA) and other signals in an isolated system. These properties have led to its use as a model system for the study of plant signaling and germination. Changes in response to GA and ABA at various time points were analyzed using one and two dimensional western-blotting for specific proteins. In order to correlate mRNA and protein, gene expression was analyzed in parallel. The experimental system also enabled anaylsis of the release of hydrolytic enzymes since these accumulate in the culture medium. In addition to α-amylase, limit dextrinase and α-glucosidase that are marker proteins for seed germination, the gene expression profile and protein appearance pattern were analyzed for several other genes and proteins including barley α-amylase/subtilisin inhibitor, thioredoxin h (Trx h) and NADPH-dependent thioredoxin reductase (NTR) in both dissected aleurone layer in response to hormones and embryo during germination. NTR/Trx system catalyzes disulfide bond reduction in a variety of target proteins in cytoplasm and mitochondrion and play important roles in seed development, germination and seedling growth. The study of this system in the present work led to isolating and cloning of two cDNAs encoding cytoplasmic or mitochondrial type NTR from barley seeds. The polypeptides deduced from these two cDNAs, HvNTR1 and HvNTR2, have 88% sequence identity. Both isoforms were expressed in *Escherichia coli* as His-tagged proteins and exhibited virtually the same affinity towards two barley Trx h isoforms (HvTrxh1 and HvTrxh2) with slightly different catalytic activity. The present study provides the first investigation of regulation and interactions between members of the NTR/Trx system

in barley seed tissues and suggests that different isoforms are differentially regulated but may have overlapping roles. The cloning and heterologous expression of both NTR and Trx h isoforms provided a basis for design and characterization of mutants using site directed mutagenesis to investigate the interaction between NTR and Trx h at the level of molecular structures. In this way, the kinetic parameters of mutants $R140A_{HvNTR2}$, $R140M_{HvNTR2}$, $I154G_{HvNTR2}$, $E86R_{HvTrxh2}$, $M88G_{HvTrxh2}$, $M88L_{HvTrxh2}$, $M88P_{HvTrxh2}$, $M88A_{HvTrxh2}$, $M82G_{HvTrxh1}$, $A106P_{HvTrxh2}$, and $G105A_{HvTrxh2}$ were determined and compared with those of wild types.

Dansk Resumé

Spiringen starter ved, at frøkimen udskiller plantehormonet gibberellinsyre, som i aleuronlagets celler aktiverer produktionen af hydrolytiske enzymer. Disse enzymer frigives efterfølgende til endospermet (frøhviden) før at celledød indtræffer. Isolering af aleuronlaget fra bygkernernes (*Hordeum vulgare*) resterende væv, muliggør, at man kan studere vævet under påvirkning af gibberellinsyre (GA) og abscisinsyre (ABA) i et isoleret system; et modelsystem som har muliggjort studier af plantesignalering og -spiring. Ændringerne i proteinsammensætningen i aleuronlaget efter behandling med GA og ABA til flere tidspunkter blev i dette projektforløb analyseret ved hjælp af 1D og 2D western blotting, samtidigt med, at mRNA nivauerne, kodende for de samme proteiner, blev moniteret, så transkript og proteinkoncentration kunne korreleres. Udover at kunne isolere vævets proteiner, var det muligt at studere frigivelsen af hydrolystiske proteiner til omgivelserne. Ekspressions- og proteinprofilerne for Limit dextrinase, α-amylase og α-glukosidase, der kan bruges som markører for spiring, blev sammen med α-amylase/subtilisin inhibitor, thioredoxin h og NADPH-dependent thioredoxin reductase analyseret i aleuronlaget behandlet med GA og ABA, og embryo under spiring. Da thioredoxin h/NADPH-dependent thioredoxin reductase-systemet katalyserer *in vivo* reduktionen af disufidbindinger i mange forskellige proteiner i cytoplasmaet og i mitokondrierne, spiller det en vigtig rolle under kerneudvikling og spiring. To cDNA kloner af NADPH-dependent thioredoxin reductase, HvNTR1 og HvNTR2, blev isoleret fra bygkerner. HvNTR1 og HvNTR2 deler 88% sekvensidentitet. Rekombinante fusionsproteiner: HvNTR1-His og HvNTR2-His blev udtrykt i *Escherichia coli*. Både HvNTR1 og HvNTR2 har den samme affinitet overfor byg thioreoxin isofomerne: HvTrxh1 og HvTrx2; dog har de lidt forskellige katalytisk aktivitet.

Denne afhandling beskriver regulationen og interaktionen af thioredoxin h/ NADPH-dependent thioredoxin reductase-systemet i bygkerner. Resultaterne indikerer, at de undersøgte isoformer reguleres forskelligt, men dog har de overlappende funktioner. Kloningen og ekspressionen af thioredoxin h og NADPH-dependent thioredoxin reductase i *E.coli* har dannet basis for mutagenese-studierne, hvis formål var at undersøge interaktionerne mellem thioredoxin h og NADPH-dependent thioredoxin reductase. De kinetiske parametre for mutanterne: $R140A_{HvNTR2}$, $R140M_{HvNTR2}$, $I154G_{HvNTR2}$, $E86R_{HvTrxh2}$, $M88G_{HvTrxh2}$, $M88L_{HvTrxh2}$, $M88P_{HvTrxh2}$, $M88A_{HvTrxh2}$, $M82G_{HvTrxh1}$, $A106P_{HvTrxh2}$, og $G105A_{HvTrxh2}$ blev bestemt og samlignet med vildtypedata.

Table of contents

Chapter 2

Hormone-dependence of transcript accumulation, protein synthesis and release from barley aleurone layer

Chapter 3

The NADPH-dependent thioredoxin reductase/thioredoxin system in germinating barley seeds: gene expression, protein profiles, and interactions between isoforms of thioredoxin h and thioredoxin reductase…

Chapter 4

Interaction between thioredoxin h (Trx h) and NADPH-dependent thioredoxin reductase (NTR) from barley studied by site directed mutagenesis

Appendix 1

Multiple alignment of primary sequences of NTRs from different sources

Appendix 2

Shahpiri A, Svensson B, Finnie C (2008) The NADPH-dependent thioredoxin reductase/thioredoxin system in germinating barley seeds: gene expression, protein profiles, and interactions between isoforms of thioredoxin h and thioredoxin reductase. Plant Phyiol 146: 789-799

Appendix 3

Bønsager BC, Shahpiri A, Finnie C, Svensson B. Monitoring enzymes of the ascorbate-glutathione cycle of the barley seed embryo during seedling growth. In Prep.

Abbreviations

1D	One -dimensional
2D	Two-dimensional
3D	Three-dimensional
ABA	Abscisic acid
ABRE	Abscisic acid response element
AL-ABA	Aleurone layer treated with abscisic acid
AL-GA	Aleurone layer treated with gibberellic acid
AL-O	Aleurone layer incubated in culture medium without hormones
AMY1	The low pI α-amylase
AMY2	The high pI α-amylase
AsA	Ascorbate
AtNTR	Arabidopsis NADPH-dependent thioredoxin reductase
AtTrx h	Arabidopsis thioredoxin h
BASI	Barley α-amylase/subtilisin inhibitor
APX	Ascorbate peroxidase
BSA	Bovine serum albumin
CAT	Catalase
CE	Coupling element
DHAR	Dehydroascorbate reductase
DHA	Dehydroascorbate
DTNB	5,5´-dithio-bis (2-nitrobenzoic acid)
EcNTR	*Escherichia coli* NADPH-dependent thioredoxin reductase
EcTrx	*Escherichia coli* thioredoxin
ER	endoplasmic reticulum
ESI	Electrospray ionization
ESP	Embryo-specific protein
EST	Expressed sequence tag
FAD	Flavin adenine dinucleotide
Fd	Ferredoxin
FDA	fluorescein diacetate
FMN	Flavin mononucleotide
FO	Flavin oxidizing
FR	Flavin reducing
FTR	Ferredoxin thioredoxin reductase
GA	Gbberellic acid
GARE	Gibberellic acid response element
GBP	Gibberellic acid binding protein
gfp	Green fluorescent protein
GR	Glutathione reductase
Grx	Glutaredoxin
GSH	Glutathione (reduced)
GSSG	Glutathione (Oxidized)
HvNTR	Barley NADPH-dependent thioredoxin reductase
HvTrxh	Barley thioredoxin h
IEF	Isoelectric focusing

IPTG	Isopropyl-β-D-thiogalactopyranoside
LD	Limit dextrinase
LDI	Limit dextrinase inhibitor
LEA protein	Late embryonic protein
LTP	Lipid transfer protein
m/z	Mass to charge ratio
MALDI	Matrix-assisted laser desorption ionization
MDHA	Monodehydroascorbate
MDHAR	Monodehydroascorbate reductase
MS	Mass spectrometry
Mw	Molecular weight
NADPH	Nicotinamide adenine dinucleotide phosphate
NCBI	National centre biological information
NTR	NADPH-dependent thioredoxin reductase
PCR	Plolymerase chain reaction
PCD	Programmed cell death
PDB	Protein data bank
PDI	Protein disulfide isomerase
pI	Isoelectric point
RNS	Reactive nitrogen species
ROS	Reactive oxygen species
RSOH	Sulfenic acid
RSO_2H	Sulfinic acid
RSO_3H	Sulfonic acid
RT-PCR	Reverse transcription polymerase chain reaction
SN-ABA	Culture supernatant corresponding to AL-ABA
SN-GA	Culture supernatant corresponding to AL-GA
SN-O	Culture supernatant corresponding to AL-O
SNO	Nitrosothiol
SOD	Superoxide dismutase
SDS	Sodium dodecyl sulfate
SDS-PAGE	Sodium dodecyl sulfate-polyacryl amide gel electrophoresis
TaNTR	Wheat NTR
TBST	Tris-buffered saline Tween-20
TC	Tentative consensus
TIGR	The institute for genomic research
TNB	2-nitro-5-thiobenzoic acid
TOF	time-of-flight
TR	Thioredoxin reductase
Trx	Thioredoxin
Wt	Wild type

Chapter 1- Introduction

1.1. Barley

Barley *(Hordeum vulgare*) is an annual cereal grain belonging to grass family "poaceae". Between various cereals, barley has adapted to the widest variety of climates. Barley is grown for food, feed and malting. In fact, about 85% of today's barley production is used for animal feed (Fischbeck et al., 2002). However, some barley properties including its diploid nature (2n=2x=14), self fertility, large chromosomes, ease of hybridization, and high adaptability have made it a favorable genetic experiment of organism and a nice model for other plants (Nilan, 1974). Obtaining barley genome sequence will be useful as it contains genes for agronomically desirable traits related to stress, pest and disease resistance. At the same time, sequence analysis will help improvement of the feed quality. Therefore, barley researchers have put their efforts into developing a dense physical map for barley and creating a large numbers of ESTs [392628 ESTs are currently available in EST database in national centre biological information (NCBI, http://www.ncbi.nlm.nih.gov)].

1.2. The barley seed

The barley seed is typical for monocot and consists of several tissues that play different roles during seed germination and seedling growth (Fig. 1.1). The seed coat protects the seed against entry of parasites, mechanical injury and unfavorable high or low temperature. Inside the seed coat is the embryo, a result of fertilization of the egg cell in the embryo sac by one of the male nuclei. The embryo comprises 3-4% of the dry weight of the seed. It is a living tissue and contains all necessary components for growth of a new plant when supported by nutrients from the endosperm. The seed is filled with endosperm that protects and contains nutrients for

the embryo, i.e. mainly starch and storage proteins, but also lipid and other nutrients. The majority of the endosperm cells are dead at the maturity but on the surrounding the endosperm remains living tissue, i.e. the aleurone layer that releases the enzymes required for degradation of endosperm storage components providing the nutrients for germinated embryo (Bewley and Black, 1994).

Seed germination comprises numerous anatomical, genetic, metabolic and hormonal events that start with water uptake by the seed (imbibition) and end with the start of elongation by the embryonic axes (Bewley, 1997).

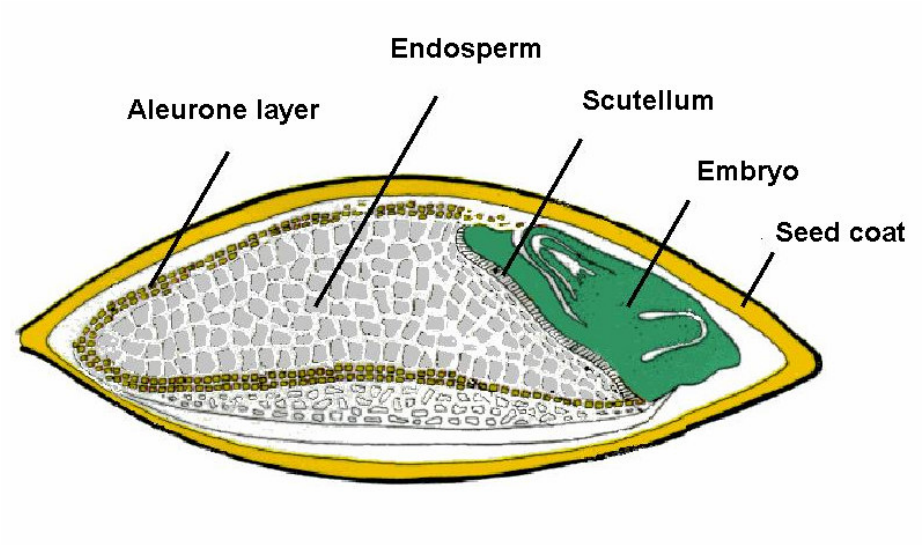

Figure 1.1. Structure of the barley seed (adapted from http://www.crc.dk/flab/the.htm)

1.2.1. Aleurone layer

The aleurone layer is a highly specialized layer of cells differentiated from the endosperm during seed development. However, it is highly different from the starchy endosperm. The aleurone layer is a living secretory tissue that responds to hormone signals whereas the starchy endosperm cells are dead in the mature seeds. In the freshly imbibed grain, aleurone cells have a dense cytoplasm filled with many small vacuoles containing proteins and phytic

acid. Upon imbibition, when aleurone layer receives gibberellic acid (GA) from the embryo the vacuole contents are hydrolyzed to provide the amino acids and inorganic materials which are used by the synthetic machinery of the cell to produce secreted hydrolases (Ritchie et al., 2000). The aleurone layer has recieved great attention for nearly 200 years because of its importance in malting and brewing (Bethke et al., 1997). The discovery of the response of deembryonated aleurone layer to exogenous hormones for first time in 1960 individually by Paleg in Australia and Yomo in Japan was the starting point for using the aleurone layer as an experimental system to understand the effect of the phytohormones GA and abscisic acid (ABA) in plant cells.

1.2.1.1. GA signaling in barley aleurone layer

GAs are tetracyclic diterpenoid growth factors that are essential for normal growth and affect a wide variety of plant developmental processes (Singh et al., 2002). During germination aleurone layer cells respond to GA and release a group of hydrolytic enzymes such as α-amylase, proteases and nucleases into the starchy endosperm (Ranki and Sopanen, 1984; Baulcombe and Buffard, 1983). At least about 40% of the newly synthesized protein in GA-treated aleurone layers is α-amylase. Therefore, this enzyme and its corresponding gene have been used as a convenient marker for study of GA action (Ho et al., 2003). Plants have two types of GA-binding proteins (GBP), including soluble and membrane-bound forms (Ueguchi-Tanaka et al., 2007). The α-amylase was induced in aleurone protoplasts in a GA-dependent manner. Such induction was observed even with GA derivatives that cannot cross the plasma membrane (Hooley et al., 1991). In contrast, α-amylase was not appeared when GA was injected into the cytoplasm of barley aleurone protoplasts (Gilroy and Jones, 1994). These experiments showed that the GA receptor has been located on the outside of the

aleurone cell plasma membrane. In the GA signal-transduction pathway DELLA proteins that are belonging to GRAS subfamily play a key role. The mutations in DELLA proteins in several plants including rice (SLR1, Ikeda et al., 2001) and barley (SLN1, Chandler et al., 2002) resulted in reduced GA responses. In barley aleurone layer the interaction between GA and its receptor on the plasma membrane activates the heterotrimeric G protein and eventually leads to decrease of SLN1 either by blocking the translation or by promoting SLN1 protein degradation (Gubler et al., 2002). SLN1 is a repressor for the gene GAMYB which itself encodes GA-regulated transcription factor. Therefore, decrease in SLN1 leads to the enhancement of expression of GAMYB. The transcription factor GAMYB binds to a GA response element (GARE) on α-amylase promoter that is necessary for GA induction of α-amylase. GAMYB has similar effect on the other GA-induced enzymes. Furthermore, the expression of GAMYB itself is up-regulated by GA and down-regulated by ABA (Gomez-Cadenas et al., 2001).

1.2.1.2. The antagonistic effect of GA and ABA in aleurone layer

The plant hormone ABA plays a major role in seed maturation and germination. ABA regulates several essential processes during seed development including induction of seed dormancy, accumulation of nutrition reserves and establishment of stress tolerance (Leung and Giraudat, 1998). In cereal aleurone layer ABA induces the synthesis of late embryonic abundant (LEA) proteins that likely relate to stress tolerance in this tissue (Hong et al., 1988). The antagonism between GA and ABA is an important factor that regulates developmental transition from embryogenesis to seed germination. The expression of GA-inducible genes in aleurone layer required for seedling growth is suppressed by ABA. In fact, ABA-signaling in aleurone layer appears to branch into two separate pathways. One involves in induction of

ABA-inducible genes and another one functions in suppression of GA effect. It has been determined that cis-acting elements called ABA response promoter complexes, consisting of either two copies of a specialized G-box element (also called ABA response element: ABRE) or one copy of G-box plus a copy of a coupling element (CE1 or CE3) are present for many ABA-inducible genes (Hobo et al., 1999; Shen et al., 1996). Furthermore, the induction of genes by ABA requires a particular class of bZIP transcription factors including ABI5 that interacts with ABARE (Finkelstein and Lynch, 2000). However, the pathway through which ABA suppresses the expression of GA-inducible genes is completely different (Fig. 1.2). The transcription factor ABI5 is not involved in the ABA suppression pathway (Casaretto and Ho, 2003). The suppression of GA-inducible genes by ABA are mediated by induction of synthesis of protein kinase PKABA (Gomez-Cadenas et al., 1999) which is a member of the snRK2 subfamily of SNF-1 related protein kinase (Yamauchi et al., 2002). It has been proposed that the effect of ABA in this pathway is blocking the GA induction of GAMYB at the transcription level which is necessary for induction of GA-inducible genes (Ho et al., 2003; Gomez-Cadenas et al., 2001; Gubler et al., 2002). Unlike LEA proteins, ABA-induction of PKABA1 can be reversed by GA. This indicates that PKABA1 could be involved in GA/ABA antagonism (Ho et al., 2003).

1.2.1.3. Aleurone layer cell death program

The aleurone layer of cereal seeds is programmed to die following the germination (Bethke et al, 1999). Programmed cell death (PCD) in aleurone layer is hormonally regulated. GA promotes and ABA postpones PCD in the barley aleurone layer (Bethke et al., 1999). Death of cells begins 24 h after incubation of barley aleurone layer in GA and almost all of the cells die during the subsequent 24 h whereas they remain viable during incubation with ABA (Fig.

1.3; Bethke et al., 2002). Reactive oxygen species (ROS) are key players of PCD in cereal aleurone layer (Bethke and Jones, 2001). The main source of production of ROS in aleurone layer is metabolism of triglycerides via β-oxidation which is necessary to provide energy and substrates for synthesis of hydrolases by aleurone layer following GA-treatment (Fath et al., 2001). Hydrogen peroxide (H_2O_2) is the major byproduct in this process and the major ROS that leads to aleurone PCD. ROS are scavenged by many enzymes including ascorbate peroxidase (APX), superoxide dismutase (SOD) and catalase (CAT). The treatment of aleurone layer with GA causes a rapid reduction of the corresponding mRNA for these enzymes leading to sensitization of the aleurone cells to H_2O_2. In contrast, a high level of these mRNAs was maintained during incubation in ABA. Therefore, ABA maintains the aleurone layer cell viability by keeping ROS under control (Fath et al., 2001).

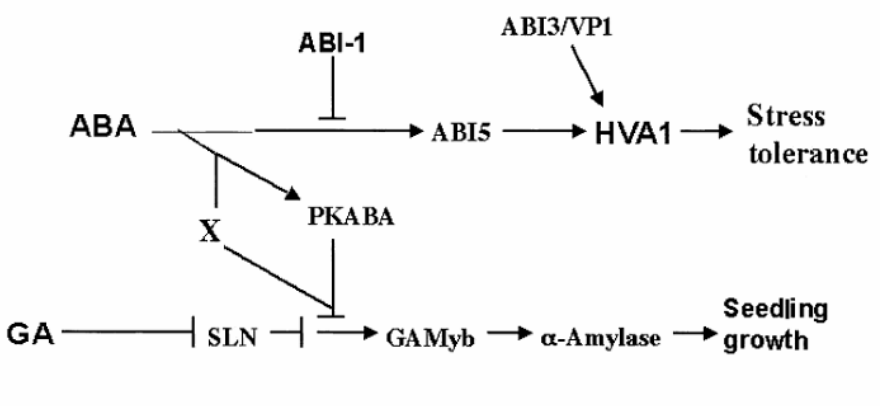

Figure 1.2. The steps involved in GA/ABA crosstalk in regulating of α-amylase or other GA-inducible genes. A repressor SLN1 and an activator GAMyb are essential components in the GA-signaling pathway. ABA suppresses the expression of GAMyb leading to suppression of α-amylase expression. An alternative route (represented by X) indicates that PKAMyb is sufficient, but not necessary for blocking of α-amylase expression. Two transcription factors, ABI5 and VP1 are required for expression of ABA-inducible genes (adapted from Ho et al., 2003).

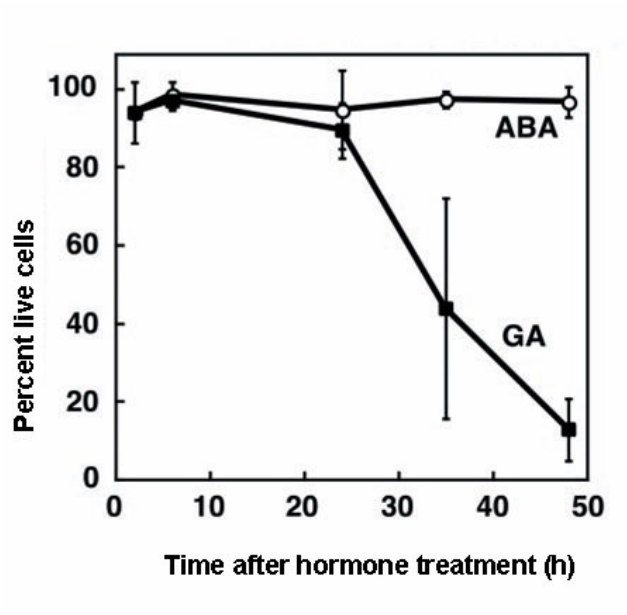

Figure 1.3. Time course of barley PCD in barley aleurone layer treated with 5 µM GA or ABA. Viable cells were identified by staining with fluorescein diacetate (FDA) and dead cells with FM 4-64 (adapted from Fath et al., 2001).

1.2.2. Seed reserves and their mobilization during germination

1.2.2.1. Carbohydrate reserves

Starch is the major carbohydrate reserve in cereal grain where it is located in nonliving starchy endosperm cells and comprises up to 60% of total grain dry weight (Aman et al., 1985). Starch consists of the essentially linear (1-4)-α-glucan (amylase) together with the branched (1-4,1-6)-α-glucan (amylopectin). Barley seeds contain 70-75% amylopectin and 25-30% amylose (MacGregor and Fincher, 1993). Amylose and amylopectin in the native starch grains are first hydrolyzed by cooperation of α-amylase and β-amyalse, which break down the (1-4)-α-glucosidic links between the glucose residues randomly through chain. But these enzymes can not hydrolyze (1-6)-α-glucosidic bonds in amylopectin and therefore highly branched cores of glucose units called limit dextrins are produced. Then debranching

enzymes like limit dextrinase (LD) in barley seeds break down (1-6)-α-glucosidic linkages and produce glucose oligomers (Figure 1.4). The released glucose oligomers are further hydrolyzed by α-amylase and β-amylase to glucose and maltose and finally α-glucosidase hydrolyzes the maltose to glucose molecules (Sun and Henson, 1991).

Whereas the β-amylase is synthesized during seed development in endosperm (Lauriere et al., 1986), other enzymes involved in starch degradation appear during germination in the aleurone layer in response to GA (Bewley and Black, 1994). Multiple forms of α-amylase are synthesized in germinated barley seeds and fall into two subfamilies, low pI α-amylase (AMY1) and high pI α-amylase (AMY2). AMY1 and AMY2 contain 414 and 403 amino acids, respectively and share approximately 80% sequence identity (Rogers and Milliman, 1983; Rogers, 1985). Despite the high sequence similarity, the isoforms show very different physiochemical and biochemical properties (Bertoft et al., 1984, Rodenburg et al., 1994). For instance, only AMY2 is sensitive to the barley α-amylase/subtilisin inhibitor (BASI; Mundy et al., 1983; Weselake et al., 1983).

The abundance of LD mRNA in GA-treated aleurone layer and in germinated seeds is in agreement with the role of this enzyme in starch hydrolysis. However, a low level of LD mRNA was also observed in the developing endosperm, suggesting involvement of LD in starch synthesis during seed development (Burton et al., 1999). A specific inhibitor for this enzyme that is called limit dextrinase inhibitor (LDI) was found in mature barley seeds, but disappears several days after germination (MacGregor, 2004).

1.2.2.2. Protein reserves

Cereal seeds contain relatively little protein compared to legumes corresponding to an average of 10-12% of the dry seed weight (Shewry and Halford, 2002). According to Osborne's

classification, seed proteins can be divided into four groups (1) albumins-soluble in water and dilute buffers at natural neutral pH; (2) globulins-soluble in salt solution but insoluble in water; (3) glutelins-soluble in dilute acid or alkali solutions; and (4) prolamins-soluble in aqueous alcohols. The major protein in the barley seed endosperm is hordein that belongs to the prolamins, whereas the major storage proteins in wheat and oat seeds are of the glutelin and globulin type, respectively (Bewley and Black, 1994). The prolamins are deficient in essential amino acids, notably lysine (Shewry, 2007). Barley seeds, therefore, are usually combined with other sources of these amino acids like legume seeds for animal feed. Proteinases for breaking down the major storage proteins in the starchy endosperm come from two sources: the aleurone layer or the starchy endosperm itself (Bewley and Black., 1994).

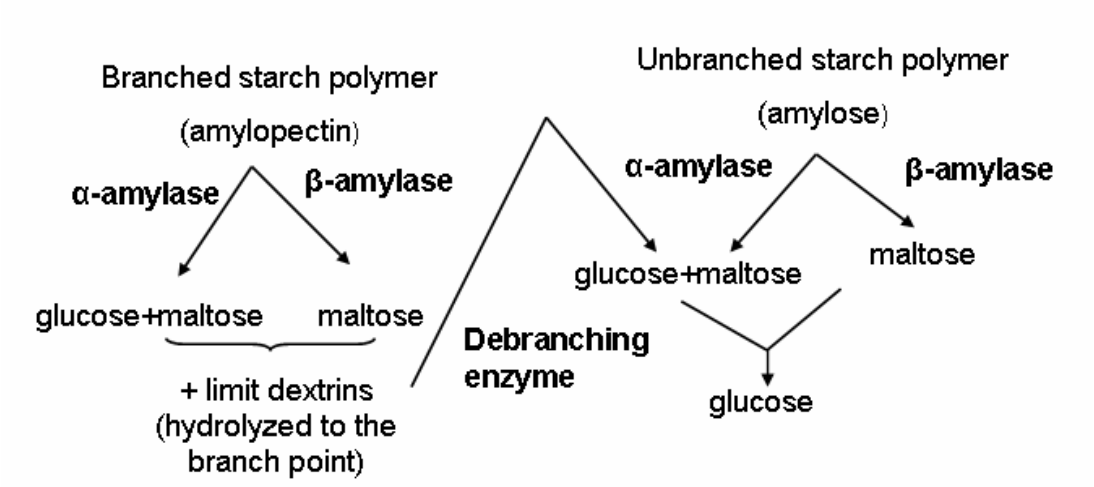

Figure 1.4. The role of α-amylase, β-amylase, debranching enzyme and α-glucosidase in degradation of amylopectin and amylose in cereal seed starchy endosperm (adapted from Ritchie et al., 2000).

1.3. Genomics and proteomics

Genomics is the study of an organism's genome and aims to determine the linear chromosomal sequence of model organisms. Annotating the genome, including defining coding and regulatory sequences is also part of genomics (de Hoog and Mann, 2004). The information in the DNA sequence is transcribed to mRNA and the sum of all mRNAs in a cell or tissue or an organism is called the transcriptome. Functional genomics by employing different techniques including northern blot, RT-PCR, DNA microarray and SAGE attempts to describe the mRNA levels. DNA microarray is a large scale method in which gene expression levels of thousands of genes can be determined simultaneously (Kurella et al., 2001). There is not necessarily a one-to-one relationship between the genome sequence and the transcript; cells use alternative splicing to produce different transcripts from one gene and a whole range of mechanisms to control the production, transcriptional status, and degradation of mRNA (Leipzig et al., 2004, Danpure, 1995). Therefore, a transcriptome is a part of the information in DNA. The products of genes are proteins which actually carry out the majority of the cellular reactions. The entire complement of proteins in a cell or tissue or organism is called the proteome. There is not always a linear relationship between the level of mRNA and protein; Cases are known where the extent of variation in mRNA and protein are widely different (Rousseau et al., 1992) or even where protein and mRNA levels vary in opposite directions (Knochbin et al., 1991). Given these limitations, proteomics as a complementary approach for genomics and mRNA expression mapping appears as a preferred tool since it directly analyzes the end product of the genome. Because some of the mRNA molecules are never translated into protein, the proteome may be expected to be less complex than transcriptome. However, the complexity of the proteome increases through post-translational

modification of the proteins thus giving the potential for more than one product to be derived from a given message. Fig. 1.5 gives an overview of the relation between the "omics".

The name proteomics is traditionally associated with the display of a large set of proteins from a given organism or cell line on two-dimensional (2D) polyacrylamide gels. The ability to associate a spot on a 2D-gel with a known protein is used to create databases of proteins that are expressed in an organism or cell line under defined conditions. This approach is complementary to the generation of databases of mRNA expression levels by microarray hybridization (Palzkill, 2002). However, the protein function depends on the precise amino acid sequence, the modifications (especially regulatory ones such as phosphorylation), the three-dimensional (3D) structure, the protein concentration, the association with other proteins, and the extracellular environment (de Hoog and Mann, 2004). Therefore, the field of proteomics is rapidly expanding and proteomics today seeks to determine protein modifications, localization, and protein-protein interaction in addition to protein expression levels.

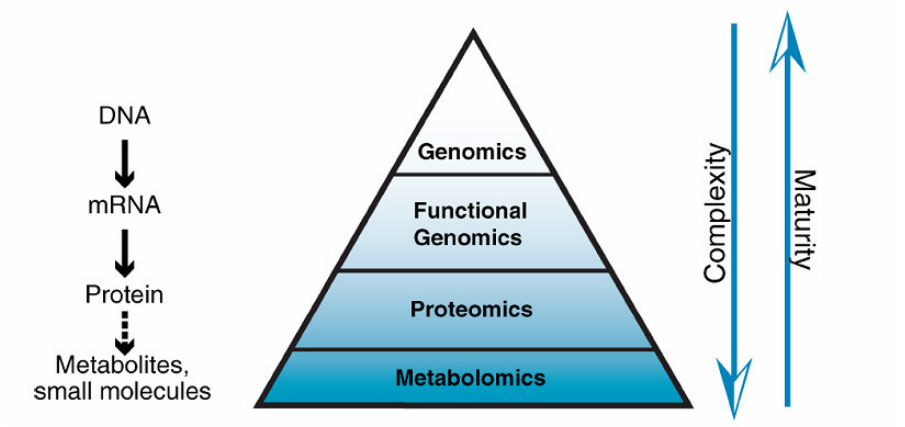

Figure 1.5. Schematic of the relationship between the different "omics" disciplines in relation to the flow of information from genome through transcript to protein and small molecule. Moving from genomics to proteomics, the complexity increases dramatically whereas the maturity of the technology decreases (adapted from de Hoog and Mann, 2004).

1.3.1. 2D-gel electrophoresis and protein identification

The classical 2D-gel electrophoresis involves first separating proteins based on their isoelectric point (pI) using isoelectric focusing (IEF). The isoelectric point is the pH at which there is no net electric charge on a protein. IEF is an electrophoretic technique where proteins are separated in a pH gradient. An electric field is applied to the gradient and proteins migrate to the position in the pH gradient equivalent to this pI. The second step in 2D-gel electrophoresis is to separate proteins based on molecular weight using SDS-PAGE. Individual proteins are then visualized by for example Coomassie Blue or silver staining techniques (Patton, 2002). Using this approach, several thousand spots can be visualized in a single gel. Despite excellent resolving power, 2D-gel electrophoresis has some limitations. One problem is sensitivity and reproducibility. Proteins are expressed in the cell with a wide range of concentration but the detection power of Coomassie or silver staining is limited. Even with loading a high protein amount on a 2D gel sometimes low abundance proteins are not detected. The development of fluorescent dyes to visualize proteins from 2D gels may increase the sensitivity and reproducibility of the technique (Steinberg et al., 1996). Staining with dyes such as SYPRO Orange or SYPRO Red is noncovalent and can be performed in a simple one-step procedure after the electrophoretic steps.

Immunoblotting can conveniently be used for identification of proteins. In this method after separation of protein on the gel electrophoresis proteins are transferred onto a nitrocellulose membrane or polyvinylidene (PVDF) where they are probed with specific antibody to the target protein. This technique, however, is limited to identify proteins for which a specific antibody is available.

During the past two decades mass spectrometry (MS) has become widely established for protein identification. In this method, 2D-gel electrophoresis is followed by excising the spots

from the gel. The next step is digestion using a sequence specific protease such as trypsin. Peptides are much more amenable to MS analysis because proteins cannot easily be eluted from gels and because the molecular weight of whole proteins is not usually sufficiently discriminating for database identification. After digestion of proteins, the peptides are often delivered to a MS for analysis. Two "soft ionization" methods, namely matrix-assisted laser desorption ionization (MALDI) and electrospray ionization (ESI), have made it possible to analyze large biomolecules, such as peptides and proteins (Cotter, 1999; Boyd, 1997). In the case of MALDI the samples of interest are solidified in an acidified matrix, which absorbs energy in a specific UV range and dissipates the energy thermally. This rapidly transferred energy generates a vaporized plume of matrix and thereby simultaneously ejects the analytes into the gas phase where they receive charge. A strong electrical field between the MALDI plate and the entrance of the MS tube forces the charged analytes to rapidly reach the entrance at different speeds based on their mass-to-charge (*m/z*) ratios. The m/z ratios are recorded and used for searching against a computer generated list of peptides of proteins in a database.

1.3.2. Barley seed proteomics

Recently 2D gel and MS has been extensively used for barley on mature, developing and germinated seeds (Finnie et al., 2002, 2006; Bak-Jensen et al., 2004, 2007; Østergaard et al., 2002, 2004). Proteome analysis of barley seeds during 5-week grain filling and seed maturation (Finnie et al., 2002) assigned around 1000 spots. Decrease in the number of spots in mature seeds compared to developing seeds reflected the greater metabolic activity in developing seeds. Noticeably, the intensity of a group of spots that were identified as α-amylase/trypsin inhibitor increased during grain filling. This observation was in accordance with the role of these proteins since they inhibit exogenous α-amylase from various insect

pests and therefore they have important role in protection of the seed against invading pathogens during grain filling. In another study proteome analysis of water-soluble proteins extracted from dissected embryo, aleurone layer and endosperm of barley seeds were compared (Finnie et al., 2003). Over 850 major spots in aleurone layer, 575 in endosperm and 1000 in embryo were visualized. The 2D-gels from different tissues showed overlapping patterns. Several spots were present in only one or two tissues. For instance the spots which were identified as α-amylase/trypsin inhibitor and chymotrypsin inhibitor were present mostly in the endosperm and in very low amount in aleurone layer, but they were absent in embryo. In contrast, the spots identified as small heat shock proteins, thioredoxin peroxidase, and Cor14b were predominantly present in embryo and aleurone layer and absent in endosperm. The location of these proteins was in agreement with their possible roles in maintaining the embryo and aleurone layer in a viable state during seed desiccation. Differences in appearance pattern of proteins in different tissues, e.g. APX, were also observed during germination and radicle elongation in dissected tissues in barley seeds (Bønsager et al., 2007). The membrane proteins in barley aleurone layer for first time using a proteome approach based on SDS-PAGE and LC-MS/MS were analyzed leading to identification of 46 proteins associated with barley plasma membrane including proteins with more than 10 transmembrane domains (Hynek et al., 2006).

1.3.3. Seed transcriptome analysis

DNA microarray is the technique most commonly used for transcriptome analysis. This method has been extensively used for plant seed transcriptome analysis. DNA microarray analysis in Arabidopsis (*Arabidopsis thalina*) seed during development (Girke et al., 2000) and seed germination (Ogawa et al., 2003), barley seeds in response to drought and salt stress

(Oztur et al., 2002), rice seeds in response to cold, drought, high salinity and ABA (Rabbani et al., 2003), dissected barley seed tissues during germination and radicle elongation (Potokina et al., 2002) are examples of employing this method for analysis of gene expression in seed under different conditions.

1.3.3.1. Transcriptome analysis in cereal aleurone layer

Transcriptome analysis has been performed to characterize changes in the transcription that occur in rice half-grains treated with GA, ABA, or no hormones for various time points using a half-genome rice microarray (Bethke et al., 2006). From 23,000 probe sets on the chip approximately 11,000 hybridized with RNA from rice aleurone treated with GA, ABA, or no hormone. This suggested that rice aleurone layer contains a surprisingly large number of mRNA species. The data as expected showed that many genes are up-regulated with GA. However, one-third of this amount was down-regulated by GA. Surprisingly ABA up-regulated as many genes as GA up-regulated. Furthermore, many genes showed a temporal change in transcript abundance during 8 h period of the experiment. In many cases, these changes did not depend on treatment with hormones, suggesting that many of these changes are resulted from imbibition and rehydration of aleurone cells.

The transcriptome pattern of over 22,000 genes was also analyzed in barley aleurone layer incubated in GA, ABA, or no hormones for 15 h (Chen and An, 2006). Approximately 50% of genes were expressed above the detection limit. This supported the data founded for the rice aleurone layer reflecting the presence of large numbers of mRNA in the seed aleurone layer. A total of 9,993 genes were expressed in all groups (GA, ABA, and control treatment). A few of genes were specifically expressed in GA-treated aleurone layer (629), ABA-treated

aleurone layer (800) and control (224). Interestingly 2.5-fold more genes were up-regulated than down-regulated by ABA.

A large number of genes encoding hydrolytic enzymes were up-regulated with GA and down-regulated with ABA. For instance, all six α-amylase genes on the GeneChip were up-regulated with GA by three to 80-fold and Four of them were down-regulated three to 50-fold by ABA. ALL seven β-amylase genes on the GeneChip were undetectable or in low levels. This confirms the previous data showing that β-amylase is synthesized in starchy endosperm during seed development rather than in the aleurone layer (Laurier et al., 1986). The expression of genes which are involved in depolymerization of the cell wall and required for secretion of enzymes from aleurone layer into the starchy endosperm were up-regulated with GA. The genes encoding cysteine proteases, serine proteases, triacylglycerol lipases that are involved in degradation of protein and lipid reserves in endosperm during germination were up-regulated with GA. Putative transcription factor genes (70 genes on the GeneChip) were differentially regulated with GA and/or ABA. For instance, two genes encoding GAMYB were up-regulated with GA. In addition, some GA-responsive genes encoded proteins involved in signal transduction pathway of jasmonates, brassinosteroids, ethylene and auxin suggesting their potential interaction with the GA response.

1.4. Heterologous protein production and protein manipulation

Advances in genetic engineering have made possible the production of therapeutics and vaccines for human and animals in the form of recombinant proteins. In addition industrial applications of recombinant proteins and enzymes in food, textile, leather and detergent are increasing exponentially.

Furthermore, recombinant DNA technology has allowed the isolation and cloning of many important genes. This approach together with heterologous protein expression has contributed a lot to analysis of gene function which is of central importance for the understanding the physiological processes.

The heterologous production of proteins and enzymes involves two major steps: (1) Introduction of foreign DNA into the host cells. This step has three major considerations. (a) Identification and isolation of the DNA to be introduced; (b) Determination of the vector and construction of recombinant vector; (c) Determination of the suitable expression system to receive rDNA. (2) Expression of the foreign DNA for protein synthesis in the chosen expression host system (Rai and Padh, 2001).

Prokaryotic and eukaryotic systems are two general categories of expression systems. Among prokaryotic systems *Escherichia coli* is the most widely employed system. Its popularity is due to complete knowledge about its genetic, physiology and complete genomic sequence, which greatly facilitate gene cloning and cultivation. Furthermore, the high growth rate of *E. coli* and large level of production of heterologous proteins are other advantages of using this host (Frommer and Ninneman, 1995). However, prokaryotic cells pose serious problems in posttranslational modification. Common bacterial expression systems such as *E. coli* have no capacity to glycosylate proteins in either N- or O-linked conjugates and therefore they have limitations for heterologous production of eukaryotic proteins (Rai and Padh, 2001). Alternatively yeast, insects and mammalian cells are eukaryotic expression systems that are used for production of eukaryotic proteins. There is no universal expression system for heterologous proteins. All expression systems have some advantages as well as some disadvantages that should be considered in selecting which one to use. Choosing the best one

requires evaluating the properties of the product from yield to glycosylation, proper folding, and economical scale-up.

One of the most exciting aspects of the recombinant DNA technology involves the design, development and isolation of proteins with improved properties such as activity, affinity, selectivity, stability, resistance to proteolytic degradation, and even design and development of completely novel proteins. This technology that is called protein engineering depends on the scientific revolutions in genetic engineering and the discoveries in molecular biology and increasing use of computers, which will enable us to design novel proteins and predict protein properties.

Specific amino acids may be replaced individually by site-directed mutagenesis. This powerful approach by altering the DNA sequence in a cloned DNA provides a way for understanding how the primary structure determines the three-dimensional structure and function of proteins. The changes can also be made in more than one base pair. Large parts of a gene can be deleted by cutting out a segment with restriction endonucleases and ligating the remaining portions to form a smaller gene. Parts of two different genes can also be ligated to create new combinations. The product of such a fused gene is called a fusion protein.

1.5. Plant redox regulation

1.5.1. Thiol/disulfide exchange regulation

It has been well established that disulfide bonds contribute in stabilization, folding and activity of proteins (Raina and Missiakas, 1997). Two cysteine residues in a protein can be oxidized to form a disulfide bond. Disulfide bonds can be formed between two cysteines in the same polypeptide (intramolecular disulfide) or different polypeptides (intermolecular disulfide). Another type of disulfide bond that can be classified as an intermolecular disulfide

is a mixed disulfide, where a cysteine reacts with its counterpart of an oxidized molecule of glutathione. This is known as glutathionylation (Dalle-Donne et al., 2008).

For a long time it was assumed that the formation of disulfide bonds in proteins is a spontaneous process. Later it was shown that this process is catalyzed by Dsb proteins in *E. coli* and by protein disulfide isomerase (PDI) in eukaryotes (Raina and Missiakas, 1997). Secreted eukaryotic proteins contain a larger number of disulfides than bacterial proteins. Therefore, eukaryotes have a more active quality control system to ensure that the correct disulfides are formed as the protein matures. Because most disulfides occur in extracellular proteins, the eukaryotic endoplasmic reticulum (ER) provides a redox environment that encourages disulfide bond formation and a network of chaperones and folding catalysts to ensure that the correct disulfides are formed prior to exiting from the ER (Kadokura et al., 2008).

In plants, disulfide bonds are especially prominent in secretory and storage proteins giving them stability. This protects proteins against denaturation and decreases their susceptibility to proteolytic degradation. Disulfide bonds are reversibly oxidized and reduced. For instance in plant seeds, storage proteins are synthesized in reduced state during seed development and become oxidized to a more stable disulfide state during maturation. Upon germination, they will revert to the reduced state that increases their solubility and susceptibility to proteases and facilitates their mobilization (Buchanan and Balmer, 2005).

In many enzymes disulfide bonds which are formed between two cysteines separated by one or two amino acids have a catalytic role. This redox active site functions either as an electron donor or acceptor. Interconversion of a disulfide to thiols provides a mechanism for the regulation of the catalytic activity of this kind of enzymes (Ziegler, 1985).

In addition to disulfide bonds exposure of protein cysteine to reactive oxygen/nitrogen species (ROS/RNS) such as hydrogen peroxide can lead to production of several reversible and irreversible forms of oxidized cysteine including sulfenic acid (RSOH), sulfinic acid (RSO_2H), sulfonic acid (RSO_3H) and nitrosothiol (SNO). Since cysteines often have catalytic or structural roles in proteins, such modifications can affect the protein function (Maeda et al., 2006b).

Several enzymes including glutaredoxin (Grx), thioredoxin (Trx) and PDI are involved in modulation of dithiol/disulfide exchange in the cell.

1.5.2. Glutaredoxin system

The glutathione/glutaredoxin system (Fig. 1.6) consists of glutathione (GSH), Grx and NADPH-dependent glutathione reductase (GR). Grx is a small protein and member of the thiol-disulfide oxidoreductase enzyme family (Holmgren, 1989). In recent years, Grx has been detected in most prokaryotes and eukaryotes, and even in viruses (Lou, 2008). The first plant Grxs were cloned and isolated from rice aleurone layer (Minakuchi et al., 1994) and spinach leaves (Morell et al., 1995). Grxs catalyze dithiol-disulfide exchange reactions or reduce protein-mixed glutathione disulfide. The reduction of Grx itself is carried out using reduced glutathione (GSH). GSH is one of the most important antioxidants in almost all organisms. The ratio of reduced (GSH) to oxidized (GSSG) glutathione is the main control of cellular redox balance including the thiol-disulfide redox state. The reduction of GSSG is dependent on NADPH and is catalyzed by GR which is an enzyme belonging to the flavoprotein disulfide oxidoreductase family.

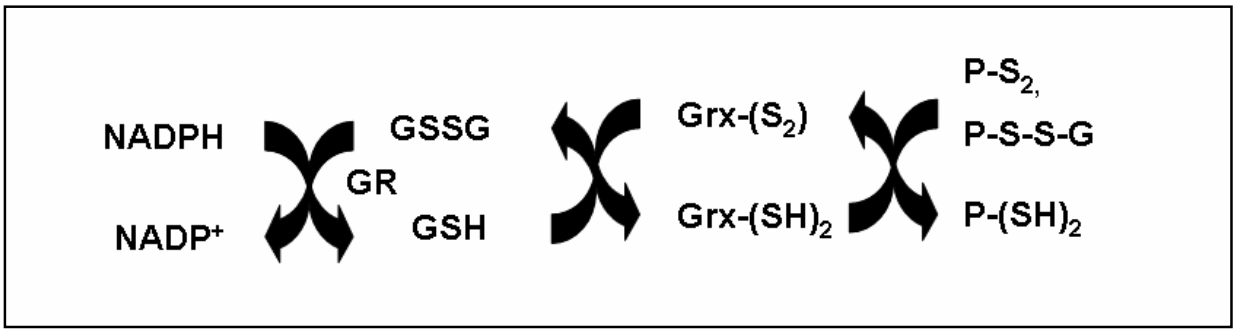

Figure 1.6. The glutathione system. Glutathione reductase (GR) reduces the oxidized form of glutathione (GSSG) in the presence of NADPH. The reduced glutathione (GSH) acts as electron donor to the enzyme glutaredoxin (Grx). Then glutaredoxin reduces disulfide bonds in target proteins (P) or glutathionylated proteins (P-S-S-G).

1.5.3. Thioredoxin systems

Thioredoxins (Trxs) are small proteins with molecular weight of 12-14 kDa with a typical WC(G/P)PC motif. These ubiquitous proteins are present in all organisms from prokaryotes and eukaryotes (Gelhaye et al., 2004). Trxs function as dithiol/disulfide catalysts. The oxidized form of Trx contains a disulfide bridge (S-S) that is reduced either by reduced ferredoxin or NADPH. In higher plants Trxs are divided into several major groups. For instance 19 different Trxs have been identified in the genome of Arabidopsis (Fig. 1.7) that can be grouped in six subfamilies (Meyer et al., 2002, 2005). In general the Trxs m, f, x and y are localized in chloroplasts whereas Trx o is localized in the mitochondrion and Trx h is distributed in multiple cell compartments: cytosol, nucleus, endoplasmic reticulum as well as mitochondrion.

Chloroplast Trxs are members of ferredoxin (Fd) /Trx system (Fig. 1.8). In this system Trxs in chloroplast are reduced by way of light. Light-driven photosynthetic electrons reduce Fd which then serves as electron donor for the enzyme ferredoxin-thioredoxin reductase (FTR). This enzyme in turn reduces Trxs. Then Trxs act as electron donor to reduce target proteins in

chloroplast and activate biosynthetic, or deactivate catabolic pathways. Trxs f and m are the major Trxs in chloroplast and Trxs x and y are present in lower abundance. Trx f was originally described as the activator protein for spinach stromal fructose 1,6-bisphosphatase and Trx m for NADP-malate dehydrogenase (Buchanan, 1980, 1991; Jacquot et al., 1997).

The second Trx system consists of NADPH, a flavin enzyme called NADP-dependent thioredoxin reductase (NTR) and a Trx (h or o type in plants). In NTR/Trx system electrons are transferred from NADPH via FAD to the active site disulfide bond of NTR, which then reduces the active site disulfide bond in Trx. Then Trx acts as electron donor to many Trx target proteins (Figure 1.9). Each enzyme in this system is individually described in the following.

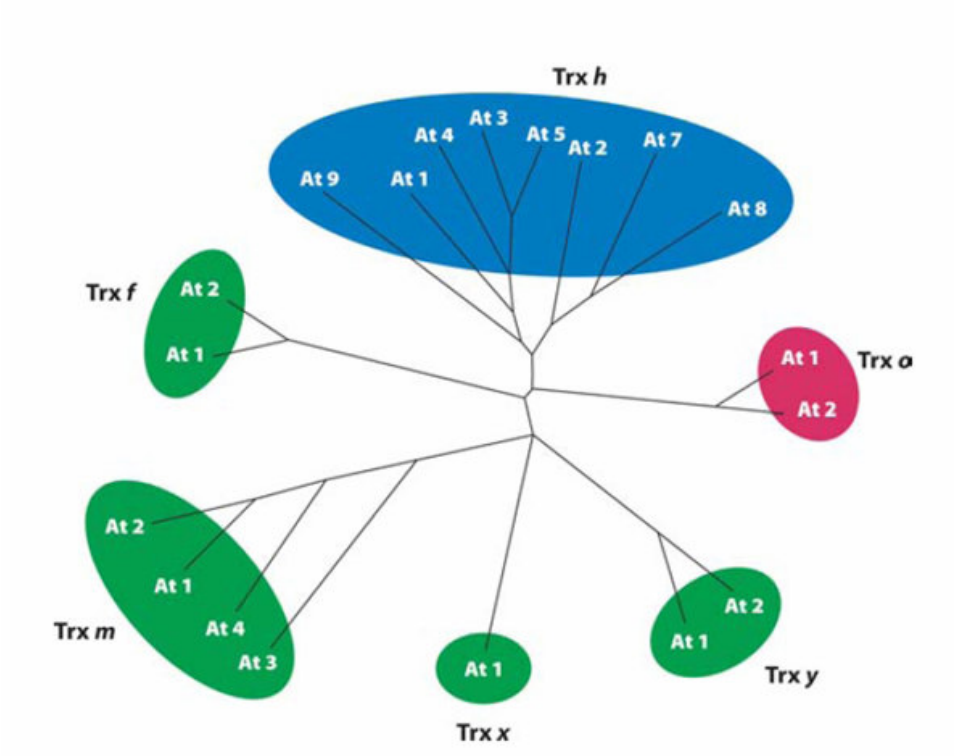

Figure 1.7. Phylogenetic tree of thioredoxins in *Arabidopsis thalina.* Thioredoxins f, m, x and y are found in the chloroplast. Thioredoxins o and h types At7 and At8 in the mitochondrion. Other members of h-type have been localized in the cytosol and ER (adapted from Buchanan and Balmer, 2005).

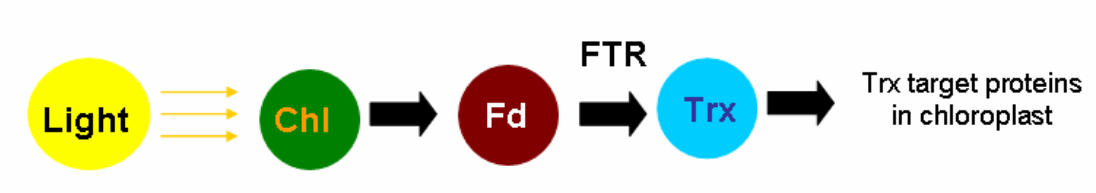

Figure 1.8. Ferredoxin (Fd) /thioredoxin (Trx) system in chloroplasts.

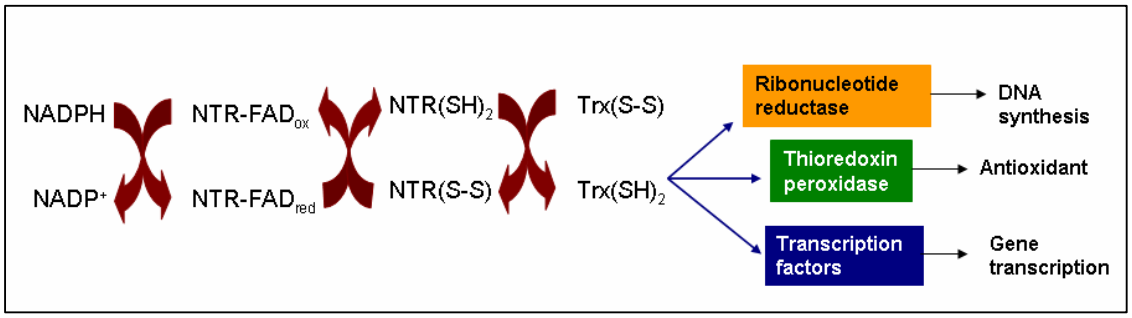

Figure 1.9. NTR/Trx system. Electrons flow from NADPH through FAD to the active site disulfide bond in NTR and then to the active site disulfide bond in Trx. Trx in turn acts as electron donor to Trx target proteins such as ribonucleotide reductase which reduces ribonucleotide to deoxyribonucleotide for DNA synthesis, Trx peroxidase, and transcription factors.

1.5.3.1. Trx h

Trx h was originally found in nonphotosynthetic tissues. However, a number of Trx h have been isolated from both nonphotosynthetic and photosynthetic tissues in Arabidopsis (Rivera-Madrid et al., 1995). Trx h similar to other types of Trxs has the following secondary structure: β1, α1, β2, α2, β3, α3, β4, β5, α4. Trx h structure presents only one major difference compared to the model of other Trx types, namely one elongated α1 helix (Schürmann and Jacquot, 2000).

Trx h receives electrons from NADPH via NTR and then acts as electron donor to many other proteins. Historically it was thought that there are a limited number of Trx targets. However in recent years the list of putative Trx target proteins identified using proteomics techniques has been growing (Yano et al., 2002, Kulmer et al., 2004).

For reduction of protein disulfides, the surface exposed thiol group of N-terminal cysteine in the active site (WC_NG/PPC_C) of reduced Trx carries out the initial nucleophilic attack to form a transient intermolecular disulfide bond. Then the C-terminal cysteine subsequently attacks the transient disulfide bond and releases the reduced substrate with formation of a disulfide bond in Trx (Kallis and Holmgren, 1980).

In plants several isoforms of Trx h are involved in a NTR/Trx system. A few of them were found to be targeted to specific subcellular locations including a mitochondrial Trx h in poplar (*Populus spp*; Gelhaye et al., 2004). The Arabidopsis genome encodes eight h-type Trx. With the possible exception of AtTrxh7 and AtTrxh8, they are thought to be cytosolic (Gelhaye et al., 2005). In proteome analysis of barley seeds two Trx h with 51% identity were identified and termed HvTrxh1 and HvTrxh2 (Maeda et al., 2003). Barley Trxh1 and Trxh2 both have typical fold of Trxs consisting of five stranded central β-sheet surrounded by four α-helix (Fig. 1.10, Maeda et al., 2008).

The presence of several isoforms of Trx h in plants has raised the question of whether different isoforms have different physiological roles. However to date there has been little success in assigning specific functions to each isoform of Trx h in Arbidopsis or other plants. The recent studies have shown that AtTrxh1 and AtTrxh4 are more correlated with the cell cycle, suggesting a role in redox control of cell proliferation. Other studies recently have shown that AtTrxh1 functions in reducing of cytosolic malate dehydrogenase (MDH; Hara et

al., 2006) and AtTrxh5 is specifically required for sensitivity to *Cochliobolus Victoria,* a fungal pathogen that causes victoria blight (Teresa et al., 2007).

1.5.3.2. NTR

Thioredoxin reductases (TRs) belong to the flavoenzyme oxidoreductase family. The essential cofactor of flavoproteins is derived from riboflavin, which consists of the isoalloxazine ring system with a ribityl side chain attached to the central *N*-10 position in the pyrazine moiety (Macheroux, 1999). This precursor is phosphorylated at the 5'-hydroxyl group by flavokinase to yield flavin mononucleotide (FMN). In a second ATP-dependent reaction, flavin adenine dinucleotide pyrophosphorylase attaches an AMP moiety to FMN yielding flavin adenine dinucleotide (FAD) (Fig 1.11). In addition to the noncovalent binding of the flavin to the protein, covalent linkage to an amino acid residue via positions of isoalloxazine ring system has been observed in some flavoproteins (Mewies et al., 1998). In fact, the structural component of flavin cofactor is responsible for light absorption in the UV and visible spectral range of the flavin and flavoproteins and giving them yellow color. TRs exist in all living cells. There is a remarkable difference in structure and mechanism between TR from vertebrates and mammals on the one hand and prokaryotes like bacteria, eukaryotes like yeast or plants on the other hand (Holmgren, 2008).

The gene encoding TR1 from human placenta is the first cloned mammalian TR. TR1 with 500 residues has a monomeric molecular weight of 54.6 kDa and exhibits 31% amino acid sequence identity with prokaryotic TRs but 44% identity with GRs (Gasadaska et al., 1995). Mammalian TRs have three domains: NADP-binding domain, FAD-binding domain and an interface domain. The redox-active site disulfide is located in the FAD-binding domain.

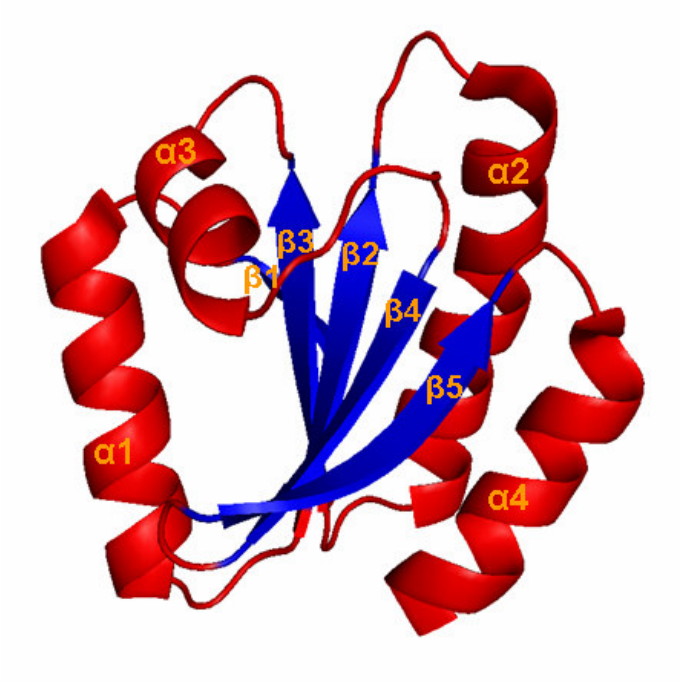

Figure 1.10. The Crystal structure of barley Trxh2 (PDB code: 2iwt). The secondary structures β-sheet (blue) and α-helix (red) have been indicated.

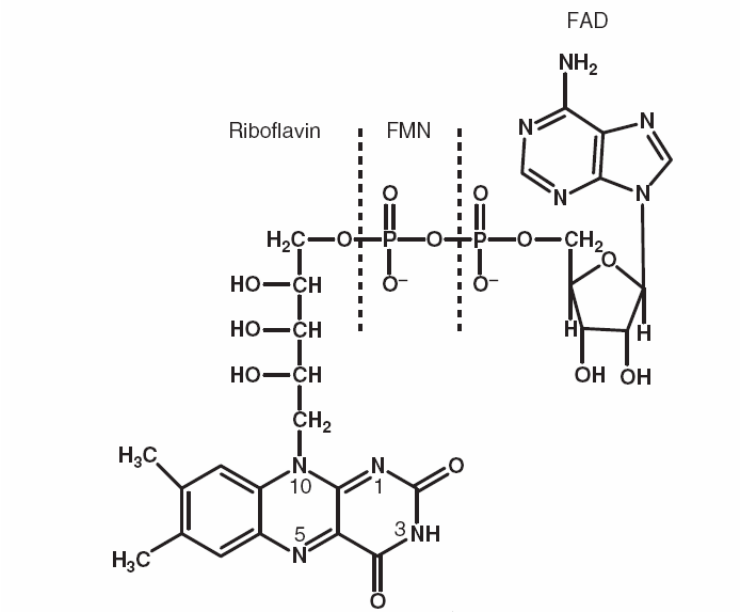

Figure 1. 11. Structure of riboflavin, flavin mono nucleotide (FMN) and flavin adenine dinucleotide.

Mammalian TRs are selenoenzymes since they have a Cys-SeCys-Gly at their C-terminal where SeCys is selenocysteine (Gladyshev et al., 1996).

The bacterial, plant and fungi TRs are homodimers consisting of 310-330 amino acids in each monomer and with a monomeric molecular weight of about 35 kDa. The crystal structure of Arabidopsis NTR-B is the only structure available for plant NTR (Fig 1.12). Arabidopsis NTR-B and *E. coli* TR exhibit 45% sequence identity and they are structurally similar. In the crystal structure of Arabidopsis NTR-B each subunit has two domains, FAD- and NADP-binding domain. A non-covalently bound FAD-molecule is formed in the FAD-binding domain and the conserved active site sequence CAT(V)CD is located in the NADP-binding domain (Dai et al., 1996).

The Arabidopsis genome encodes three types of NTR (NTR-A, B, C). The initially identified NTR-B efficiently reduces cytosolic Trx type-h (Jacquot et al., 1994). NTR-A is translated from two different mRNAs: the shorter transcript produces a cytosolic form of NTR-A, while the longer and less-abundant transcript is translated to a protein product that is localized in the mitochondrion (Laloi et al., 2001). The third NTR-C contains an extended N-terminal with an additional Trx-like active site and is localized in chloroplasts (Serrato et al., 2004). The identification of NTR-C in chloroplasts suggested the presence of a NTR/Trx system in addition to Fd/Trx system, which may allow reduction of Trxs in dark and independently from photosynthetic electron transport (Brehelin et al., 2004).

1.5.3.3. NTR/Trx function in plants

The NTR/Trx system regulates different systems in plants via thiol redox control. Redox control processes involve changes in activity of an enzyme, a receptor or a transcription factor via dithiol/disulfide exchange reactions. In mitochondria the role of this system has been

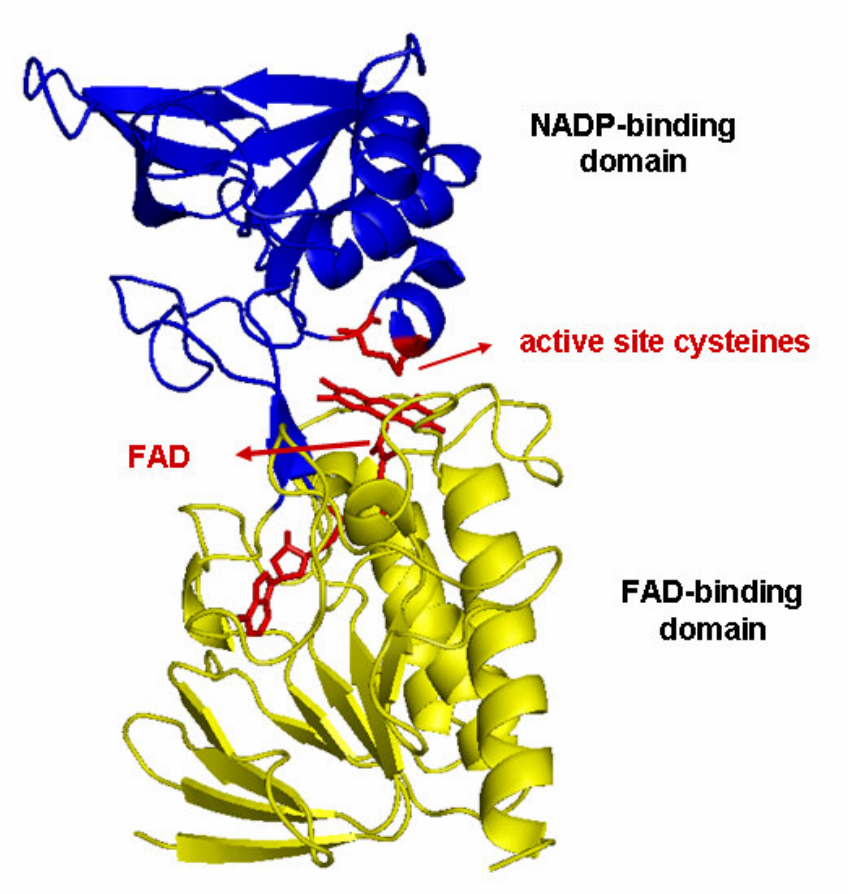

Figure 1.12. Crystal structure of AtNTR-B (PDB code:1vdc). Active site cysteines and the bound FAD molecule are shown in stick display and colored red. FAD- and NADP-binding domain are shown in cartoon display and colored yellow and blue, respectively.

linked to many fundamental process such as photorespiration, citric acid cycle and associated reactions, lipid metabolism, electron transport, ATP synthesis/transformation, translation, protein assembly/folding, nitrogen metabolism, sulfur metabolism, hormone synthesis and stress-related reactions (Buchanan and Balmer, 2005). In the cytosol of plant cells this system might be involved in detoxification of H_2O_2 via the enzyme thioredoxin peroxidase or peroxiredoxin, since peroxiredoxin has been isolated as *in vivo* target of Trx h in yeast by stabilization of a mixed disulfide intermediate (Verdoucq et al., 1999).

The role of the NTR/Trx system in seed development and seed germination has been well documented. As mentioned before disulfide bonds provide an increase in stability on the one hand and decrease in solubility on the other in seed storage proteins. Both features provide protection of proteins against proteolysis. There are several reports showing that disulfide bonds in storage proteins are converted to reduced state to facilitate mobilization. The NTR/Trx system appears to play a critical role in reduction of disulfides in storage proteins in both cereal (Kobrehel et al., 1992) and legume seeds (Alkhalfioui et al., 2007b) upon germination. The inactivation of inhibitors of amylolytic enzymes, such as BASI, and activation of a calcium-dependent substrate specific protease, thiocalsin (Besse et al., 1996) are other suggested roles for this system leading to promotion of seed germination. In addition, the overexpression of Trx h in barley starchy endosperm accelerated the appearance of α-amylase in respect to both amount of enzyme and enzyme activity (Wong et al., 2002). The enhancement of GA synthesis by embryo in Trx overexpressed grains suggests that the increase of α-amylase may be partly due to the possible role of Trx h in the enhancement of the synthesis of GA by embryo. However, the acceleration of α-amylase was also observed in deembryonated Trx overexpressed grains indicating a direct effect of Trx h on the aleurone layer (Wong et al., 2002). These experiments shows that Trx h provides a communication between endosperm, embryo and aleurone layer in cereal seeds upon germination (Fig 1.13)

Trx h was found as one of the major proteins in the phloem sap of rice (Ishiwatari et al., 1995) suggesting that Trx h can act as a messenger in plants. Trx h has also role as a regulator of membrane-bound, receptor-like kinase in plants (Bower et al., 1996).

In barley seeds by application of a highly sensitive Cy5 maleimide dye, 2D-gel and MS analysis in total 16 different putative target proteins for Trx h were identified (Maeda et al., 2004). Between Trx h target proteins BASI, α-amylase/trypsin inhibitor, chitinase isoenzymes

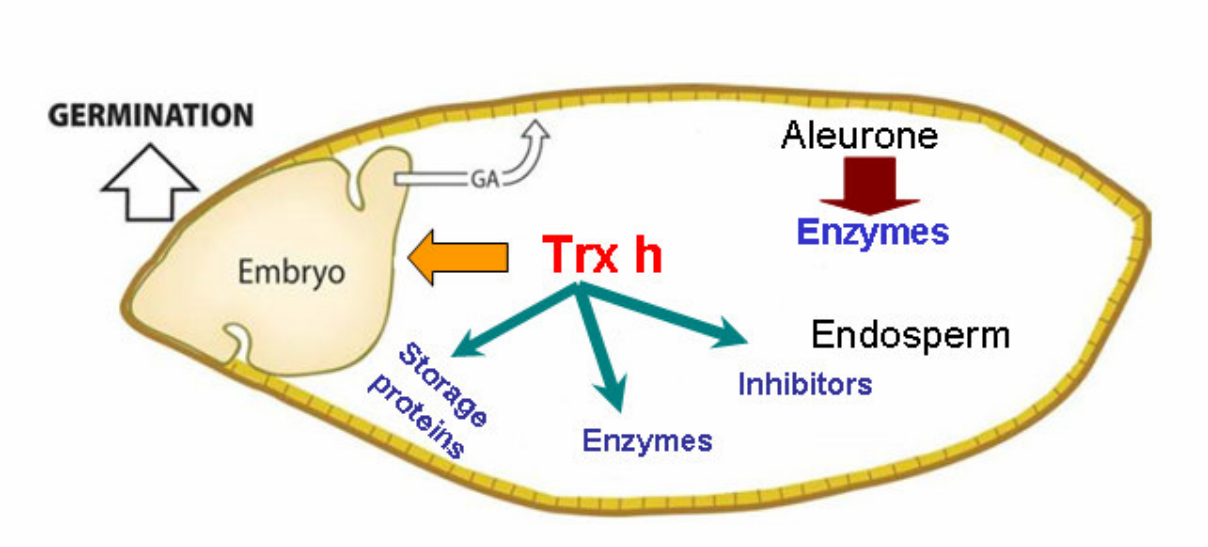

Figure 1.13. Role of Trx *h* in barley seeds. Trx h acts in the endosperm to facilitate the mobilization of nitrogen and carbon by (*a*) reducing storage proteins in the endosperm, leading to increased solubility and susceptibility to proteolysis; (*b*) inactivating small proteins that inhibit enzymes of starch degradation; and (*c*) directly reductively activating individual enzymes. Trx h also seems to function as a member of a communication network linking the endosperm to the embryo and aleurone. The increase in GA affected by Trx h is partly, but not fully, responsible for the enhanced production of hydrolytic enzymes by the aleurone layer. (adapted from Wong et al., 2002)

and lipid transfer protein 1 (LTP1) were related to seed defense. Cyclophilin was identified as Trx h target protein only in germinated seeds (72 h of germination). This protein catalyzes *cis-trans* isomerization of proline residues to accelerate protein folding. Embryo-specific proteins (ESP) and single-domain glyoxalase-like protein are other Trx h target proteins identified in this study. However, the functions of these proteins are still unknown.

In a recent study in Arabidopsis both genes encoding cytoplasmic NTR (NTR-B) and mitochondrial NTR (NTR-A) were inactivated by T-DNA insertion and thereby the role of NTR/Trx system in several plant development programs including pollen fitness, seed development and cell proliferation was evidenced (Reichheld et al., 2007). Furthermore, a

triple mutant containing homozygous *ntra ntrb* mutants together with rootmeristem less1 (*rml1*), which is disrupted in glutathione biosynthesis, provided genetic evidence of crosstalk between the GSH/Grx system and NTR/Trx system in setting up postembryonic meristematic activity (Reichheld et al., 2007).

1.5.4. ROS and antioxidants in seed biology

ROS are involved in various aspects of seed physiology. They are generated during seed desiccation, seed germination and aging. There are several sources for production of ROS/RNS in plant seeds. The mitochondrial respiratory chain is one of the major sources of ROS; electron leakage from the transport chain generates superoxide and subsequently H_2O_2 by dismutation of the former (Møller, 2001). Seed germination is associated with increased respiratory activity. Therefore, during seed germination the production of ROS is enhanced. Peroxisomes are another source of ROS; glyoxysomes, representing one type of this organelle, play a key role in mobilization of lipids in oily seeds via β-oxidation that leads to production of H_2O_2 (Huang et al., 1983). In aleurone layer of cereal seeds the lipids are reserved in large amounts. The fatty acids in aleurone layer are mobilized via β-oxidation following GA treatment leading to production of H_2O_2 as the main by-product. H_2O_2 is the main ROS that causes the aleurone layer PCD (Bethke et al., 2001). The function of NADPH oxidase in the plasma membrane, pH dependent cell-wall peroxidases, amine oxidases and finally non-enzymatic autooxidation of lipids are other potential sources of ROS in plant seeds (Bailly, 2004). If ROS are not controlled, they can lead to damage of lipids, proteins, carbohydrates and nucleic acids, resulting in seed deterioration. Therefore, the cells are endowed with detoxifying enzymes and antioxidant compounds that scavenge ROS and participate in seeds survival. The enzyme SOD that is present in mitochondrion, cytosol or

chloroplast dismutes superoxide radicals into H_2O_2 and oxygen (Bowler et al., 1992). Then H_2O_2 can be eliminated by either enzyme CAT that is located in peroxisomes and glyoxysomes (Willekens et al., 1995) or by the ascorbate-glutathione cycle. The ascorbate-glutathione cycle is a series of coupled redox reactions involving the enzymes APX, monodehydroascorbate reductase (MDHAR), dehydroascorbate reductase (DHAR) and GR which are present in cytoplasm, mitochondria, peroxisomes and the apoplasts (Noctor and Foyer, 1998). In this cycle APX converts H_2O_2 to H_2O with oxidation of ascorbate (AsA) to monodehydroascorbate (MDHA). Two molecules of MDHA can be non-enzymatically converted to dehydroascorbate (DHA) and AsA. The additional three enzymes in this cycle are involved in regeneration of AsA. The enzymes MDHAR and DHAR reduce MDHA and DHA to AsA, respectively, and GR reduces oxidized glutathione (GSSG) to reduced form (GSH) which functions as electron donor to DHAR. The enzymes GR and MDHAR use NADPH as an electron donor. The main mechanisms involved in cellular detoxification in plants are shown in Fig. 1.14.

Antioxidant mechanisms in seeds seem to control ROS rather than to eliminate them completely. This may be due to the important roles of ROS in cellular signaling pathways and their involvement in growth processes including embryogenesis during seed development and radicle protrusion during seed germination. The interplay of ROS with other molecules such as the hormone ABA suggests that ROS may be involved in many aspects of seed physiology (Bailly, 2004).

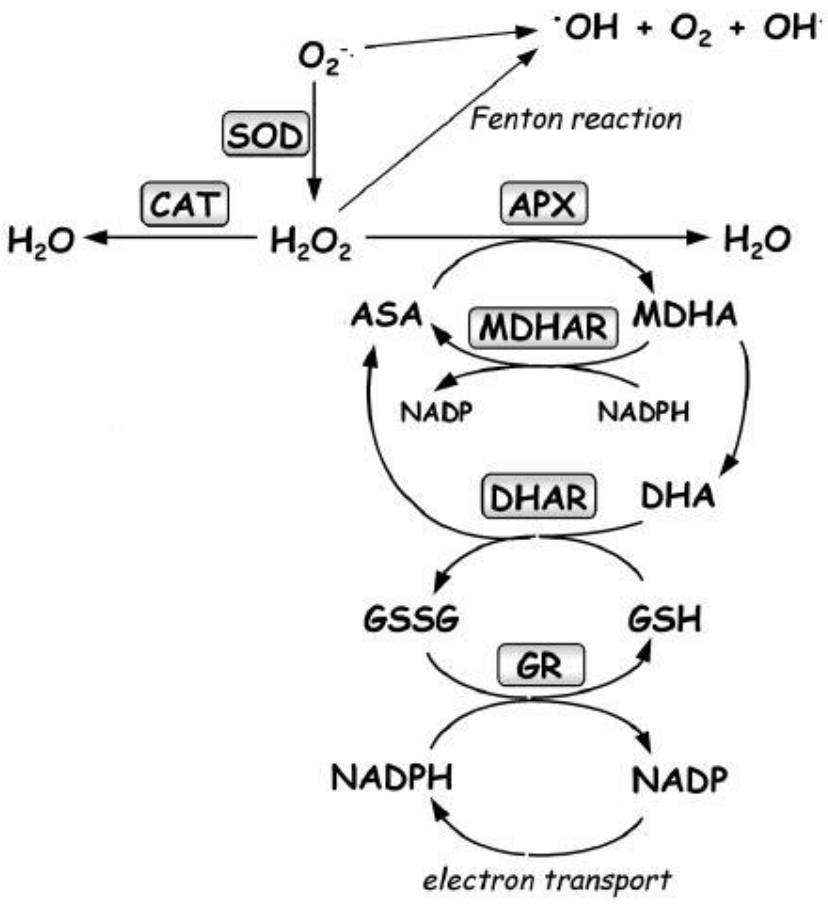

Figure 1.14. Main ROS detoxifying systems in plants. CAT, catalase; SOD, superoxide dismutase; APX, ascorbate peroxidase; MDHAR, monodehydroascorbate reductase; DHAR, dehydroascorbate reductase; GR, glutathione reductase; ASA, ascorbate; MDHA, monodehydroascorbate; DHA, dehydroascorbate; GSSG, oxidized glutathione; GSH, reduced glutathione (adapted from Bailly at al., 2004).

1.6. Objectives of the present study

Chapter 2- Hormonal-dependence of transcript accumulation, protein synthesis and release from barley aleurone layer

The cereal aleurone layer is a model system for studying the regulation of transcription and protein appearance by GA and ABA. DNA microarray analysis in recent years has provided a comprehensive and global view of transcript expression accompanying the GA and ABA responses in barley aleurone layer (Bethke et el., 2006; Chen and An, 2006), but the effect of these hormones in regulation of many genes and their corresponding proteins are still unknown. In the present study, we aimed to monitor the transcript profile and spatio-temporal pattern of proteins α-amylase, LD, α-glucosidase as important temporal markers for the events of germination. The dissected aleurone layers were therefore maintained in culture medium with or without addition of GA/ABA. In addition to the intracellular protein fractions, this system enabled analysis of the release of hydrolytic enzymes, since these accumulate in the culture medium. Therefore, the aleurone layer system was carefully characterized with respect to analyze these marker genes. This provided a frame work for study of other proteins and their corresponding genes including proteins involved in the NTR/Trx system.

Chapter 3- NTR/Trx system in germinating barley seeds: gene expression, protein profiles and interactions between isoforms of thioredoxin h and thioredoxin reductase

The NTR/Trx system has been proposed to function in seed germination, defense against pathogens and oxidative stress by reducing disulfide bonds in a variety of target proteins. Two isoforms of the plant cytosolic Trx h were previously identified in the barley seed proteome, the genes encoding them were cloned and recombinant proteins produced and characterized (Maeda et al., 2003). The *in vivo* activity of Trx h, however, depends on its reduction by

NTR in the presence of NADPH. In the present study we aimed to use a combination of protein profiling on 2D-gels, transcript profiling and functional characterization of NTR and Trx isoforms in dissected embryo during germination and aleurone layer in response to hormonal signals. This led to isolation and cloning of genes encoding two NTR isoforms from barley seed (HvNTR1 and HvNTR2). Subsequently the production of recombinant proteins allowed the first study of reciprocal interactions between NTR and Trx h isoforms from the same organism.

Chapter 4- Interaction between thioredoxin h (Trx h) and NADPH-dependent thioredoxin reductase (NTR) from barley studied by site directed mutagenesis

The cloning and heterologous expression of both NTR and Trx h isoforms provided a basis for design and characterization of mutants to investigate the interaction between NTR and Trx h at the level of molecular structures. We aimed to identify the critical residues which are involved in barley NTR-Trx h interaction. We also observed that barley NTR has much lower affinity (more than 100-fold) towards *E. coli* Trx compared to HvTrx isoforms, indicating the existence of interaction specificity between NTR and Trx from the same organism. Therefore, we were interested to determine the residues which may function in determining barley NTR-Trx h interaction specificity. In addition, the role of residues in Trx h which was previously shown to be involved in recognition of Trx target proteins (Maeda et al., 2006a), was examined in barley NTR-Trx h interaction.

Chapter 2: Hormone-dependence of transcript accumulation, protein synthesis and release from barley aleurone layer

2.1. Summary

Cereal seed germination involves mobilization of the storage reserves in the starchy endosperm necessary to support seedling growth. The aleurone layer plays a key role in germination by responding to hormone signals from embryo and producing hydrolases that are secreted into the starchy endosperm for degradation of storage products. In the present work, the transcript profiles and spatio-temporal patterns of α-amylase, limit dextrinase (LD), α-glucosidase and α-amylase/subtilisin inhibitor (BASI) were monitored in dissected aleurone layers from barley (*Hordeum vulgare*) seeds incubated for different times (6-72 h) in the presence of the hormones gibberellic acid (GA) and abscisic acid (ABA). The release of the proteins from the aleurone layer to the culture supernatant was also monitored by immunoblotting and the timing of the release of LD was found to differ from that of α-amylase and suggested to depend on the programmed cell death (PCD). The release of both α-glucosidase and α-amylase from aleurone layer to culture supernatant, however, was observed before PCD. The proteins studied here, all appeared in multiple spots on 2D-western blots that may stem from the presence of multiple isoforms of these proteins or/and their post-translational modifications.

2.2. Introduction

In cereal seeds the carbohydrates and proteins stored in the dead starchy endosperm cells are mobilized during germination for use by the developing seedling (see review Ritchie et al., 2000). Upon imbibition, the aleurone layer cells, which remain alive in the mature grain, synthesize and secrete a range of enzymes including hydrolases for degradation of the storage products in endosperm (Mundy and Rogers, 1986) and for depolymerization of endosperm cell walls (Caspers et al., 2001). Complete hydrolysis of starch, the major carbohydrate reserve in cereal seeds, is resulted from the action of four enzyme types: α-amylase is the key enzyme attacking α-1,4-glucosidic bonds to produce a range of linear and branched maltodextrins; β-amylase removes maltose from the non-reducing ends of maltodextrins and starch polymers; the debranching enzyme limit dextrinase (LD), also known as pullulanase, catalyses hydrolysis of α-1,6-glucosidic bonds which are resistant to attack by α-amylase (Sun and Henson, 1991); α-glucosidase (maltase) converts maltose to glucose (Nakai et al., 2006). Despite β-amylase that is synthesized during seed development (Hara-Nishimura et al., 1986; Shewry et al., 1988), *de novo* synthesis of hydrolases involved in starch degradation is induced in aleurone layer in response to gibberellic acid (GA) from embryo after seed imbibition. Abscisic acid (ABA) has an antagonist effect on the GA action and suppresses expression of genes encoding hydrolytic enzymes in aleurone layer (Ho et al., 2003). However, ABA stimulates expression of many genes that may function in stress tolerance and seed dormancy (Ho et al., 2003). In a microarray analysis in deembryonated barley *(Hordeum vulgare*) aleurone layer treated with ABA for 15 h, approximately 2.5-fold more genes were up-regulated than down-regulated (Chen et al., 2006).

Most of the hydrolytic enzymes synthesized in aleurone layer are anticipated to be secreted into the starchy endosperm. In the secretory pathway, proteins travel from endoplasmic

reticulum (ER) where the signal peptide is removed and the protein is *N*-glycosylated and folded. Then proteins are transported to the Golgi apparatus and loaded in vesicles for transfer to the plasma membrane and/or vacuole. Finally, the transport vesicles fuse with the plasma membrane and their contents are released to the outside of the cell (Sharova, 2002). The release of hydrolases from aleurone cell wall is facilitated by wall channels and plasmodesmata (Gubler et al., 1987). The aleurone layer is programmed to die after completion of its secretory function. The programmed cell death (PCD) in aleurone layer is stimulated with GA, but postponed by ABA (Bethke et al., 1999).

Isolated aleurone layer provides a unique system for analysis of plant signaling because i) aleurone layer does not synthesize endogenous hormones, but can respond strongly to exogenous GA or ABA ii) aleurone layer composed of one living cell type responding to hormones uniformly iii) aleurone layer can be easily separated from other seed tissues iv) aleurone layer can be maintained and manipulated in culture medium.

In the present study, isolated aleurone layers were maintained in culture medium. This isolated system enabled monitoring of effects of GA and ABA on the protein appearance patterns of hydrolytic enzymes involved in starch degradation as well as barley α-amylase/subtilisin inhibitor (BASI). The aleurone layer cultures allowed analysis of both intracellular proteins and the release of hydrolytic enzymes accumulating in the culture supernatant. In parallel, the mRNA accumulation was analyzed of genes encoding these proteins. In the present study, the expression pattern of α-amylase, which has well been documented was used as a reference to enable comparison with other studies. The data presented here provide new insights for understanding the role of aleurone layer in regulation of starch degradation in the endosperm and form the basis for monitoring the changes in aleurone layer transcriptome and proteome in response to hormones.

2.3. Results

2.3.1. The changes in amount of total soluble protein in aleurone layer

The soluble proteins were extracted from the same amount of aleurone layer treated with GA (AL-GA), ABA (AL-ABA) or buffer without hormones (AL-O) at different time points (6-72 h). The amount of total soluble protein extracted from AL-ABA and AL-GA was similar to that from AL-O up to 24 h. After 48 h the amount of total protein significantly decreased in AL-GA compared to that from AL-O and AL-ABA (Fig. 2.1A). The amount of total soluble protein decreased in all samples after 72 h.

These changes in total extractable soluble protein across samples were also visualized by SDS-PAGE, where equal volumes of aleurone layer extracts were loaded (Fig. 2.1B). The culture supernatants from incubations with GA (SN-GA), ABA (SN-ABA) or no hormones (SN-O) were also harvested and equal volumes from different samples were loaded on SDS-PAGE. The analysis of culture supernatants is considered to show the proteins released from aleurone layers into the starchy endosperm. This is a very important property of the aleurone layer culture system that is difficult to analyze in intact seeds. The total soluble protein in SN-GA and SN-ABA was low and similar to that in SN-O up to 24 h. However, after 48 and 72 h incubation the total soluble protein in SN-GA was higher than that in SN-O and SN-ABA (Fig. 2.1B).

The comparison of the total soluble proteins in the aleurone layer with that of the culture supernatant revealed that a substantial amount of soluble proteins are released from aleurone layer extreated with GA after 48 h incubation. Accordingly, a previous study has shown that

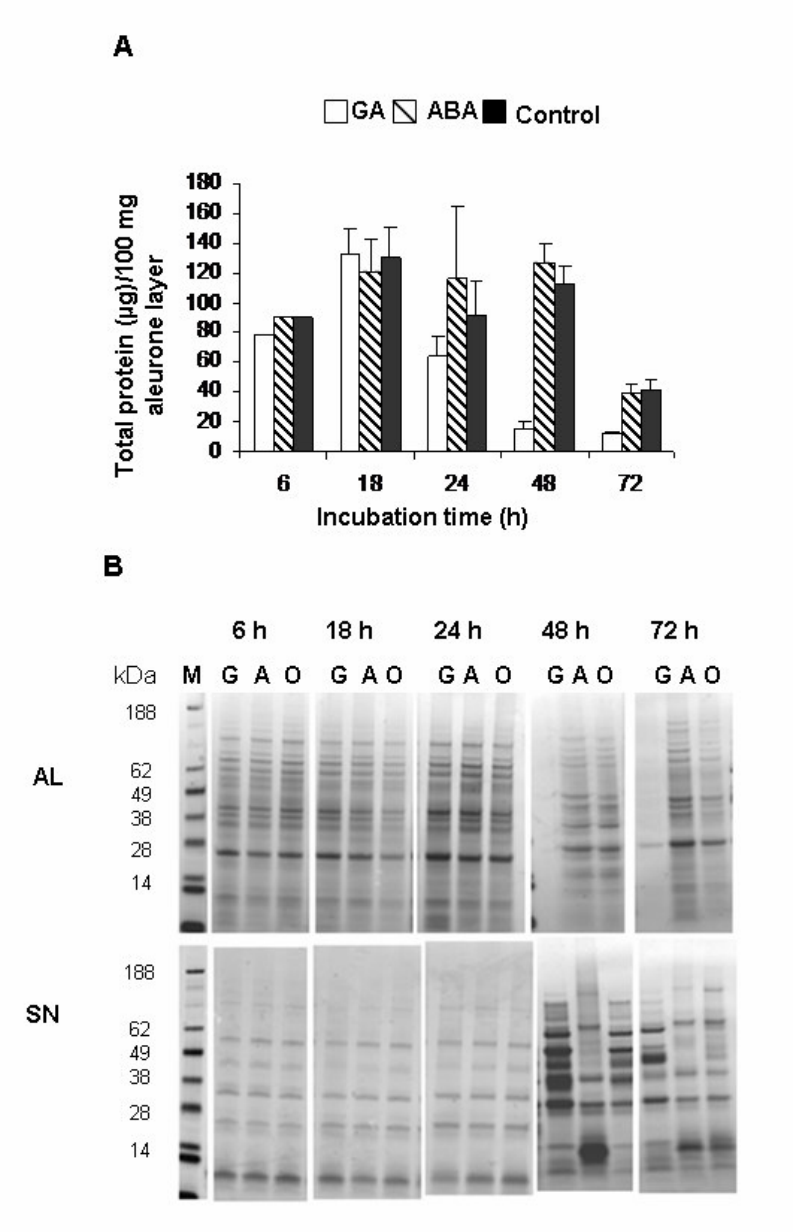

Figure 2.1. Changes in total extractable soluble protein in dissected aleurone layer (AL) and released proteins into culture supernatants (SN) after treatment with GA (G), ABA (A) and no hormones (O) during incubation (6-72 h). A, The total soluble protein was extracted from aleurone layer and the protein concentration was determined. Each histogram represents the mean ± SD obtained from five independent experiments. B, Equal volumes (10 µl) of protein extracts from aleurone layer or culture supernatant were loaded on SDS-PAGE and stained with Coomassie Brilliant Blue.

the aleurone layer cells remain viable during the first 24 h incubation in GA. Death of cells begins after 24 h incubation in 5 µM GA and almost all cells die during the subsequent 24 h (Bethke et al., 2002). Therefore, the release of interacellular proteins after prolonged incubation in GA may stem from a PCD-regulated disintegration of aleurone cells which is stimulated with GA but postponed by ABA.

2.3.2. Protein appearance pattern and transcript profiling

2.3.2.1. α-amylase

Northern blot analysis was performed using equal amounts of total RNA purified from AL-GA, AL-ABA and AL-O at various time points (6-72 h). Before hybridization blots were stained in methylene blue and two sharp bands representing plant ribosomal RNA (18S and 25S) were observed in all samples (Fig. 2.2A) except in aleurone layers incubated for 72 h in which the ribosomal bands appeared with lower molecular mass. This may suggest that RNA in aleurone layer is degraded after prolonged incubation.

The DNA probe was prepared from the α-amylase isozyme 2 (AMY2) coding sequence. However, due to high identity (~80%) between genes encoding isoforms of two subfamilies (AMY1 and AMY2), the northern blot analysis represents a combination of transcript profiles from several isoforms of both subfamilies. mRNA transcripts were detected in 12 h AL-GA, increased up to 18 h and then decreased (Fig. 2.2A). This pattern was in agreement with transcript profile of α-amylase obtained using RT-PCR. The RT-PCR analysis also represents a combination of transcript profiles from all genes encoding α-amylase since the primers were designed from conserved region in all barley α-amylase nucleotide sequences available in the NCBI database (Fig. 2.2B). α-amylase transcripts were not detected with northern blotting in AL-ABA or AL-O (data not shown), but low levels of α-amylase transcripts in these samples

were detected using RT-PCR (Fig. 2.2B) which is more sensitive than northern blotting. This is in agreement with a previous study showing that low levels of α-amylase transcripts are present in aleurone layers before treatment with GA (Rogers, 1985).

At the protein level, α-amylase was detected in both aleurone layer and culture supernatants at the early time points of incubation (6 h) with GA, and its abundance increased up to 48 h (Fig. 2.2C), but decreased after 72 h which could be due to decrease in total soluble protein at this time point. Low levels of α-amylase were detected in AL-ABA and AL-O which increased after 48 h. No α-amylase however, was detected in SN-ABA and SN-O. It should be noted that western-blot profiles for α-amylase in this study represent the combination of all isoforms in both α-amylase isozyme subfamilies 1 and 2.

Several α-amylase spots appeared on 2D-western blot between pI 5-6.2 in 24 h AL-GA suggesting the appearance of multiple isoforms of both AMY1 (theoretical pI 4.2-5.2) and AMY2 (theoretical pI 5.9-6.6) subfamilies (Fig. 2.2D). In agreement, in a study in our group using 2D-gel and mass spectrometry four isoforms of α-amylase were identified in 10 spots in aleurone layer treated with GA (Finnie et al., unpublished data). In addition, 29 2D-gel spots containing products from one and two genes encoding α-amylase 1 and α-amylase 2, respectively were identified in barley germinated seeds (Bak-Jensen et al., 2007).

A few numbers of spots that appeared in 24 h AL-GA were also observed with low intensity in 24 h AL-ABA and 24 h AL-O indicating the presence of low amounts of α-amylase in aleurone layer before treatment with GA in agreement with the results from 1D-western blotting and RT-PCR as explained above.

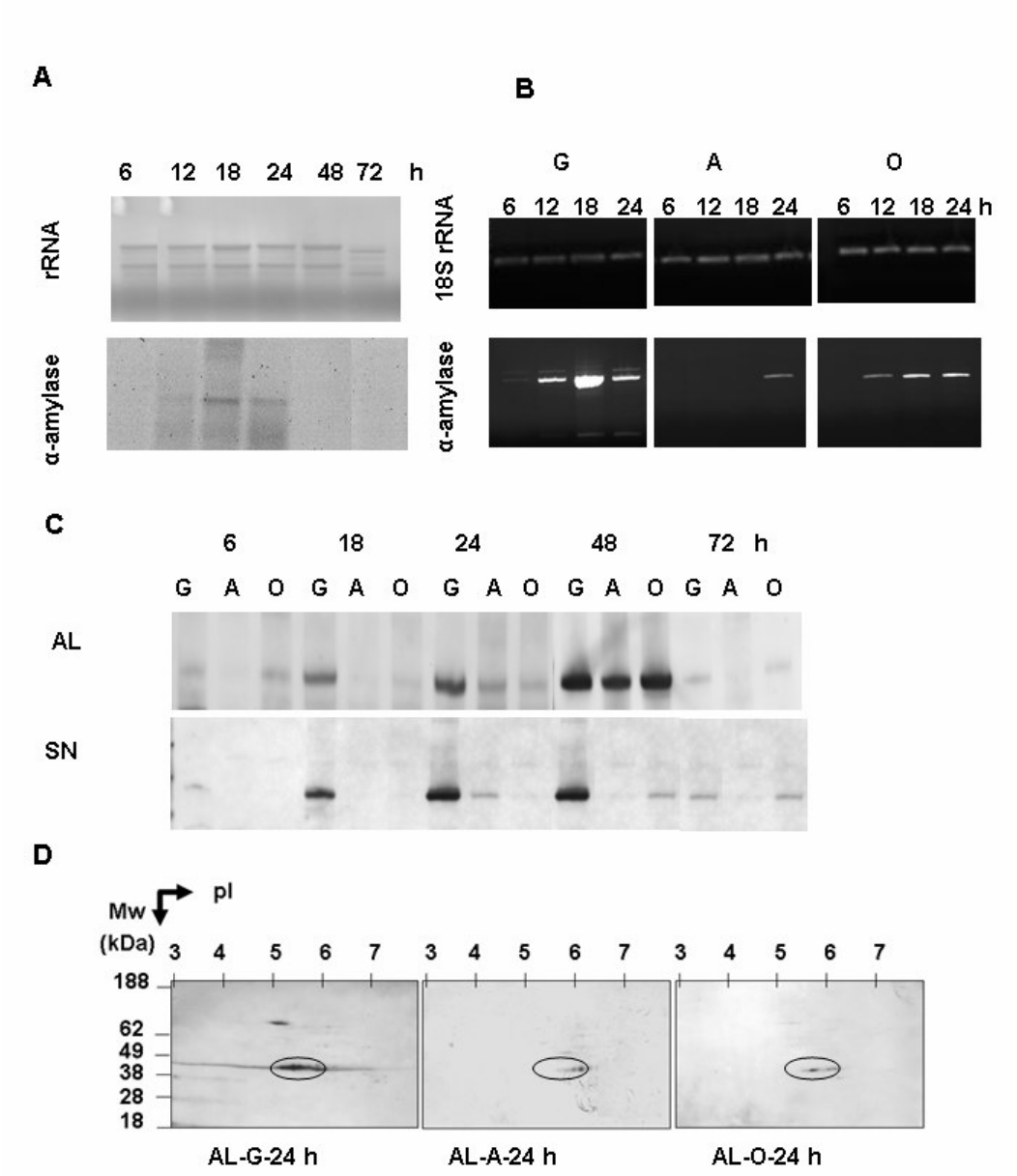

Figure 2.2. Time-course study of transcript profiling and protein appearance pattern of α-amylase in aleurone layer (AL) and culture supernatant (SN) treated with GA (G), ABA (A) and no hormones (O) during incubation (6-72 h). A, Northern blot analysis with total RNA extracted from AL-GA. The blot before hybridization was stained with methylene blue showing small and large subunits of rRNA that was used as an equal loading control. B, RT-PCR analysis of α-amylase**.** 18S rRNA was equally expressed across samples and used as control. C, 1D-western blot analysis of α-amylase. D, 2D-western blot analysis of α-amylase in 24 h AL-GA, AL-ABA and AL-O. The circles show the position of α-amylase spots. The appearance of extra spots is due to the poor specificity of antibody.

2.3.2.2. LD

LD mRNA transcripts were detected in12 h AL-GA and their abundance increased up to 24 h and then decreased (Fig. 2.3A). No LD mRNA transcripts were detected in AL-ABA and AL-O showing that the expression of LD is stimulated with GA. The transcript profile of LD obtained here is in agreement with that reported by Burton and co workers (1999).

The LD protein was detected in 18 h AL-GA and its abundance increased during incubation up to 48 h and then decreased at 72 h (Fig. 2.3B). This decrease was due to decrease in total soluble protein extracted from aleurone layer at this time point. LD was not detected in AL-ABA or AL-O up to 24 h, but it was detected in considerable amount in 48 h AL-ABA and AL-O. This may stem from the presence of LD synthesized and stored in insoluble form during seed development (Burton et al., 1999; Sissons et al., 1993) that may be converted gradually to a soluble and extractable form during incubation. In agreement, a previous study has shown that LD is synthesized first in inactive bound form and converted to active free form during germination (Longstaff et al., 1993).

The release of LD from aleurone layer into the culture supernatant happened after 48 h incubation in GA, much later than its detection inside of aleurone layer (Fig. 2.3B). At this time point, it is likely that the AL-GA is undergoing PCD and releases most of its protein contents. A low level of LD was also detected in 48 h SN-O, while LD was not detected in 48 h SN-ABA. This also supports a PCD-dependent release of LD that is postponed by ABA treatment.

The protein LD appeared in several spots with pI 5-6 in 24 h AL-GA (Fig. 2.3C). The presence of a single LD gene in barley genome suggested by a southern blot analysis (Kristensen et al., 1999) may exclude the presence of multiple isoforms in different spots. Therefore, the multiple spots may stem from post-translational modifications. In agreement

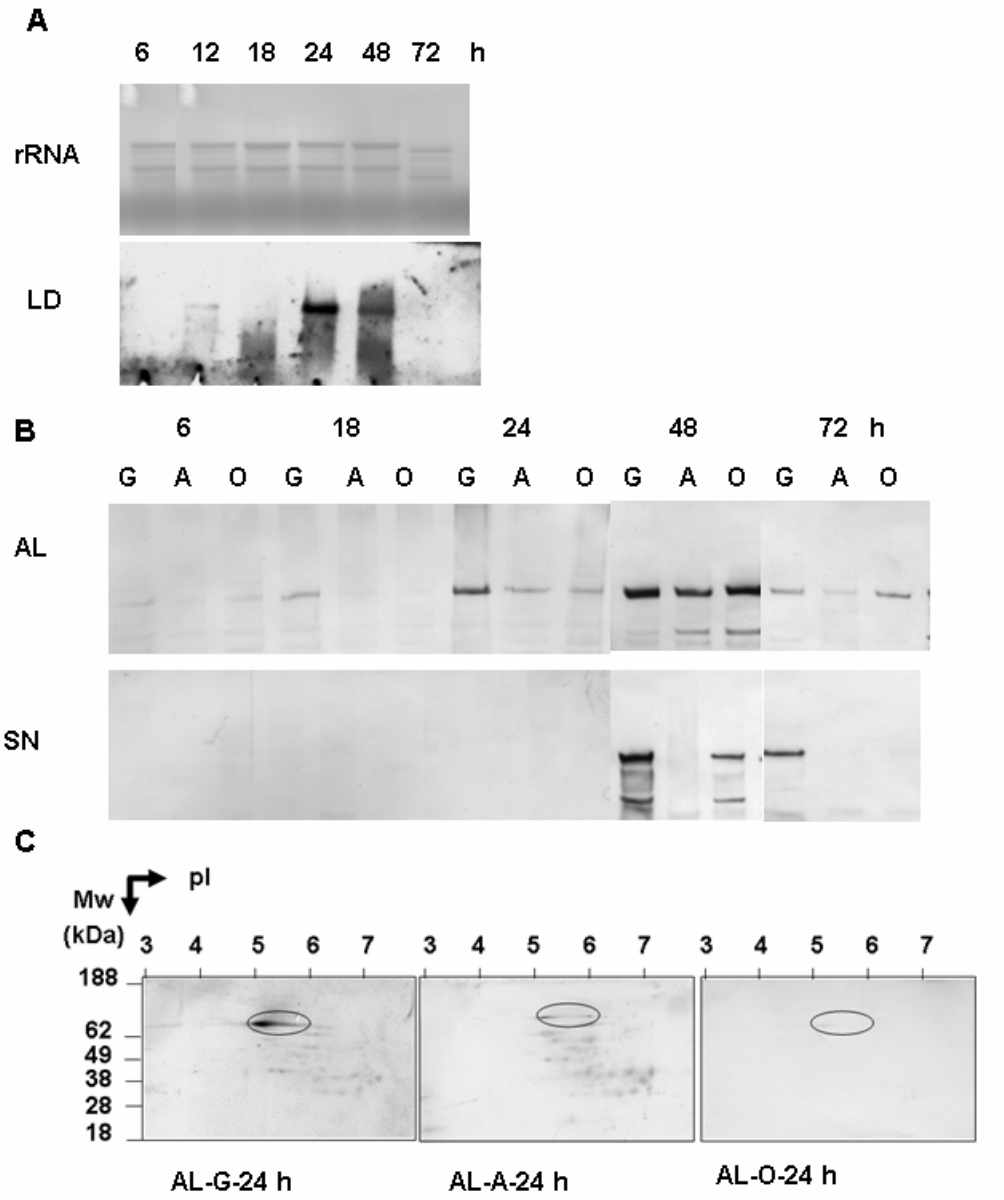

Figure 2.3. Time-course study of transcript profiling and protein appearance pattern of LD in aleurone layer (AL) and culture supernatant (SN) treated with GA (G), ABA (A) and no hormones (O) during incubation (6-72 h). A, Northern blot analysis with total RNA extracted from AL-GA at various time points (6-72 h). The blot before hybridization was stained with methylene blue showing small and large subunits of rRNA that was used as an equal loading control. B, 1D-western blot analysis of LD C, 2D-western blot analysis of LD at 24 h AL-GA, AL-ABA and AL-O. The circles show the position of LD spots. The appearance of extra spots is due to drgradation of LD or/and poor specificity of antibody.

with 1D-western blot the intensity of LD spots was very low in 24 h AL-ABA and 24 h AL-O compared to that in 24 h AL-GA.

2.3.2.3.α-glucosidase

mRNA transcripts encoding α-glucosidase were detected in 12 h AL-GA and the abundance increased up to 18 h and followed by a slight decrease up to 48 h (Fig. 2.4A). No α-glucosidase mRNA transcripts were detected in AL-ABA or AL-O indicating that the expression of α-glucosidase in aleurone layer is stimulated with GA.

Detection of α-glucosidase protein in aleurone layer extracts was failed even with using 10 µg of aleurone layer extracts (4-fold of the total protein that was normally loaded for analysis of the other proteins in this study). However, α-glucosidase was detected in low amounts in 24 h and 48 h SN-GA, using 10 µg of total protein (Fig. 2.4B), but it was not detected in SN-ABA or SN-O. Due to the inability to detect α-glucosidase in aleurone layer intracellular, the sensitivity of the anti-α-glucosidase antibody was compared with that of the anti-α-amylase antibody. The anti-α-glucosidase recognized 1 ng of purified recombinant α-glucosidase, whereas the amounts lower than 5 ng of purified recombinant α-amylase were not detected by anti-α-amylase suggesting a higher sensitivity for anti-α-glucosidase compared to anti-α-amylase. Therefore the lack of α-glucosidase detection in aluerone layer may stem either from the presence of α-glucosidase in a low level in aleurone layer as compared to α-amylase or from rapid release of protein into the culture supernatant. However, the activity of this enzyme in aleurone layer extracts after treatment with GA has been previously reported (Tibbot et al., 1998).

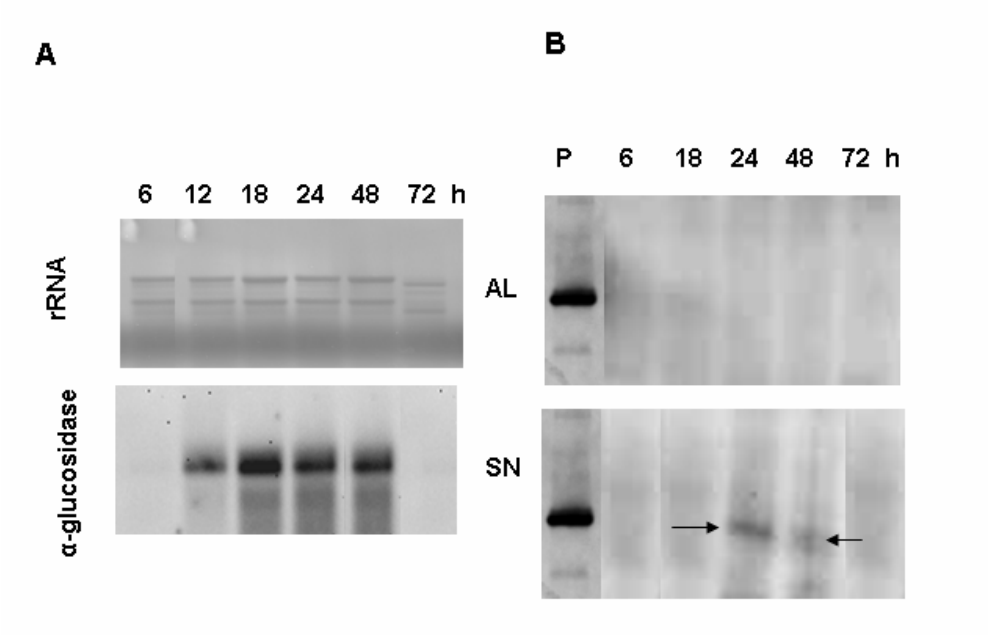

Figure 2.4. Time-course study of transcript profiling and Protein appearance pattern of α-glucosidase in aleurone layer (AL) and culture supernatant (SN) treated with GA (G), ABA(A) and no hormones (O) . A, Northern blot analysis with total RNA extracted from AL-GA at various time points (6-72 h). The blot before hybridization was stained with methylene blue showing small and large subunits of rRNA that was used as an equal loading control. B, 1D-western blot analysis of α-glucosidase in aleurone layer and culture supernatants after treatment with GA at various time points (6-72 h). Purified recombinant α-glucosidase (P) was loaded as positive control.

2.3.2.4. BASI

Barley α-amylase/subtilisin inhibitor (BASI) is an endogenous inhibitor synthesized in the barley seeds and encoded by the the *asi* gene. Although the physiological function of this protein has not completely been understood, it is known that BASI selectively inhibits the high-pI group of α-amylase (Mundy et al., 1983; Weselake et al., 1983). Another function of this protein is apparently associated with defense of the plant against bacterial serine protease that is called subtilisin (Mundy et al., 1983).

In a transient gene expression assay in which the *asi* promoter was studied using a gene encoding green fluorescent protein (*gfp*) as reporter, GA and ABA had no effect on the *gfp*

expression (Furtado et al., 2003). By contrast, in dissected aleurone layers BASI mRNA accumulation was promoted by ABA and reduced by GA as opposed to effect of these hormones on expression of α-amylase (Mundy and Rogers, 1986). However, in the present study BASI was detected at similar levels in AL-GA, AL-ABA and AL-O up to 24 h (Fig. 2.5A), suggesting that the appearance of BASI is not affected with GA or ABA. BASI was not detected in 48 h and 72 h AL-GA but observed in both AL-ABA and AL-O at these time points. This may stem from the decrease in total protein in aleurone layer extracts after long time treatment with GA.

BASI was detected in similar levels in 6-24 h SN-GA, SN-ABA and SN-O (Fig. 2.5A), and was accumulated in larger amounts after 48 and 72 h. However, the presence of BASI in culture supernatant does not only reflect the portion released from aleurone layers, but can also be originated from residual starchy endosperm in aleurone layer preparations, as BASI is abundant in barley seed endosperm (Bak-Jensen et al., 2004; Finnie et al., 2006).

The BASI protein appeared in two weak and one intense spots with pI 7.0-7.7 in 24 h AL-O, AL-ABA and AL-GA (Fig. 2.5B). However, the question of whether these spots are different isoforms or they are arising from post-translation modification is still remaining to be answered.

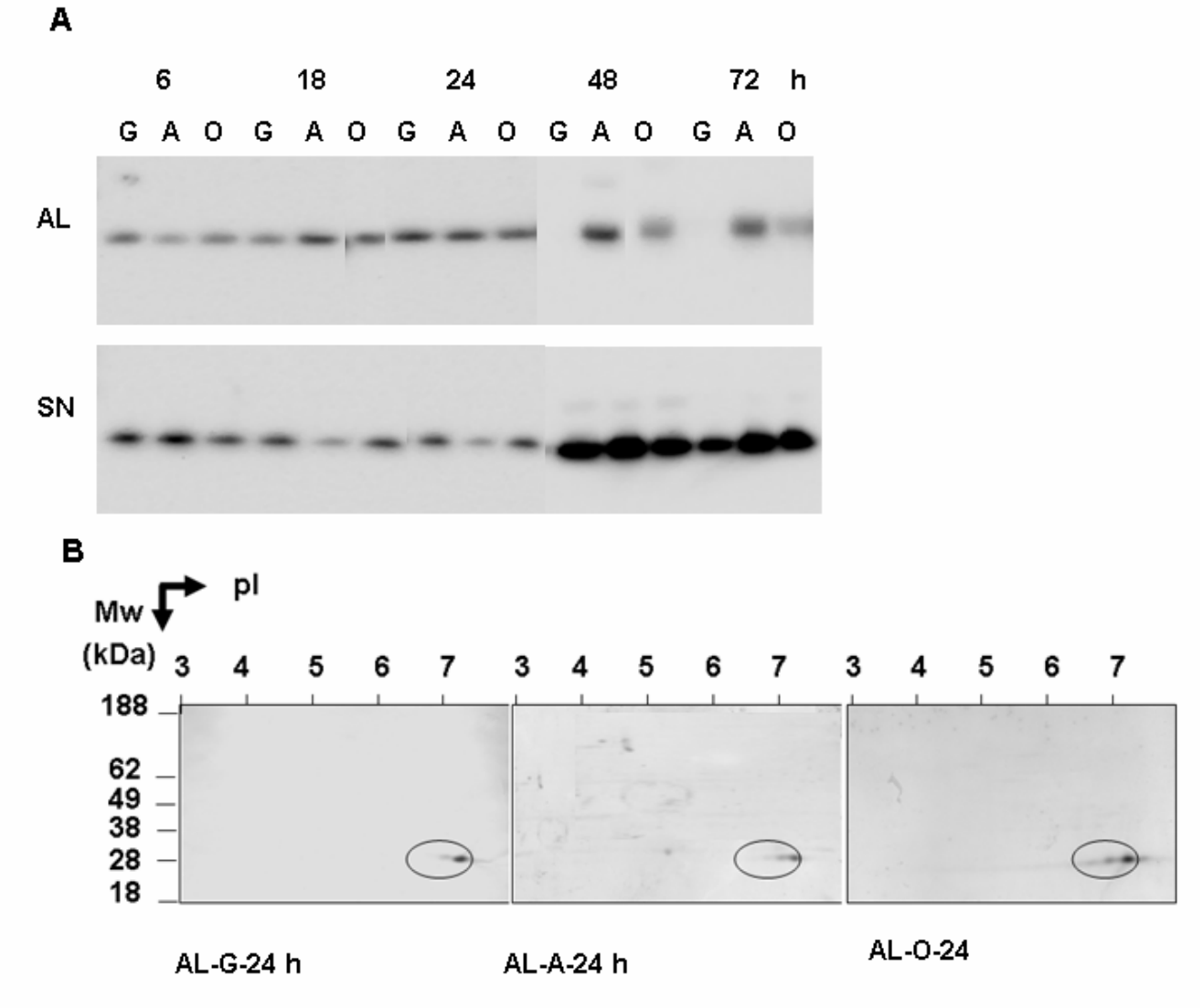

Figure 2.5. Time-course study protein appearance pattern of BASI in aleurone layer (AL) treated with GA (G), ABA (A) and no hormones (O). A, 1D-western blot analysis of BASI in dissected aleurone layer from dry seeds (D), treated aleurone layer and culture supernatants (SN) at various time points (6-72 h). C, 2D-western blot analysis of BASI at 24 h AL-GA, AL-ABA and AL-O. The circles show the position of BASI spots

2.4. Discussion

The present study confirms that genes encoding α-amylase, LD and α-glucosidase necessary for starch degradation in barley seed endosperm are induced in aleurone layer at the initial hours of incubation with GA. Accordingly, α-amylase and LD proteins were detected in the aleurone layer after treatment with GA with a slightly later appearance of LD compared to α-amylase. However, a significant difference was observed in the timing of appearance of these two enzymes in culture supernatants representing proteins released from the aleurone layer. Whereas α-amylase appeared in the culture supernatant at the same time as it was detected in the aleurone layer intracellular (6 h), the release of LD to the culture supernatant was delayed by 48 h, suggesting different mechanisms may be involved in the release of these two enzymes from the aleurone layer to the starchy endosperm. The enzyme α-amylase has a primary role in degradation of starch in endosperm whereas LD has a secondary role in starch hydrolysis. Therefore, the priority of the release of these two enzymes seems to be in agreement with their role in starch degradation.

Barley α-amylase in aleurone layers contains an N-terminal signal peptide and is proposed to be routed in a secretion pathway after synthesis. Secretion of α-amylase across the plasma membrane is an energy dependent process while the passage of this enzyme across the cell wall is diffusion-limited (Varner and Mense et al., 1972) and depends on the presence of cations like Ca^{2+} (Benjamin and Jones et al., 1982). However, LD in contrast to proteins destined for the secretory pathway does not carry signal peptide targeting proteins to the endoplasmic reticulum (ER). A 78-amino acid leader sequence at the N-terminus of LD was found to be similar to transit peptides that target the polypeptides to plastids rather than the ER (Burton et al., 1999). Here we demonstrate that LD is released from aleurone layer cells after 48 h incubation in GA corresponding to time point when the PCD has extensively

progressed and almost all of the aleurone layer cells have died (Bethke et al., 2002). Therefore, the release of LD from aleurone layer seems to be dependent on PCD in aleurone layer. This is supported by the fact that LD did not appear in culture supernatants from aleurone layers incubated with ABA since PCD is postponed by ABA in aleurone layer. Noticeably, the release of endo-β-1,4-xylanase, required for the degradation of the inner cell wall of aleurone layers coincides with PCD, tissue integrity is thus maintained until secretion of α-amylase and other hydrolases is completed (Caspers et al., 2001). By contrast, enzymes like β-glucanase that are involved in the degradation of endosperm cell walls and the initial degradation of aleurone layer outer cell walls, are the first enzymes to be released from aleurone layer (Fincher, 1992).

The enzyme α-glucosidase was found to be synthesized at low levels compared to α-amylase and LD in aleurone layer. The release mechanism of this enzyme from aleurone layer is similar to that of α-amylase, since it appeared in the culture supernatant during the first 24 h incubation with GA.

Here we also demonstrated that the appearance of BASI is not affected by GA or ABA at least at the level of protein appearance. The role of BASI in inhibition of high pI α-amylase (AMY2) is important with regard to premature sprouting and protection of seed against subtilisin-like proteases from pests or pathogens (Mundy et al., 1983). However, BASI may have role in modulating starch hydrolysis during seed germination.

Moreover the present study enabled comparison of the transcript profiling of genes with the corresponding protein patterns in aleurone layer. The accumulation of α-amylase and LD mRNA in GA-treated aleurone layer peaks after 18 h and 24 h, respectively, whereas synthesis of enzymes encoded by these genes peaks after 48 h. These differences may be due to the higher stability of proteins than mRNA transcripts.

By following the protein appearance patterns on 2D-western blotting, all of enzymes studied here were found in several spots. Further work, however, is required to determine whether different spots contain different isoforms or if they are the same isoform with different post-translational modifications.

2.5. Materials and Methods

2.5.1. Plant material

Seeds from barley cultivar Himalaya were purchased from Washington State University, Pullman, WA, U.S.A. The embryo-containing part of the seeds was removed using a scalpel. The embryoless half grains were soaked for four days in sterile water with 50 µg/ml ampicillin and 5 µg/ml nystatin. The endosperm was scraped away from the aleurone layers and 100 mg (fresh weight) aleurone layers were incubated in 2 ml buffer (20 mM $CaCl_2$, 20 mM Na succinate pH 4.2, 50 µg/ml ampicillin, 5 µg/ml nystatin). Where required, either 5 µM GA or ABA was added. Incubation was performed at room temperature for 6-72 h with continuous gentle shaking. Aleurone layers were harvested at various time points, washed four times with incubation buffer without antibiotics or hormones, frozen in liquid nitrogen and stored at -80 ^{o}C until use. For analysis of released protein from aleurone layer the culture supernatants were collected, centrifuged for 10 min at 12,000 rpm to remove debris, transferred to new tubes and stored at -80 ^{o}C for later analyses.

2.5.2. Protein extraction

Frozen aleurone layers (100 mg fresh weight) were dried under vacuum and ground to a fine powder using a pre-cooled ceramic mortar and pestle. The powder was resuspended in 580 µl ice cold extraction buffer (5 mM Tris HCl, 1 mM $CaCl_2$, pH 7.5) containing of protease

inhibitor cocktail "complete" (Roche) and transferred to an eppendorf tube. Two glass beads were added to aid homogenization of the tissue. The samples were shaken for 30 min at 4 ^{o}C. and were centrifuged at 18000 × g for 30 min at 4 ^{o}C to pellet debris. Supernatants (500 µl) were transferred to clean tubes. Protein concentrations were determined by the Popov assay (Popov et al., 1975) with bovine serum albumin (BSA) as standard.

2.5.3. 1D-gel electrophoresis and western blotting

For SDS-PAGE analysis and western blotting 10 µl of aleurone layer extracts or culture supernatanrs were separated on 4-12% Bis-Tris NuPAGE gels (Novex system, Invitrogen) with NuPAGE MES running buffer (Invitrogen). Gels were stained with colloidal Coomassie Brilliant Blue G-250 (Candiano et al., 2004). For western blotting separated proteins on the gel were transferred to a nitrocellulose membrane (Hybond-N, GE Healthcare) using the Novex system (Invitrogen) according to the manufacturer's instructions. The blots were blocked overnight in TBST (150 mM NaCl, 25 mM Tris-HCl, pH 7.5, 0.1% [v/v] Tween 20). Primary antibodies: rabbit anti-α-amylase raised against barley AMY2 (customer preparation, DAKO A/S, Denmark), rabbit anti-LD (Kristensen et al., 1998), rabbit anti-α-glucosidase (Næsted et al., unpublished) or mouse anti-BASI (Rodenburg et al., 1995), were diluted in 1:1000 in TBST. The antigen-antibody interaction was carried out at room temperature for one hour. The blots were washed (3 × 10 min) in TBST and were probed with secondary antibodies conjugated with alkaline phosphatase (AP) or horseradish peroxidase (DAKO Cytomation) diluted 1:2000 in TBST. After washing the membrane (3 × 10 min) in TBST, the immunoblots were developed using nitro blue tetrazolium/bromochloro indolyl phosphate colorimetric method or enhanced chemiluminescence (Thorpe and Kricka, 1986).

2.5.4. Determination of sensitivity of primary antibodies

The antibody efficiency was tested for anti-α-glucosidase and anti-α-amylase using dot blotting and purified recombinant barley α-glucosidase and barley α-amylase, respectively. The recombinant proteins were diluted to give final concentrations in the range of 1 ng/µl to 500 ng/µl. The diluted proteins were dotted onto nitrocellulose membrane strips using 1 µl volume for each dot and one dot without protein for negative control. The membrane strips were allowed to dry, blocked overnight in TBST, and probed with a different dilution of primary antibody in TBST (1:2000-1:1000). The blots were then washed, incubated with secondary antibody, and developed as above.

2.5.5. 2D-western blotting

Protein extracts from 100 mg (fresh weight) aleurone layers were desalted on a NAP^{TM}-5 column (GE, Healthcare) in extraction buffer (5 mM Tris HCl, 1 mM $CaCl_2$, pH 7.5). After determination of protein concentration, 10 µg protein was precipitated using 0.1 M ammonium acetate in methanol (Vensel et al., 2005) and resuspended in reswelling buffer (7 M urea, 2 M thiourea, 2% [v/v] CHAPS, 0.5 % [v/v] immobilized pH gradient [IPTG] ampholytes 3-10 [Amersham Bioscience, 1.2% [v/v] Destreak reagent [hydroxyethyl disulfide], and a trace of bromophenol blue) as described (Finnie et al., 2002). First dimension electrophoresis was carried out using 11 cm immobilized linear pH gradiant IPG strips, pI 3-10, on an IPGphor (Amersham Biosciences). After isoelectric focusing, IPG strips were equilibrated as previously described (Finnie et al., 2002). For the second dimension, the IPG strips were cut to give 7 cm covering pI 3-8. The NuPAGE Novex 4-12% Bis-Tris Zoom Gel (Invitrogen) with NuPAGE MES running buffer (Invitrogen) were used for SDS-PAGE

according to the manufacturer's instructions. Western blotting was performed as described above.

2.5.6. DNA labeling

The plasmids PHIL-D2-AMY2 (Juge et al., 1996), pET11a-LD (Jensen et al., Unpublished) and pPIC9K/α-Glc (Næsted et al., 2006) were purified using HiSpeed Plasmid Midi Kit (Qiagen). The purified plamids containing coding sequences for enzymes AMY2 (AAA98790), LD (AAF98802) and high pI α-glucosidase (AAF76254) were digested with restriction enzymes *Bam*HI-*Eco*RI, *Nde*I-*Bam*HI, and *Eco*RI-*Avr*II, respectively to excise the inserts. DNA probes were prepared with the random primed labeling method using DIG High prime DNA labeling and detection starter Kit II (Roche) and the labeling efficiency was tested according to the manufacturer's instructions.

2.5.7. RNA extraction

Total RNA was extracted from 50 mg (fresh weight) aleurone layer using the RNeasy plant mini kit (Qiagen) and treated with RNase–Free DNase set (Qiagen) to remove any contaminating genomic DNA. The total RNA was quantified by the UV absorbance at 260 nm.

2.5.8. Northern blotting

Purified total RNA (6 µg) was separated on a denaturing agarose/formaldehyde gel and transferred under RNase-free conditions onto a positively charged nylon membrane (Roche). RNA was fixed to the membrane by UV cross-linking. The blotted RNA was stained with

0.02% methylene blue, 0.3 M Na acetate, pH 5.5 for 3 min. The stained RNA was controlled for RNA quality and equal loading of different samples before hybridization.

Blots were prehybridized with pre-heat Dig Easy Hyb (Roche) for 30 min at 50 ^{o}C. The heat denatured DNA probes were added to hybridization buffer in a final concentration of 50 ng/ml. Hybridization was carried out overnight in a hybridization oven at 50 ^{o}C. The unbound DIG-labeled DNA was removed by post-hybridization washes as follows: membranes were washed twice with 2 × SSC (0.3 M NaCl, 0.03 M Na Citrate) containing 0.1% SDS for 5 min at room temperature followed by two washes with 0.1% SSC containing 0.1% SDS at 50 ^{o}C for 15 min. Blots were immunodetected with anti-DIG-AP and visualized with by chemiluminescence substrate CSPD according to the procedure described by the manufacturer's instruction (Roche).

2.5.9. RT-PCR analysis

RT-PCR was performed in a PTC-200 DNA Engine Peltier Thermal cycler (BioRad) using the one step RT-PCR kit (Qiagen). The RT-PCR mixture was set up according to the manufacturer's recommendations using 0.6 μM of each primer and 100 ng total RNA as starting material. Barley 18S rRNA showing invariant expression across the samples was amplified in parallel. The optimum number of amplification cycles for each set of primers was determined at the exponential phase range of amplification. To control for possible presence of genomic DNA contamination, parallel reactions were carried out where reverse transcriptase activity was inactivated by starting the reaction at 95 ºC. One negative control lacking template RNA was included for each set of RT-PCR reactions.

The primers were 5´-CTACGTCCCTGCCCTTTGTACA-3´and 5´-ACACTTCACCGGAC CATTCAA-3´ for analysis of 18SrRNA and 5´-AGCGGCG GGTGGTACAACAT-3´ and 5´-AGCCTTGCATGACCTTGTCG-3 for analysis of α-amylase.

Chapter 3: The NADPH-dependent thioredoxin reductase/ thioredoxin system in germinating barley seeds: gene expression, protein profiles, and interactions between isoforms of thioredoxin h and thioredoxin reductase

3.1. Summary

The NADPH-dependent thioredoxin reductase (NTR)/thioredoxin (Trx) system catalyzes disulfide bond reduction in the cytoplasm and mitochondrion. Trx h is suggested to play an important role in seed development, germination, and seedling growth. Plants have multiple isoforms of Trx h and NTR; however, little is known about the roles of the individual isoforms. Trx h isoforms from barley (*Hordeum vulgare*) seeds (HvTrxh1 and HvTrxh2) were characterized previously. In this study, two NTR isoforms (HvNTR1 and HvNTR2) were identified, enabling comparison of gene expression, protein appearance, and interaction between individual NTR and Trx h isoforms in barley embryo and aleurone layers. Although mRNA encoding both Trx h isoforms is present in embryo and aleurone layers, the corresponding proteins differed in spatiotemporal appearance. HvNTR2, but not HvNTR1, gene expression seems to be regulated by gibberellic acid. Recombinant HvNTR1 and HvNTR2 exhibited virtually the same affinity toward HvTrxh1 and HvTrxh2, whereas HvNTR2 has slightly higher catalytic activity than HvNTR1 with both Trx h isoforms, and HvNTR1 has slightly higher catalytic activity toward HvTrxh1 than HvTrxh2. Notably, both NTRs reduced Trx h at the acidic conditions residing in the starchy endosperm during germination. Interspecies reactions between the barley proteins and *Escherichia coli* Trx or *Arabidopsis thaliana* NTR, respectively, occurred with 20- to 90-fold weaker affinity. This

first investigation of regulation and interactions between members of the NTR/Trx system in barley seed tissues suggests that different isoforms are differentially regulated but may have overlapping roles, with HvNTR2 and HvTrxh1 being the predominant isoforms in the aleurone layer.

3.2. Introduction

Thioredoxins (Trxs) are small, ubiquitous proteins participating in thiol-disulfide reactions via two Cys residues found in a conserved active-site motif (CXXC; Jacquot et al., 1997). A wide range of genes encoding Trx have been identified in plants, as opposed to animals, fungi, and bacteria. Trxs are classified based on primary structures and subcellular localization. Trxs f, m, x, and y are found in the chloroplast, whereas Trxs o and h are localized to the cytoplasm or mitochondrion (Gelhaye et al., 2004). Trx f is reduced by ferredoxin-thioredoxin reductase (Hirasawa et al., 1999). In contrast, Trx o and two large Trx h subgroups are reduced by NADPH via NADPH-dependent thioredoxin reductase (NTR; Laloi et al., 2001; Gelhaye et al., 2004). Finally, a new Trx h subgroup, first reported in poplar (*Populus* spp.; Gelhaye et al., 2003), is reduced via the glutathione/glutaredoxin system.

NTRs belong to a superfamily of flavoprotein disulfide oxidoreductases (Reichheld et al., 2005) and transfer electrons from NADPH to the active-site disulfide bridge of oxidized Trx h via FAD and a redox-active disulfide (Mustacich and Powis, 2000). NTRs from plants, bacteria, fungi, and archaea are homodimers of 35 kDa (Dai et al., 1996), whereas mammalian NTRs are homodimers of 55 kDa, usually containing an active-site seleno-Cys (Tamura and Stadtman, 1996). The NTR/Trx system in plants has a variety of functions. Trx h was suggested to act as a signal in the phloem sap (Ishiwatari et al., 1995) and it was reported to participate in the self-incompatibility reaction (Cabrillac et al., 2001). In addition, Trx h

functions during seed development (Serrato and Cejudo, 2003). Many of the Trx h target proteins identified in cereal seeds suggest that cellular redox-regulated processes are necessary for germination. Thus, the NTR/Trx system may control the activity of α-amylase and trypsin inhibitors (Kobrehel et al., 1991), increase activity of pullulanase (limit dextrinase) that specifically cleaves α-1,6 linkages from starch amylopectin (Cho et al., 1999), reduce storage proteins, facilitating their mobilization (Kobrehel et al., 1992), and activate a seed-specific Ser protease, thiocalsin (Besse et al., 1996). Finally, enhancement of gibberellic acid (GA) synthesis in embryos and accelerated appearance of α-amylase in transgenic barley overexpressing Trx h in the starchy endosperm suggest that Trx h plays a role in the communication between endosperm, embryo, and aleurone layer (Wong et al., 2002).

The presence of multiple Trx h and NTR isoforms in plants makes the NTR/Trx system particularly complex compared with other organisms. For instance, in Arabidopsis (*Arabidopsis thaliana*), eight genes encoding Trx h have been identified (Meyer et al., 2002, 2005) and three NTR isoforms have been characterized (Serrato et al., 2004; Reichheld et al., 2005). Five Trx h (Gautier et al., 1998; Serrato et al., 2001; Cazalis et al., 2006) and one NTR (Serrato et al., 2002) were described from wheat (*Triticum aestivum*). In barley (*Hordeum vulgare*), two seed Trx h isoforms were characterized (Maeda et al., 2003), but no barley NTR was identified until now.

The mechanisms regulating expression of Trx h and NTR in seed tissues are poorly understood; indeed, specific isoforms of Trx h and NTR may be localized in different tissues and have diverse roles during plant development. Expression of Trx h in endosperm seems to be controlled by hormones via the embryo (Lozano et al., 1996). Furthermore, an increase of Trxh1, Trxh2, and Trxh3 transcripts at the beginning of seed desiccation and a transient increase of Trxh1 after seed imbibition were observed in wheat (Cazalis et al., 2006). Others

reported that Trx h (Marx et al., 2003) and NTR (Montrichard et al., 2003) increase during germination in the embryo of barley and pea (*Pisum sativum*), respectively.

Knowledge lags behind on the individual roles played by Trx and NTR isoforms from the same organism. In particular, insight is lacking on specificity and structural requirements for interactions between NTRs and Trxs. To address these fundamental questions, two barley NTR isoforms are cloned and characterized in this work and their gene expression and protein appearance in seed tissues are described in parallel with two Trx h isoforms. The effects of GA and abscisic acid (ABA) on the members of this NTR/Trx system were monitored in isolated aleurone layers. Production of all four proteins in recombinant form allowed the interactions between isoforms of Trx h and NTR from the same source to be characterized.

3.3. Results

3.3.1. Isolation, cloning, and sequence analysis of two cDNAs encoding NTR

Two cDNAs encoding NTR in barley seeds were isolated by a PCR-based cloning strategy. Each contained an open reading frame of 996 bp encoding proteins designated HvNTR1 and HvNTR2 with theoretical molecular mass (kDa)/pI of 34.818/5.7 and 34.793/5.7, respectively. Nucleotide sequences of HvNTR1 and HvNTR2 are very similar to tentative consensus (TC) sequences TC142091 and TC141301 from The Institute for Genomic Research (TIGR) barley gene index. One additional sequence in the database (TC132362) showed lower identity with HvNTR1 and HvNTR2, but was still related to NTR. TCs were assembled from few EST sequences, indicating that NTR transcripts are not highly represented in barley cDNA libraries. It therefore cannot be excluded that barley has other NTR isoforms than the three discussed here. The EST sequences originated predominantly from seed tissues.

HvNTR1 and HvNTR2 proteins have 88% sequence identity. A multiple alignment, including the protein sequence deduced from TC132362 and NTR sequences from other sources (Appendix 1), was used to generate a phylogenetic tree (Fig. 3.1). The tree is divided into three major clusters. One cluster contains NTR from cyanobacteria and plant chloroplast-type (C-type) NTRs that have an extra Trx active-site sequence (CGPC) in a C-terminal extension (Serrato et al., 2004; Alkhalfioui et al., 2007a). The second cluster has two main branches; one contains fungal NTRs and the other contains plant cytoplasmic or mitochondrial type NTRs (A/B type; Reichheld et al., 2005), which are further subdivided into sequences from monocots and dicots. Bacterial NTRs constitute the third cluster. HvNTR1 and HvNTR2 belong to the monocotyledon subgroup of the plant A/B type. Despite their high sequence identity, both have even higher similarity to other cereal NTRs. HvNTR1 is thus 97% identical with wheat NTR (TaNTR) and HvNTR2 is 91% identical to a putative rice (Oryza sativa) NTR (Os1; see Fig. 3.1). HvNTR1 and HvNTR2 are each 75% identical to an Arabidopsis NTR (At3; Fig. 3.1). Barley enzymes are thus expected to share tertiary and quaternary structure with Arabidopsis NTR—the only plant NTR for which the three-dimensional (3-D) structure has been solved (Dai et al., 1996).

Plant NTRs are homodimers with each subunit containing an FAD- and an NADP-binding domain. HvNTR1 and HvNTR2 contain both FAD-binding motifs GXGXXA and TXXXXVFAAGD (residues 17–22 and 283–293, respectively), the NADP-binding motif GXGXXA (residues 164–169), and the two active-site Cys residues in the motif CAVC (residues 145–148). A C-terminal extension containing an additional Trx active site, characteristic for C-type NTRs, is present in the third, NTR-related sequence in barley TC132362 (Hv3; Fig. 3.1).

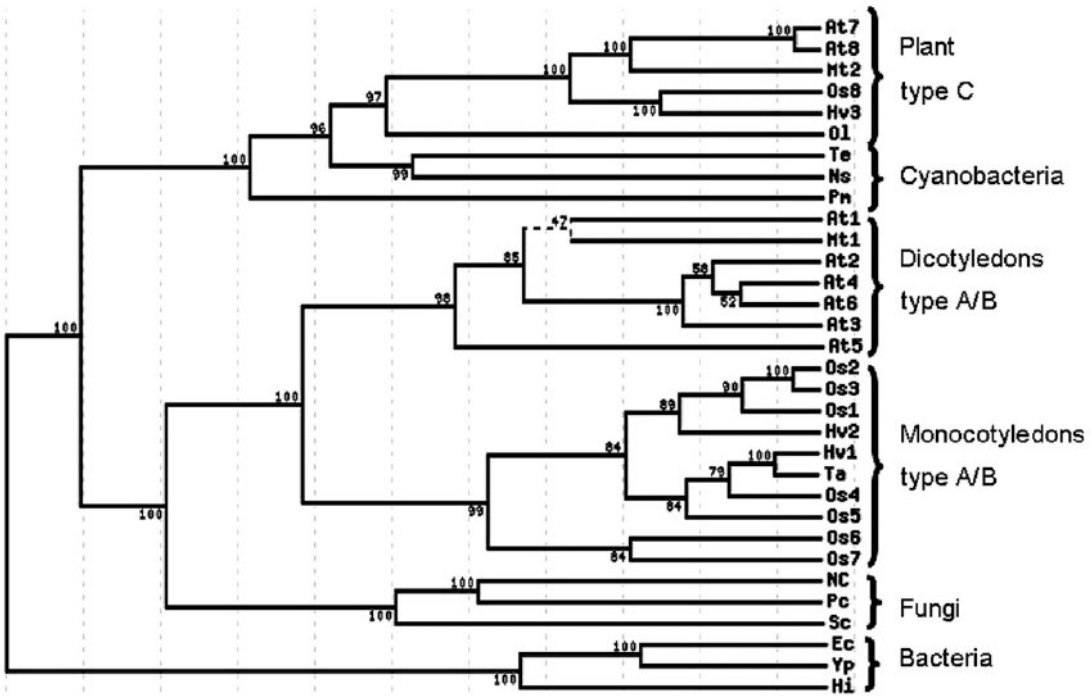

Figure 3.1. Phylogenetic tree of NTR sequences. Values indicate percent bootstrap support for each branch. For accession numbers and organisms, see ‘‘Materials and Methods.’’

3.3.2. Gene expression and protein profiling of NTR and Trx h in germinating embryos

Expression of HvTrxh1, HvTrxh2, HvNTR1, and HvNTR2 genes was analyzed by semiquantitative reverse transcription (RT)-PCR using total RNA from embryos dissected from mature seeds and seeds at different time points during germination. The appearance of the corresponding proteins was monitored by western-blot analyses of soluble proteins extracted from the embryo during germination. Transcripts of both HvTrxh1 and HvTrxh2 were present in embryos from mature seeds and remained constant during germination (Fig. 3.2A). Trx h protein, however, increased slightly in amount from 24 h after imbibition (Fig. 3.2B), corresponding to the time of radicle protrusion, and then remained constant up to 144 h. HvNTR1 and HvNTR2 transcripts were both detected at low levels in embryos from

mature seeds (Fig. 3.2A). Expression increased considerably up to 72 h after imbibition, then started to decrease. NTR protein (Fig. 3.2B) was detected at low levels in embryo 4 h after imbibition, increased up to 48 h, and then remained essentially constant. For both Trx h and NTR, the western-blotting profiles represent the combined appearance of all isoforms.

3.3.3. Gene expression and protein profiling of NTR and Trx h in aleurone layers responding to hormones

The cereal seed aleurone layer has a key role in germination, responding to hormone signals from the embryo and producing storage reserve mobilizing enzymes. Isolated aleurone layers can be maintained in buffer, providing a well-defined system for analysis of hormonal regulation of seed germination (Fath et al., 2001). Aleurone layers were incubated in buffer containing GA or ABA and harvested at time points between 6 and 48 h. HvTrxh1 and HvTrxh2 expression was detected in aleurone layers incubated with or without the addition of GA or ABA and the expression level varied only slightly (Fig. 3.3A). Trx h protein, however, was hardly detected in aleurone layers after 6-h incubation (Fig. 3.3B) and the level increased slightly during the course of the incubation. A similar increase was observed in aleurone layers treated with GA or ABA, suggesting that these hormones do not regulate gene expression or protein accumulation of HvTrxh1 and HvTrxh2.

HvNTR1 transcripts were only detected in aleurone layers after 45 amplification cycles in contrast to 35 cycles in embryos, suggesting that HvNTR1 is expressed at a much higher level in embryos than aleurone layers. In contrast, HvNTR2 transcripts were detected in both tissues after 35 amplification cycles. Noticeably, expression of HvNTR1 and HvNTR2 in aleurone layers showed distinct differences. HvNTR1 expression increased considerably after 12-h incubation with or without GA or ABA, and then decreased up to 24 h (Fig. 3.3A).

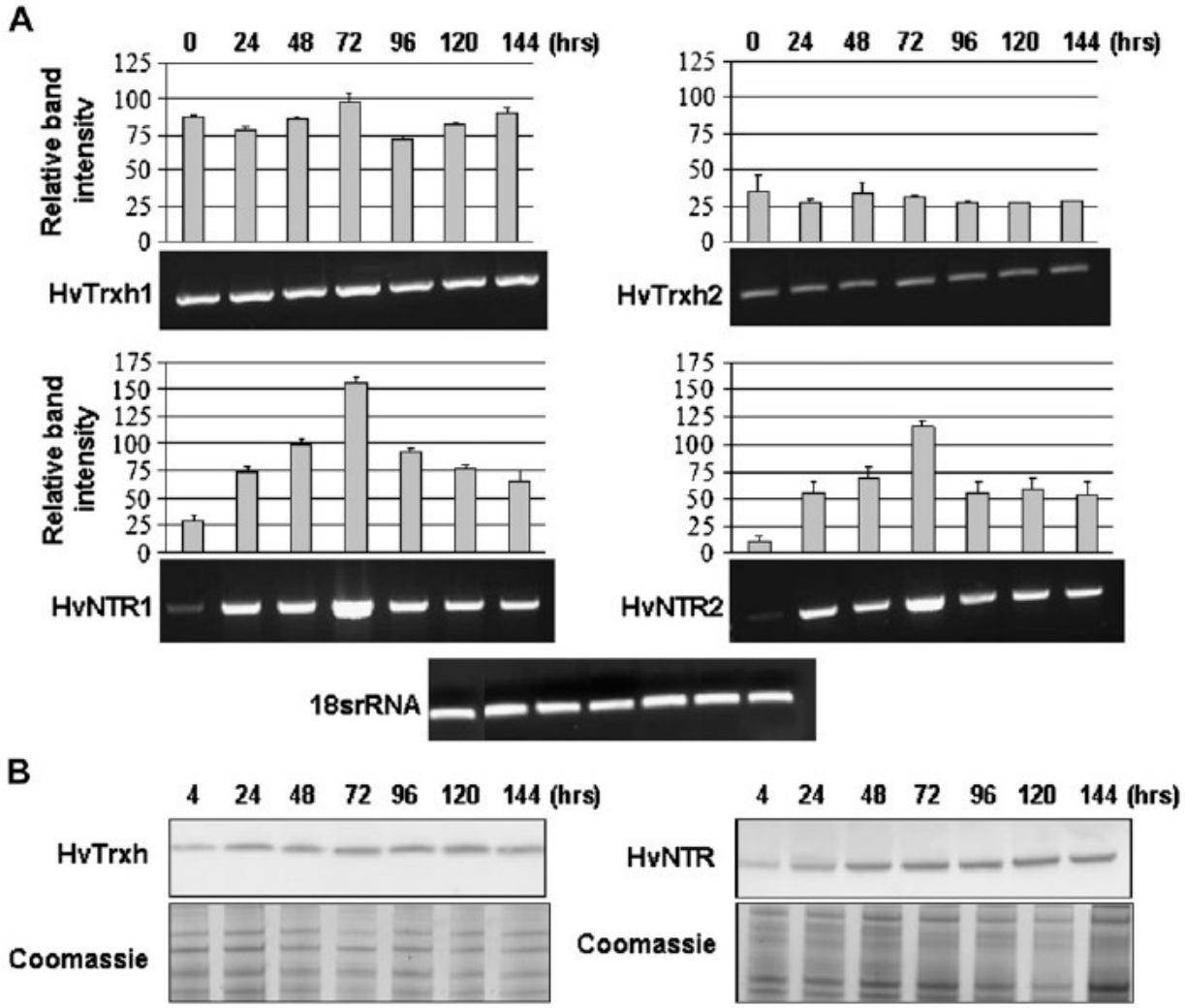

Figure 3.2. Gene expression and protein appearance for Trx h and NTR isoforms in barley embryos during germination (0–144 h). A, RT-PCR analysis of HvTrxh1, HvTrxh2, HvNTR1, and HvNTR2. One representative gel is shown from three independent replicates. Relative band intensities were normalized to the 18S rRNA band intensity (100%). Each histogram represents the mean ± SD obtained from three independent RT-PCR reactions. B, Western blot of embryo protein extracts using antibodies against Trx h and NTR.

No clear trend in expression of HvNTR2 was observed; however, the expression was significantly lower in the presence of GA than in control or ABA-treated aleurone layers, in particular at early time points, suggesting that GA down-regulates HvNTR2 expression. This was supported by the western blot (Fig. 3.3B) showing very little NTR protein after 6- and 18-h GA treatment compared with control or ABA-treated aleurone layers. After 24 h, the NTR level was essentially the same in all three samples, supporting early-phase down-regulation by GA. Because the protein profile clearly reflected HvNTR2 gene expression, HvNTR2 might be the dominant isoform in aleurone layers.

3.3.4. 2-D gel electrophoresis pattern of Trx h in aleurone layers

HvTrxh1 and HvTrxh2 were identified in two and one 2-D gel spots, respectively, in mature barley embryos (Maeda et al., 2003). One HvTrxh1 spot and the HvTrxh2 spot decreased at radicle elongation (Bønsager et al., 2007). In aleurone layers dissected from mature seeds, HvTrxh2 was absent and HvTrxh1 appeared in one spot (Maeda et al., 2003). Trx h transcript levels in aleurone layers appear to be independent of GA and ABA. Therefore, 2-D western blotting was performed to examine whether the individual protein isoforms were affected by hormone treatment. A single spot with approximate 12.5 kDa molecular mass and pI 5.0 was detected in all blots and on 2-D gels stained with Coomassie Blue and silver nitrate (Fig. 3.3C). The spot was excised from the Coomassie-stained gel for in-gel digestion with trypsin and analysis by matrix-assisted laser desorption/ionization time-of-flight mass spectrometry (MALDI-TOF MS). Five peptide masses matched HvTrxh1 (AAP72290), giving 20% sequence coverage. The abundance of the spot was similar in aleurone layers treated with or without GA or ABA, in agreement with gene expression and the 1-D western blot, indicating that synthesis of the protein was not regulated by hormones. The HvTrxh1 spot was hardly

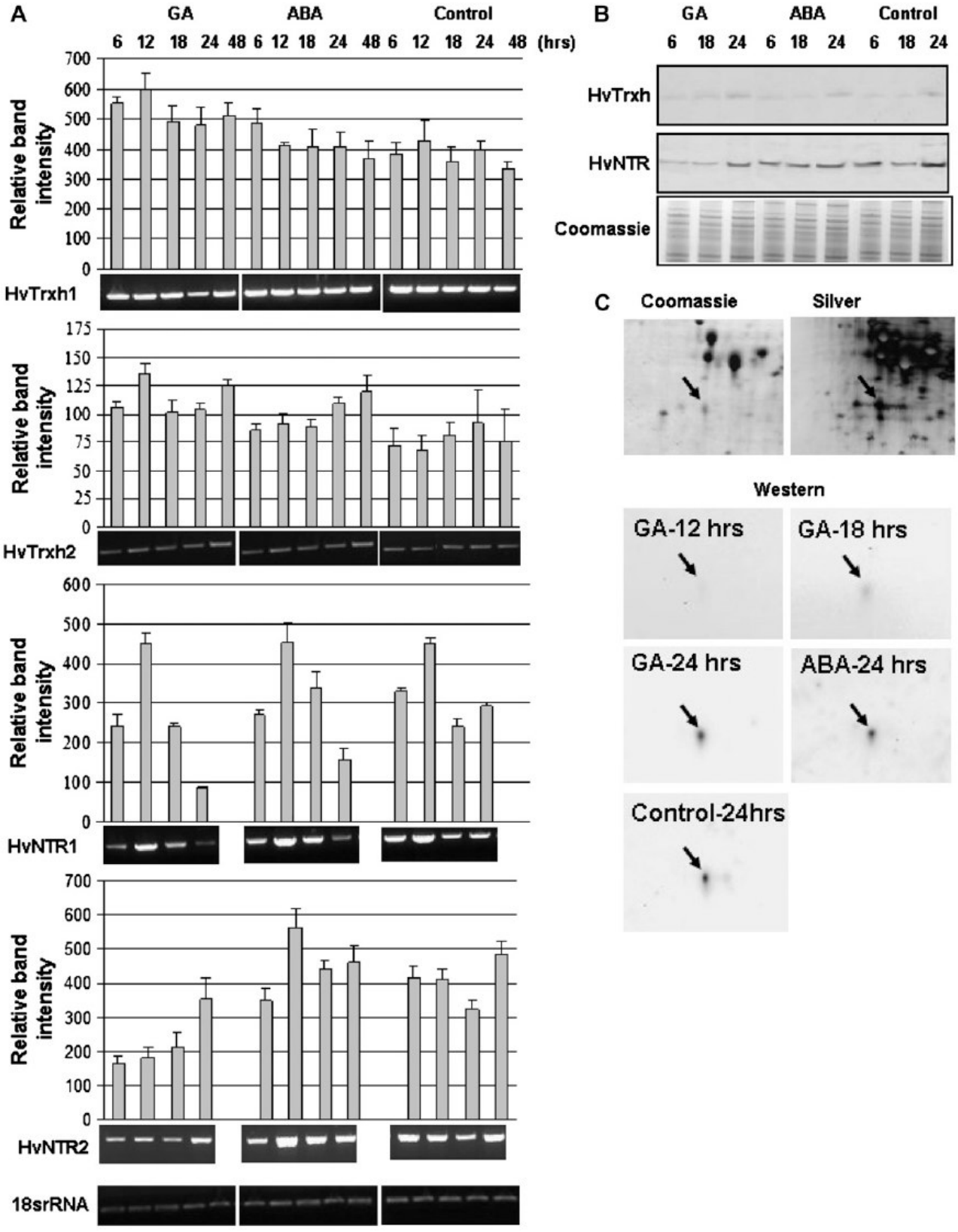
A
GA
ABA
Control
6 12 18 24 48 6 12 18 24 48 6 12 18 24 48 (hrs)
Relative band intensity
HvTrxh1
HvTrxh2
HvNTR1
HvNTR2
18srRNA
B
GA
ABA
Control
6 18 24 6 18 24 6 18 24
HvTrxh
HvNTR
Coomassie
C
Coomassie
Silver
Western
GA-12 hrs
GA-18 hrs
GA-24 hrs
ABA-24 hrs
Control-24hrs

Figure 3.3. Gene expression and protein appearance for Trx h and NTR isoforms in aleurone layers responding to GA, ABA, and buffer without hormones (control) at various time points (6–48 h). A, RT-PCR analysis of HvTrxh1, HvTrxh2, HvNTR1, and HvNTR2. One representative gel is shown from three independent replicates. Relative band intensities were normalized to18S rRNA band intensity (100%). Each data point represents the mean ± SD obtained from three independent RT-PCR reactions. B, Western blot of aleurone protein extracts using antibodies against Trx h and NTR. C, Coomassie- and silver-stained 2-D gels and 2-D western blotting using Trx h antibody in aleurone layers treated in the presence and absence of GA and ABA. The Trx h spot is marked by an arrow.

detected in aleurone layers incubated for 12 or 18 h (Fig. 3.3 C) and increased in intensity during incubation, in agreement with the 1-D western blot. Identification of only the HvTrxh1 protein in aleurone layers is in agreement with previous findings (Maeda et al., 2003), but is in contrast to detection of transcripts corresponding to both Trx h genes.

3.3.5. Expression, purification, and biochemical characterization of HvNTR1 and HvNTR2

To confirm that the cDNA sequences encoded active NTR and to compare the kinetic properties of the two isoforms, recombinant proteins carrying an amino-terminal His6-tag were produced in *Escherichia coli*. HvNTR1 and HvNTR2 were found in the soluble fraction of the *E. coli* transformant culture after induction with β-D-thiogalactopyranoside (IPTG) and were recognized both by an antibody recognizing the His-tag and an antibody raised against wheat NTR (data not shown). SDS-PAGE of cell extracts showed a prominent polypeptide band of the expected molecular mass (Fig. 3.4 A, lanes 2 and 5), and the recombinant His6-HvNTR1 and His6-HvNTR2 were purified from the crude extracts by nickel affinity chromatography (Fig. 3.4 A, lanes 3 and 6) in yields of 30 and 10 mg/L, respectively. Proteins

were yellow with absorption maxima at 270, 378, and 454 nm (Fig. 3.4B) typical for flavoproteins (Jacquot et al., 1994; Serrato et al., 2002).

One FAD-binding site is predicted per NTR subunit. Remarkably, the MALDI-TOF mass spectrum for His_6-HvNTR2 showed a series of peaks differing by 787 Da corresponding to the molecular mass of $FADH_2$ (Fig. 3.4C). The peaks were assigned to $[M+H]^+$ of His_6-HvNTR2 lacking FAD, and His_6-HvNTR2 with one or more associated FAD molecules, respectively. The N-terminal His_6-tag was subsequently removed from the recombinant proteins by thrombin cleavage (Fig. 3.4A, lane 7). Three amino acids (Gly, Ser, His) originating from the His-tag remain at the N-terminus of NTR after thrombin cleavage. The MALDI-TOF mass spectrum for cleaved HvNTR2 exhibited a prominent peak at *m/z* 35050.02 Da in agreement with the theoretical mass of cleaved HvNTR2 lacking FAD (35052.54 Da). No additional series of peaks was observed (Fig. 3.4C), and it is concluded that FAD is non-covalently bound to HvNTR allowing disassociation from the FAD-binding site and formation of adducts associated with the N-terminal His_6-tag under MALDI conditions.

3.3.6. Enzyme activity

Kinetic parameters for activity of HvNTR1 and HvNTR2 were determined using barley HvTrxh1 and HvTrxh2, and for comparison, also with *E. coli* Trx as substrate (Table 3.1). K_m values indicate that HvNTR1 and HvNTR2 have similar affinities for HvTrxh1 and HvTrxh2. Activity of HvNTR1 with HvTrxh1, represented by k_{cat}, was almost twice that with HvTrxh2. In contrast, the k_{cat} of HvNTR2 was the same for HvTrxh1 and HvTrxh2. The k_{cat} of HvNTR2 with *E. coli* Trx was similar to that of barley HvNTR1 with barley Trx h isoforms, whereas the K_m for *E. coli* Trx was very high. The catalytic efficiency (k_{cat}/K_m) for *E. coli* Trx was thus 100-fold lower than for HvTrxh1 and HvTrxh2 indicating that a non-cognate Trx is not a

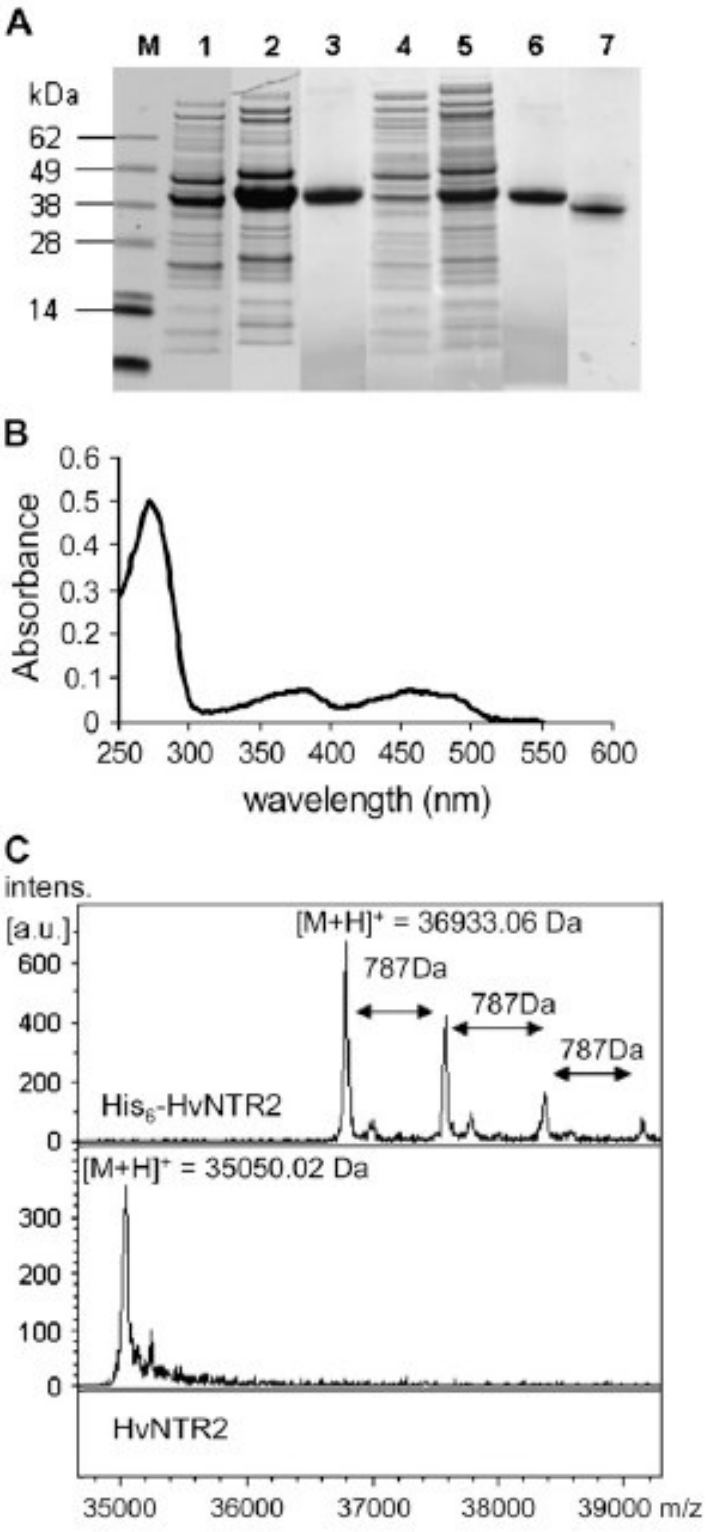

Figure 3.4. Expression, purification, and chemical properties of NTR. A, SDS-PAGE of NTR overexpression in *E. coli*, purification, and thrombin cleavage. Total protein from *E. coli* harboring pET15b-HvNTR1 (lanes 1 and 2) and pET15b-HvNTR2 (lanes 4 and 5), respectively, before (lanes 1 and 4) and 3.5 h after (lanes 2 and 5) induction with IPTG; purified His-HvNTR1 and His-HvNTR2, respectively (lanes 3 and 6); and HvNTR2 after thrombin cleavage to remove the His-tag (lane 7). B, Absorption spectrum of recombinant HvNTR2. C, MALDI MS spectrum of intact His-HvNTR2 and after cleavage with thrombin.

Table 3.1. Kinetic parameters of barley (HvNTR1, HvNTR2) and Arabidopsis (AtNTR) NTR for barley Trx h isoforms (HvTrxh1, HvTrxh2) and *E. coli* Trx.

Enzyme	Substrate	K_m (μM)	k_{cat} (s^{-1})	k_{cat}/K_m (s^{-1} M^{-1})
(pH 7.4)				
HvNTR1	HvTrxh1	1.18±0.25	2.25± 0.08	1.90×10^6
HvNTR1	HvTrxh2	1.79± 0.40	1.31±0.08	0.73×10^6
HvNTR2	HvTrxh1	1.12±0.04	3.26±0.09	2.91×10^6
HvNTR2	HvTrxh2	1.29±0.25	2.98± 0.16	2.31×10^6
HvNTR2	*E. coli* Trx	107	1.6	1.55×10^4
AtNTR	HvTrxh1	24.70±5.00	1.04 ±0.09	0.42×10^5
AtNTR	HvTrxh2	26.70 ±6.50	0.80±0.07	0.30×10^5
(pH 5.7)				
HvNTR1	HvTrxh2	1.45	0.43	0.30×10^6
HvNTR2	HvTrxh2	0.90	0.8	0.89×10^6

good substrate for the NTR. Similarly, thioredoxin reductases from *Caenorhabditis elegans* (Lacey and Hondal, 2006) and *Plasmodium falciparum* (Krnajski et al., 2001) also show high activity towards *E. coli* Trx, but with a high K_m. Kinetic parameters were also determined using Arabidopsis NTR (AtNTR) (Jacquot et al., 1994), which had lower affinity and lower activity for barley Trx h isoforms compared with the barley NTRs (Table 3.1). Conversely, both AtNTR and *E. coli* NTR showed high affinity for their own thioredoxins, K_m being 1.1 (Jacquot et al., 1994) and 1.9-2.4 μM (Miranda-Vizuete et al., 1997), respectively, similar to the K_m values determined here for the barley NTR/Trx h pairs. These data underline that NTR from different species prefer their cognate Trx h as substrate.

The pH used here and by others to determine NTR activity is significantly higher than that expected in some barley seed tissues, since the aleurone layer acidifies the starchy endosperm to about pH 5.0 during germination (Dominguez and Cejudo, 1999). As Trx h may have a number of roles in the starchy endosperm during germination (Buchanan and Balmer, 2005),

the activity of HvNTR2 was analyzed between pH 5.0-7.4 using 3 µM oxidized HvTrxh1 or HvTrxh2 as substrate (Fig. 3.5). The velocity of 5,5´-dithio-bis (2-nitrobenzoic acid) (DTNB) reduction decreased from pH 7.4 to 5.0, but considerable reduction of DTNB was still obtained at pH 5, indicating that HvNTR2 has the capacity to reduce Trx h in the slightly acidic environment found in the starchy endosperm during germination. HvNTR1 showed a similar pH dependence (data not shown). The K_m of HvNTR1 and HvNTR2 determined towards HvTrxh2 at pH 5.7 was not altered (Table 3.1), therefore it is concluded that the decrease to pH 5.7 reduced the catalytic activity 3 to 4 times.

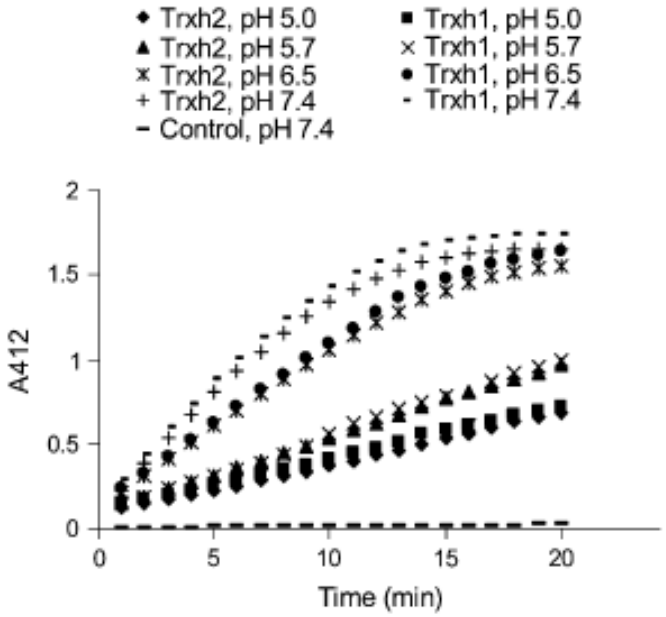

Figure 3.5. Time course of HvTrxh1 and HvTrxh2 reduction by HvNTR2 as monitored by reduction of DTNB at various pH values (5, 5.7, 6.5, and 7.4). Control shows the time course of DTNB reduction by HvNTR2 without addition of Trx h.

3.3.7. An initial study for identification of HvNTR isoforms on 2D-gel electrophoresis in barley aleurone layer

The obtained protein profile of NTR in aleurone layer and embryo using 1D-western blotting reflected the combined appearance of all isoforms of NTR because anti-wheat NTR antibody can not discriminate between different isoforms. In addition the molecular masses of barley NTR isoforms (HvNTR1 and HvNTR2) are similar, the bands corresponding to two isoforms are therefore overlapped on 1D-gel electrophoresis. In order to determine the protein pattern of each NTR isoform a proteomics approach consisting of 2D-wetern blotting, 2D-gel electrophoresis and mass spectrometry was exploited.

To locate spots containing NTR in aleurone layer proteome, a 2D-gel with proteins extracted from aleurone layer treated with GA after 18 h incubation (18 h AL-GA, Fig. 3.6) was electroblotted and probed with antibody raised against wheat NTR. Between several spots appeared on the blot only one spot (Fig. 3.6, Spot # 7) had molecular mass/pI (35.0/6.0) close to that of HvNTR isoforms (theorical molecular mass/pI for HvNTR1 and HvNTR2 are 34.818/5.7 and 34.793/5.7, respectively). However to identity the proteins in the extra cross-reacting spots, the position of all of spots on the blot were determined on the Coomassie-stained 2D-gel. The spots were excised from the 2-D gel for in-gel trypsin digestion and analyzed with MALDI-TOF MS. As Table 3.2 shows the obtained peptide mass fingerprinting enabled us to identify the following proteins; cytosolic NADP-malic enzyme in spots 1 and 2, low pI α-amylase (AMY1) in spots 3 and 4, and high pI α-amylase (AMY2) in spots 5 and 6 indicating an unspecific interaction between this antibody with other proteins. However, we were not able to get a successful MS spectra for identification of spot # 7 which was due to very low abundance of protein in this spot.

A similar experiment was performed with extracted protein from aleurone layer treated with ABA after 18 h incubation (18 h AL-ABA, Fig. 3.6). This decreased the number of unspecific spots corresponding to α-amylase, but the spots # 1, 2 and 7 were still present. Although the intensity of spot # 7 on 2D-western blot from 18 h AL-ABA was higher than 18 h AL-GA, the intensity of corresponding spot on Coomassie-stained 2D-gel was still very low and we still couldn't identify it by MS analysis. In another experiment where the purified recombinant HvNTR2 together with extracted protein from 18 h AL-ABA were loaded on 2D-gel, the molecular mass/pI of spot # 7 (35.0/ 6.0) was very close to that from the observed spot for recombinant HvNTR2 (35.0/5.7). This experiment raised the possibility of the spot # 7 to be NTR. However these observations can not exclusively prove that this spot is containing NTR, further MS and MS-MS analysis are necessary for identification. Moreover, making antibody against each HvNTR isoforms is possible since the recombinant HvNTR1 and HvNTR2 are now available.

Table 3.2. Identification of proteins in 18 h AL-GA which made unspecific interaction with rabbit-anti wheat NTR

Spot Number	Accession number	Protein	Matched peptides	Sequence coverage (%)
1	TC139309	Cytosolic NADP malic enzyme	14	22
2	TC139309	Cytosolic NADP malic enzyme	14	20
3	gi|113765	α-amylase, low pI isozyme (AMY1)	10	24
4	gi|166979	α-amylase, low pI isozyme (AMY1)	7	25
5	gi|1065365	α-amylase, High pI isozyme (AMY2)	11	36
6	gi|1065365	α-amylase, High pI isozyme (AMY2)	10	22
7	----------	----------	----------	----------

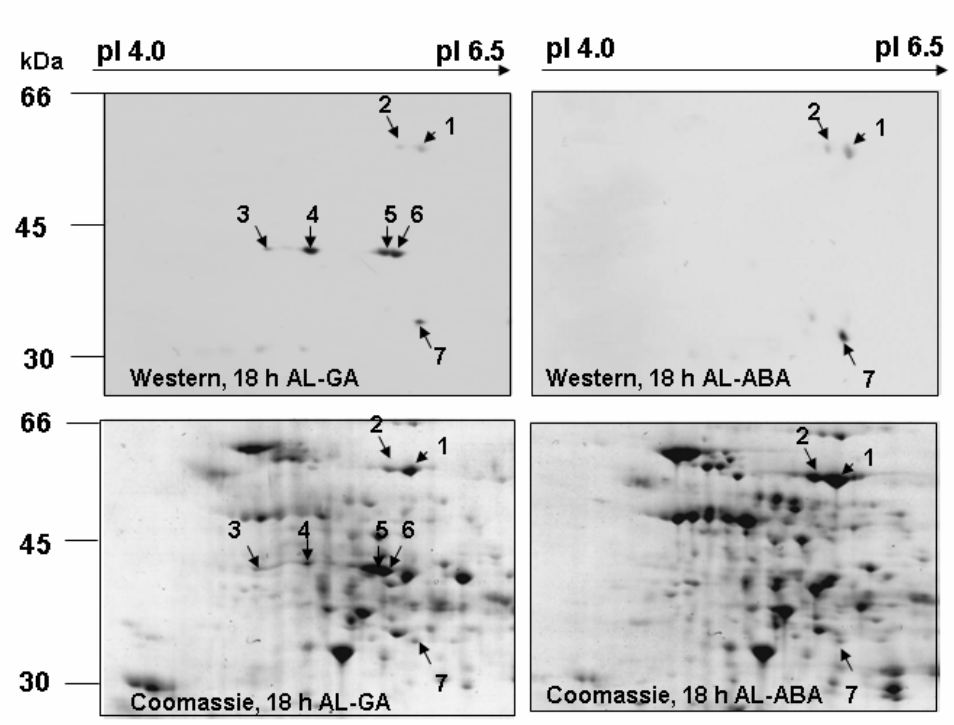

Figure 3.6. 2D-western blots and Coomassie-stained 2D gels to follow up the identification of HvNTR isoforms in aleurone layers treated with GA (Al-GA) or ABA (AL-ABA) during 18 h incubation.

3.3.8. An initial study shows that a C-type NTR is expressed in barley leaves

As mentioned before in addition to NTR type A/B localized in either cytoplasm or mitochondrion, plants pose an NTR with a C-terminal extension containing a Trx active site in chloroplast of green tissues (NTR-C; Serrato et al., 2004). Expression of barley TC132362 (Hv3; Fig. 3.1) corresponding to a putative NTR-C was analyzed by RT-PCR using total RNA from dissected embryo of germinated seeds (24 h after imbibition), aleurone layer treated with or with out addition of GA or ABA for 24 h and finally in 2-week seedling leaves.

The transcript of TC132362 was detected in barley leaves (Fig. 3.7) but not in embryo or aleurone layer. This supports that TC132362 encodes a C-type NTR expressed in photosynthetic tissues.

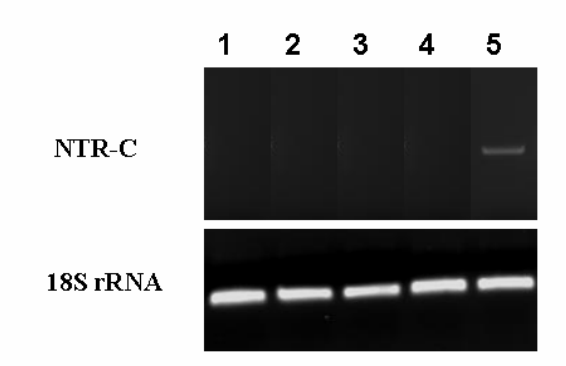

Figure 3.7. Gene expression analysis of NTR-C in aleurone layer treated with GA (1), ABA (2), No hormones (3) for 24 h. embryo of germinated seeds after 24 h imbibition (4), and 2-week seedling leaves (5) using RT-PCR.

3.4. Discussion

Production of recombinant forms of two isoforms each of barley NTR and Trx h allowed the first investigation of interactions between NTR and Trx isoforms from the same organism. The finding that both NTR isoforms have similar affinity toward the Trx h isoforms is in accordance with the high sequence identity of HvNTR1 and HvNTR2 and the conservation of residues surrounding the active site in HvTrxh1 and HvTrxh2. The higher catalytic activity of HvNTR1 toward HvTrxh1 suggests that the overall activity of an NTR/Trx system could be modulated by exploiting different isoforms under different circumstances.

Despite the different tasks proposed for the NTR/Trx system during germination (Wong et al., 2002, 2004), most experimental evidence was obtained at more basic pH values than expected to be present in vivo. Under weak acidic conditions in the starchy endosperm during germination, the Trx N-terminal active-site Cys (e.g. $C46_{HvTrxh2}$), acting as a nucleophile in catalysis of the disulfide exchange reaction (Kallis and Holmgren, 1980; Maeda et al., 2006a) and with pKa of 6.3 to 7.5 (in *E. coli* Trx; Setterdahl et al., 2003), may be protonated and hence inactive. Therefore, the central question of whether the NTR/Trx system is active at the pH of the endosperm during germination was not clearly addressed. This work demonstrates, however, that recombinant HvNTR1 and HvNTR2 are able to reduce Trx h at pH 5.0 with

essentially retained affinity, but slightly decreased activity, which supports that the NTR/Trx system operates in germination.

Functional analysis was complemented by gene expression and protein profiling during germination because, for NTR/Trx pairs to interact, they must be present in the same tissue at the same time. Profiling experiments also provide information about gene expression, posttranscriptional, and posttranslational regulation. Transcripts corresponding to both Trx h and NTR isoforms were detected in embryos and aleurone layers at all time points, suggesting that the NTR/Trx system is active in these tissues during germination. Levels of Trx h transcripts were relatively constant, whereas NTR transcript accumulation showed greater modulation, as characteristic for genes encoding important regulatory proteins. The comparison of Trx h gene expression and protein profiles illustrates the general problem with predicting protein expression levels from mRNA data. Differences can be due to posttranscriptional modification controlling the protein translation rate (Day and Tuite, 1998), protein modification or degradation, and protein transport to or from cytoplasm (Gygi et al., 1999; You and Yin, 2000). Distinct transcript accumulation patterns were observed for HvNTR1 and HvNTR2, indicating that the isoforms are differentially regulated and may have individual functions in seed germination. HvNTR2 perhaps has a specific role in germination because its expression in the aleurone layer was affected by GA. HvNTR1 expression level is much lower in aleurone than embryo and the NTR protein profile in the aleurone layer closely resembles the HvNTR2 gene expression pattern. In combination, gene expression and protein profiling suggest that, whereas both NTR and Trx h isoforms are present in the embryo, with HvTrxh1 protein more prominent during germination, HvNTR2 and HvTrxh1 may be the dominant isoforms in the aleurone layer during germination. Isolation of the promoter regions for the two genes would be one way to further study the regulation.

The observed increase of NTR gene expression in germinating embryos would be expected to lead to an increase in the proportion of reduced Trx h and hence reduced Trx h target proteins. These results agree with protein disulfides becoming more reduced during germination (Marx et al., 2003; Alkhalfioui et al., 2007b). The reported elevated activity during germination of oxidative pentose phosphate pathway enzymes (Lozano et al., 1996) could provide the NADPH required for activation of the NTR/Trx system in embryos. In contrast, the decrease of HvNTR2 expression in aleurone layers in response to GA at early incubation time points suggests an initial low level of reduced Trx h and target proteins in the aleurone layer. Several potential Trx target proteins (Yamazaki et al., 2004; Gelhaye et al., 2006) are involved in protection against reactive oxygen species, generated as by-products of lipid metabolism in the aleurone layer (Bethke et al., 2002) and implicated in the initiation of the cell death program (Fath et al., 2001). Down-regulation of HvNTR2 expression by GA is predicted to decrease the proportion of reduced Trx h, resulting in modulation of target protein activity. Therefore, regulation of the NTR/Trx system by hormones could affect cell death signaling in aleurone layer cells.

It still remains to be determined whether NTR isoforms are localized in the same cell compartments. In Arabidopsis, both mitochondrial and cytosolic forms (Reichheld et al., 2005) of NTR have been identified.

3.5. Conclusion

This study shows for the first time interactions between two NTR and two Trx h isoforms from the same organism. The results support a functional role of the NTR/Trx system during germination and suggest that the members of the barley seed NTR/Trx system can function interchangeably. Future proteomics-based studies of individual NTR and Trx isoforms in

conjunction with determination of intracellular localization and promoter structure may clarify their differential expression pattern in response to hormones and their possibly divergent in vivo functions. Finally, heterologous expression of both NTR and Trx h isoforms provides a basis for design and characterization of mutants to investigate the interaction between NTR and Trx h at the level of molecular structures.

3.6. Materials and methods

3.6.1. Plant material

Embryos from germinated seeds were prepared from the malting barley (*Hordeum vulgare* 'Barke') provided by Sejet Plantbreeding. Mature seeds were sterilized in 5% sodium hypochlorite for 30 min and rinsed several times with water. Seeds were germinated for 0, 4, 24, 48, 72, 96, 120, and 144 h, frozen, and stored as described (Bønsager et al., 2007). Embryos were dissected from seeds prior to protein and RNA extraction. Aleurone layers were prepared from embryoless half-grains (Hynek et al., 2006) of barley 'Himalaya' (purchased from Washington State University). Isolated aleurone layers (100 mg fresh weight) were incubated in 2 mL of 20 mM Na succinate (pH 4.2), containing 20 mM CaCl2, 50 mg/mL ampicillin, and 5 mg/mL nystatin. Where appropriate, GA or ABA (5 mM) was added. Incubation was performed at room temperature with continuous gentle shaking. Aleurone layers were harvested at various time points (6–48 h), washed four times with 2 mL of the incubation medium without addition of antibiotics or hormones, frozen in liquid nitrogen, and stored at -80 ^{o}C until use.

For preparation of barley leaves the barley seeds were grown in soil for 14 days in growth-chambers with 16 h light followed by 8 h dark at 18-20 ^{o}C (provided by A.L.B. Møller). The leaves were harvested and frozen at -80 ^{o}C until analysis.

3.6.2. RT-PCR analysis

Total RNA was extracted from tissues using the RNeasy plant mini kit (Qiagen) and treated with RNase-Free DNase (Qiagen). RT-PCR was performed in a PTC-200 DNA Engine Peltier thermal cycler (Bio-Rad) using the one-step RT-PCR kit (Qiagen). The RT-PCR mixtures were set up according to the manufacturer's recommendations using 0.6 μM primers and 50-100 ng total RNA as starting material. Barley 18S rRNA showing invariant expression across the samples was amplified in parallel. The optimal number of amplification cycles (between 15 and 45) for each set of primers was determined at the exponential phase range of amplification. To control for possible genomic DNA contamination, parallel reactions were carried out where reverse transcriptase activity was inactivated by incubation at 95 ^{o}C. A negative control lacking template RNA was included for each set of RT-PCR reactions. Reactions were performed in triplicate. Amplification products were separated by agarose gel electrophoresis and quantified using ImageJ software (W.S. Rasband; 1997–2007; National Institutes of Health; http://rsb.info.nih.gov/ij). Signal intensities were normalized with respect to 18S rRNA from the same sample. Primers used were trxh8 and trxh9 for HvTrxh1, trxh10F and trxh10R for HvTrxh2, ntr3F and ntr3R for HvNTR1, and ntr4F and ntr4R for HvNTR2 and ntrc1F and ntrc1R for analysis of NTR-C (primers were designed based on the regions of TC132362 encoding NTR and Trx-active site in putative NTR-C). The sequence of primers are listed in Table 3.3.

3.6.3. Sequence analysis

Multiple alignment of the region marked in Appendix 1 was performed using ClustalW (http://www.ebi.ac.uk/Tools/clustalw). A phylogenetic tree was constructed using the GeneBee TreeTop phylogenetic tree prediction server (http://www.genebee.msu.su/

genebee.html). National Center for Biotechnology Information (NCBI) accessions used for the analysis were: Os, rice (*Oryza sativa*), Os1 (NP_001047911), Os2 (EAY87270), Os3 (EAZ24372), Os4 (BAD33510), Os5 (NP_001057531), Os6 (EAZ00754), Os7 (EAZ36842), Os8 (NP_001060515); At, Arabidopsis (*Arabidopsis thaliana*), At1 (Q39242), At2 (NP_195271), At3 (1VDC), At4 (AAO42318), At5 (AAO42318), At6 (CAA80656), At7 (AAL08250), At8 (NP_565954); Hv, barley (*Hordeum vulgare*), Hv1 (ABY27300), Hv2 (ABX09990), Hv3 (TC132362); Ta, wheat (*Triticum aestivum*; CAD19162); Mt, *Medicago truncatula*, Mt1 (ABH10138), Mt2 (ABH10139); Ol, *Ostreococcus lucimarinus* (XP_001422184); Te, *Thermosynechococcus elongates* (NP_682714); Ns, *Nostoc* sp. (NP_484780); Pm, *Prochlorococcus marinus* (NP_893267); Nc, *Neurospora crassa* (P51978); Pc, *Penicillium chrysogenum* (P43496); Sc, *Saccharomyces cerevisiae* (P29509); Ec, *Escherichia coli* (P09625); Yp, *Yersinia pestis* (NP_404967); and Hi, *Haemophilus influenzae* (P43788).

3.6.4. Protein extraction and western-blot analysis

Frozen tissues were dried under vacuum and ground to a fine powder using a mortar and pestle. Soluble proteins were extracted in 5 mM Tris-HCl, 1 mM CaCl2 (pH 7.5) with the protease inhibitor cocktail Complete (Roche; Finnie and Svensson, 2003). Protein concentration was determined using the Popov assay with bovine serum albumin as standard (Popov et al., 1975). Proteins (1.5 mg total protein from the aleurone layer or 6 mg total protein from the embryo) were separated on 4% to 12% Bis-Tris NuPAGE gels (Invitrogen) and stained with colloidal Coomassie Brilliant Blue G-250 (Candiano et al., 2004). Proteins were electroblotted onto a nitrocellulose membrane (Hybond-N; GE Healthcare) and probed using rabbit anti-wheat Trx h or rabbit anti-wheat NTR antibodies. Secondary antibodies

conjugated to horseradish peroxidase or alkaline phosphatase (Dako Cytomation) were detected by enhanced chemiluminescence (Thorpe and Kricka, 1986) or the nitroblue tetrazolium/bromochloro indolyl phosphate colorimetric method, respectively.

3.6.5. 2-D gel electrophoresis and western- blotting

Protein extracts from 100-mg aleurone layers were desalted on NAP-5 columns (GE Healthcare). Aliquots containing 50 µg of protein were precipitated by ammonium acetate (0.1 M) in methanol (Vensel et al., 2005) and redissolved in reswelling buffer (7 M urea, 2 M thiourea, 2% [v/v] CHAPS, 0.5% [v/v] immobilized pH gradient [IPG] ampholytes 3–10 [Amersham Biosciences], 1.2% [v/v] Destreak reagent [hydroxyethyl disulfide], and a trace of bromphenol blue). First-dimension isoelectric focusing was done using 18-cm linear IPG strips, pI 3 to 10, and an IPG phor (GE Healthcare). IPG strips were subsequently equilibrated as described (Finnie et al., 2002) for second-dimension electrophoresis on Excel SDS XL (18 3 24 cm) 12% to 14% gradient gel (GE Healthcare) using Multiphor II (GE Healthcare) according to the manufacturer's recommendations and stained with either silver nitrate (Heukeshoven and Dernick, 1985) or colloidal Coomassie Brilliant Blue G-250 (Candiano et al., 2004). For electroblotting onto nitrocellulose, gels were first equilibrated for 30 min in NuPAGE transfer buffer (Invitrogen) containing 15% methanol.

3.6.6. In-Gel Digestion and Protein Identification

Spots cut out from Coomassie-stained gels were in-gel digested with trypsin (Promega) as described (Finnie et al., 2002). Peptides were micropurified (Gobom et al., 1999) and eluted directly onto the MALDI target in 5 mg/mL α-cyano-hydroxy-cinnamic acid in 70% acetonitrile and 0.1% trifluoroacetic acid. An Ultraflex II MALDI-TOF-TOF mass

spectrometer (Bruker-Daltonics) was used in positive ion reflector mode and spectra were analyzed using FlexAnalysis software (Bruker-Daltonics). Spectra were calibrated externally using a tryptic digest of β-lactoglobulin. Internal calibration was carried out with trypsin autolysis products (m/z 842.51 and m/z 2211.10). Peptide mass data were searched against the NCBI nonredundant database and TIGR database barley gene index using Biotools (Bruker Daltonics) software and Mascot (MatrixScience) with the following parameters: monoisotopic mass tolerance, 80 ppm; allowed missed cleavages, 1; allowed modifications, carbamidomethylation of Cys (global) and oxidation of Met (partial).

3.6.7. Isolation and cloning of HvNTR1 and HvNTR2

Total RNA was extracted from embryos and contaminating genomic DNA was removed as described above. Conserved regions from plant genes encoding NTR were used to design primers (ntr1F and ntr1R). RT-PCR was performed using the one-step RT-PCR kit (Qiagen) according to the manufacturer's instructions. The amplified fragment (700 bp) was cloned in the pDrive cloning vector (Qiagen). Sequencing of cloned fragments (MWGBiotech AG) distinguished two types of internal NTR sequences, cDNA1 and cDNA2. Because cDNA1 was 98% identical to TC142091 and cDNA2 was 100% identical to TC141301, these TC sequences were used to design genespecific primers for RT-PCR amplification from embryo RNA and sequencing of the 5´ end (primers ntr4F and ntr4R) and 3´ end (primers ntr5F and ntr5R) of the cDNA2 coding sequence and the 3´ end of the cDNA1 coding sequence. Because TC 142091 did not include a complete coding sequence and lacked the 5´ untranslated region, the untranslated region from wheat NTR (accession no. AJ421947, 97% identical to cDNA1) was used to design primers (ntr2F and ntr2R) for isolation of the 5´ end of the cDNA1 coding sequence. Amplicons were cloned in pDrive cloning vectors and

sequenced. Finally, cDNAs containing the entire coding regions of HvNTR1 and HvNTR2 were amplified by RT-PCR from embryo RNA using primers ntr2F and ntr6R and ntr4F and ntr5R, respectively, and cloned to give pDrive-HvNTR1 and pDrive-HvNTR2. Primer sequences are listed in Table 3.3.

3.6.8. Expression, purification, and chemical properties of recombinant HvNTR1 and HvNTR2

The restriction sites *Nde*I and *Bam*HI were introduced at the ends of the HvNTR1 coding sequence by primers ntr10F and ntr10R, using HotStar HiFidelity PCR (Qiagen) and pDrive-HvNTR1 as template. pDrive-HvNTR2 was used as template with primers ntr8F and ntr8R to introduce *Nde*I and *Xho*I sites. After cleavage by the appropriate restriction enzymes, the inserts were ligated into pET15b (Novagen) to give pET15b-HvNTR1 and pET15b-HvNTR2. Sequences were verified and constructs were used to transform *E. coli* strain Rosetta (DE3). Cells were grown at 37 ^{o}C in Luria-Bertani medium supplemented with 100 mg/mL ampicillin and 5 mg/mL chloramphenicol to an OD600 of 0.6. Cultures were induced by 100 mM IPTG for 3.5 h. Cells were harvested by centrifugation and frozen at 220 ^{o}C until use. Frozen pellets were resuspended in Bugbuster protein extraction reagent including Benzonase (Novagen) and shaken for 20 min at room temperature. After centrifugation (14,000g for 20 min, 4 ^{o}C), recombinant protein in the supernatant was purified by a His-Trap HP column (Amersham Biosciences) as described (Maeda et al., 2006a) and eluted fractions were analyzed by SDS-PAGE. Purified proteins were desalted on PD-10 columns (GE Healthcare)

Table 3.3. List of forward (F) and reverse primers (R).

Primers name	Sequences (5´-3´)
ntr1F	caccgacgtcgagaactt
ntr1R	aaagacccctccacact
ntr2F	ggccgccaacgggatgga
ntr2R	gtggccacgtacccctcggagtc
ntr3F	cgagctcgactcaaaggggtacg
ntr3R	ccagtgcccaacttatattcccatcca
ntr4F	ccgtagccaagcctagcag
ntr4R	atacccatcggcatggag
ntr5F	gagctccatgccgatg
ntr5R	agacatgttctcactccaaaca
ntr6R	ggatcctcaatcagtcttcccttcctgtgc
ntr8F	atacatatggagggatccgccgcg
ntr8R	ataatactcgagtgcggctttcggcgag
ntr10F	catatggaggaggcggccg
ntr10R	ggatcctcaatgagtcttccctt
trxh8	ttcatatggccgccgaggagggag
trxh9	ggggatcctaaccgggcaatcactcttc
trxh10F	aggtgatctcggtccaca
trxh10R	cggtcagttcctccttgata
18srRNAF	ctacgtccctgccctttgtaca
18srRNAR	acacttcaccggaccattcaa
ntrc1F	gcatgtgcaatatgtgatgga
ntrc1R	gcagggaccacatgttggag

in 10 mM Tris-HCl (pH 8.0). Protein concentration was determined by amino acid analysis. The absorption spectrum was recorded for 8.7 μM NTR in 10 mM Tris-HCl (pH 8.0) at room temperature. For cleavage of the N-terminal His-tag, purified His6-tag HvNTR2 (0.1 mg/mL) was treated with immobilized thrombin (Calbiochem) at 1:100 (w/w) thrombin:fusion in 0.6 mM NaCl, 50 mM Tris-HCl (pH 6.0) for 24 h at 24 ^{o}C. Mass spectrometric analysis of intact proteins was performed using 20 pmol His-HvNTR2 or cleaved HvNTR2 after micropurification of samples as described above, but using Poros 20 R1 (Applied Biosystem) as column material and eluting in sinapinic acid (10 mg/mL) in 70% acetonitrile and 0.1%

trifluoroacetic acid. External calibration of spectra was performed using protein standard II (Bruker-Daltonics).

3.6.9. Enzyme activity assay

Activity of NTR was measured at 25ºC using DTNB as the final disulphide substrate as described (Miranda-Vizuete et al., 1997) with slight modifications. The reaction mixture contained 100 mM potassium phosphate (pH 5.0-7.4), 10 mM EDTA, 200 µM DTNB (Sigma-aldrich), 200 µM NADPH (Sigma-Aldrich), and Trx (1-10 µM) from barley or *E. coli* (Promega). The reaction was started by the addition of NTR (40 nM) and the rate of reduction of DTNB was calculated from A_{412}. As 1 mol Trx-$(SH)_2$ reduces 1 mol DTNB to yield 2 mol of TNB (2-nitro-5-thiobenzoic acid) with a molar extinction coefficient of 13, 600 $M^{-1}cm^{-1}$ (Ellman, 1959), a molar extinction coefficient of 27, 200 $M^{-1}cm^{-1}$ was applied for quantification. The extinction coefficient of TNB varied by 1-4% from this value in the pH range 5.0-7.4 employed in this work (data not shown).

Chapter 4: Interaction between thioredoxin h (Trx h) and NADPH-dependent thioredoxin reductase (NTR) from barley studied by site directed mutagenesis

4.1. Summary

In plants, the reduction of disulfide bonds of thioredoxin h (Trx h) is catalyzed by the enzyme NADPH-dependent thioredoxin reductase (NTR) in the presence of NADPH. However, to our knowledge there is no study on the structural basis for plant NTR-Trx h interaction. Here we have used the crystal structure of the NTR-Trx complex from *Escherichia coli* as a guide for mutagenesis of barley NTR (HvNTR) and Trx h (HvTrxh). The general aim has been to identify residues which play critical roles in the interaction between these redox important enzymes in plants, and in particular to identify residues that provide specificity between plant proteins and lead to suboptimal interaction between plant and *E. coli* proteins. The replacement of $R140_{HvNTR2}$ by alanine and methionine resulted more than 10-fold decrease in catalytic efficiency (k_{cat}/K_m) towards HvTrxh isoforms suggesting that $R140_{HvNTR2}$ has a role in HvNTR-HvTrxh interaction. The replacement of $I154_{HvNTR2}$ by glycine increased the affinity towards *E. coli* Trx (EcTrx), although a significant decrease in activity was observed compared to wild type (wt) HvNTR2. We also examined the role of some residues in the HvTrxh isoforms which are involved in Trx-target protein recognition to see whether they have role in the HvNTR-HvTrxh interaction. In this way the mutants $M88_{HvTrxh2}$ and $M82G_{HvTrxh1}$ exhibited an increase in the K_m value compared to their corresponding wild types in reaction with HvNTR2, suggesting $M88_{HvTrxh2}$ ($M82_{HvTrxh1}$) may have role in HvNTR-HvTrxh interaction.

4.2. Introduction

Thioredoxins (Trxs) are small proteins (~ 12-14 kDa) with the highly conserved active site sequence motif, WC(G/P)PC, and protein disulfide reductase activity (Jacquot et al., 1997). Trxs act as electron donors to enzymes of metabolism such as ribonucleotide reductase, and play a critical role in the maintenance of reduced environment inside the cell (Arner and Holmgren, 2000). Trxs themselves are maintained in the reduced form in the presence of NADPH by the action of NADPH-dependent thioredoxin reductase (NTR), a member of the flavoprotein disulfide oxidoreductase family (Williams, 1995). In plants, Trxs are present in multiple forms. The cytoplasmic Trxs as called h-type are reduced by NTR, whereas the chloroplastic Trxs are reduced by ferredoxin-dependent thioredoxin reductase (Gelhaye et al., 2004). The NTR/Trx system in plants has important biological roles in regulation of seed germination and seed development (Buchanan and Balmer, 2005).

NTRs in bacteria, archaea, fungi and plants are homodimers of ~35 kDa subunits, each containing a NADP-binding domain and a FAD-binding domain (Gelhaye et al., 2005; Dai et al., 1996). The NADP-binding domain of NTR contains two redox-active cysteines in a conserved active site sequence motif, CAV(T)C (Thon et al., 2007). The cysteines form a disulfide bond in the oxidized NTR and receive electrons from NADPH via the coenzyme FAD. For the reduction of Trx, one of the two cysteine thiols in the reduced NTR attacks the active-site disulfide bond in the oxidized Trx, and an intermolecular disulfide bond is formed as a reaction intermediate (Wang et al., 1996). Structural information of this intermediate is available in an engineered NTR-Trx complex from *Escherichia coli* (*E. coli*) obtained at a resolution of 3.0 Å (Lennon et al., 2000). Comparison of the crystal structures of *E. coli* NTR (EcNTR) in the free, oxidized form (Waksman et al., 1994) and in a disulfide-linked complex with *E. coli* Trx (EcTrx) (Lennon et al., 2000) has revealed a large conformational change, in

which the NADP-binding domain is rotated by 67 degrees. The two conformations are termed as the flavin-reducing (FR) and flavin-oxidizing (FO) conformations as they allow the transfer of electrons between NADPH and FAD and between FAD and the redox-active cysteines, respectively. *Arabidopsis thaliana* NTR (AtNTR) is the only plant NTR for which the 3D structure has been solved so far (Dai et al., 1996).

The plant NTR/Trx system has been extensively studied in barley. Two barley Trx h isoforms, HvTrxh1 and HvTrxh2, have been characterized for their appearance in different tissues in mature and germinating seeds (Maeda et al., 2003) and the crystal structures determined (Maeda et al., 2008). Moreover, the crystal structure of HvTrxh2 has been determined in complex with an *in vitro* target protein, barley α-amylase/subtilisin inhibitor (BASI) (Maeda et al., 2006a). We have recently identified two cytoplasmic or mitochondrial type NTR isoforms, HvNTR1 and HvNTR2, in barley seeds, cloned and produced them recombinantly and carried out an extensive analysis on the reaction kinetic of the barley NTR/Trx system (Shahpiri et al., 2008).

NTR-Trx interaction is highly specific and NTR from different species prefer Trx from the same species as substrate (Jacquot et al., 1994; Juttner et al., 2000; Miranda-Vizuet et al., 1997). For instance AtNTR shows 80-fold higher K_m value towards EcTrx than Arabidopsis Trx h (AtTrxh) despite the high structural conservation between NTRs and Trxs from the two organisms (Jacquot et al., 1994). Moreover, HvNTR isoforms with high sequence identify to AtNTR (75%) show 20-fold higher affinity towards HvTrxh isoforms in comparison with AtNTR (Shahpiri et al., 2008). These incompatibilities between NTR and Trx from different sources show the high specificity in the interaction between NTR and Trx. In the present work, the structural background for the highly specific interaction between NTR and Trx h in plant was studied using site-directed mutagenesis and the barley NTRs and Trxs as a model

system. We aimed to identify residue-residue interactions conserved among NTR/Trx system from different organisms as well as those, which are unique for the barley NTR/Trx system.

4.3. Results

4.3.1. The involvement of $R140_{HvNTR2}$ in HvNTR-HvTrxh interaction

The design of HvNTR and HvTrxh mutants was based chiefly on the 3D structure of the EcNTR-EcTrx complex (PDB entry 1F6M). We focused here on a surface groove in the NADP-binding domain of EcNTR (Fig. 4.1) which makes a complementary structure with Trx loop between the α3 and β4, consisting of residues 70-76. From one side of the groove, the backbone CO group of $R130_{EcNTR}$ forms two hydrogen bonds with the guanidine group of $R73_{EcTrx}$. In addition the guanidine group of $R130_{EcNTR}$ forms a hydrogen bond to the backbone CO group of $Y70_{EcTrx}$. The alignment of the primary and 3D structures of HvTrxh2 with EcTrx (from the EcNTR-EcTrx complex) showed the residues 83-89 of HvTrxh2 corresponds to the EcTrx $loop_{70-76}$ (Fig 4.2A and Fig 4.2C). A multiple sequence alignment of AtNTR, HvNTR2, HvNTR1 and EcNTR (Fig. 4.2B) showed that $R130_{EcNTR}$ corresponded to $R142_{AtNTR}$, $R140_{HvNTR1}$ and $R140_{HvNTR2}$. A structural alignment of the NADP-binding domains of AtNTR (PDB entry 1VDC) and EcNTR (PDB entry 1F6M) (Fig. 4.2D) showed a well superimposition of the corresponding residues. A sequence logo was performed using a multiple alignment of 23 plant NTR sequences. This showed that $R140_{HvNTR2}$ is highly conserved in plant NTRs (Fig. 4.3A). To investigate whether this residue has an important role in HvNTR-HvTrxh interaction, $R140_{HvNTR2}$ was replaced by alanine ($R140A_{HvNTR2}$) to highly shorten the side chain and by methionine ($R140M_{HvNTR2}$) to remove the side chain guanidine group that is supposed to be necessary for making a side chain-hydrogen bond with $F83_{HvTrxh2}$ ($Y70_{EcTrx}$) as observed in the EcNTR-EcTrx complex (Lennon et al., 2000).

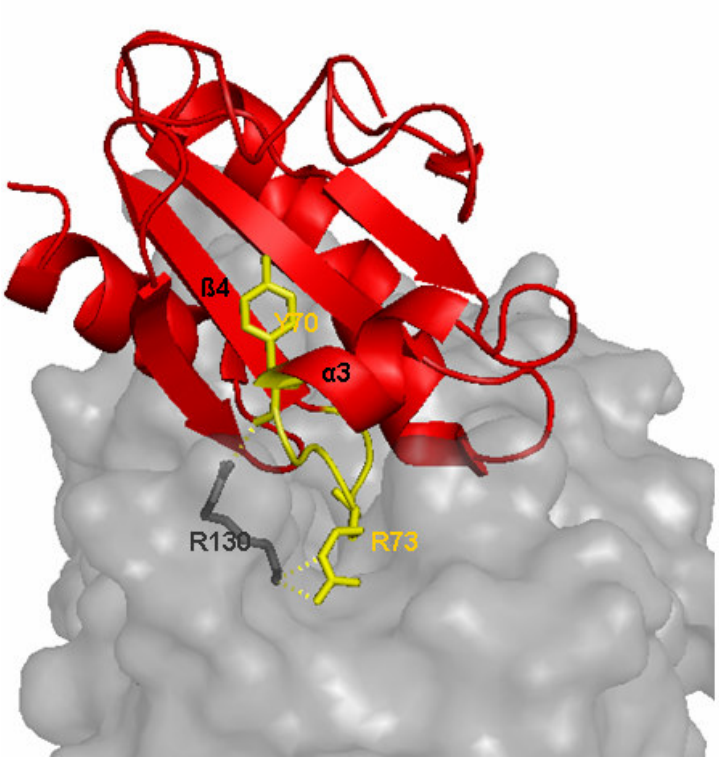

Figure 4.1. 3D structure of EcNTR-EcTrx complex (PDB code: 1F6M). The structure of EcTrx in cartoon display is colored red. The structure of Ec NTR in transparent surface is colored gray. The Trx loop constituting residues 70-76 is colored yellow. The secondary structures around this loop are labeled. The residues $R73_{EcTrx}$, $Y70_{EcTrx}$ and $R130_{EcNTR}$ are shown as sticks and labeled. The hydrogen bonds between $Y70_{EcTrx}$ and $R73_{EcTrx}$ with $R130_{EcNTR}$ are shown in yellow dashes.

4.3.1.1. Production of mutants, spectrophotometric and mass spectrometric (MS) analysis

The purified recombinant His-tagged NTR mutants $R140A_{HvNTR2}$ and $R140M_{HvNTR2}$ were obtained with a yield of 4.6 and 4.4 mg/L, respectively, corresponding to 50% of wild-type and showed prominent polypeptide bands of the expected molecular mass for both monomeric and dimeric forms of NTR, in a manner similar to wild-type, on Coomasssie-stained SDS-PAGE (Fig. 4.5A). The solutions of purified mutants in similar to wt were yellow with

absorption maxima at 270, 378, and 454 nm (Fig. 4.5B) typical for flavoproteins (Jacquot et al., 1994).

Verification of NTR mutants at the protein level was performed by comparing the tryptic peptide fingerprint patterns of His-tagged HvNTR2 mutants and wt HvNTR2 using MALDI-TOF-MS. Since trypsin cleaves protein peptide bonds on the carboxylic side of the basic residues arginine and lysine, the peak of $[M+H]^+$ 1508.680 Da for the peptide $_{129}$LYFSGSDTYWNR$_{140}$ was present in the spectrum from wt HvNTR2, but confirmed to be absent in mutants R140A$_{HvNTR2}$ and R140M$_{HvNTR2}$ (Fig. 4.6) as expected.

4.3.1.2. NTR assay with Trx

Both produced mutants, R140M$_{HvNTR2}$ and R140A$_{HvNTR2}$, exhibited activity towards wt HvTrxh1 and HvTrxh2. However, they showed 3-fold decrease in the k_{cat} value and 4- to 5-fold increase in K_m towards wt HvTrxh2 and HvTrxh1 compared to wt HvNTR2. This resulted in a decrease in catalytic efficiency of 11 to 15-fold towards wt HvTrxh2 and HvTrxh1 (Table 4.1).

4.3.1.3. NTR assay with DTNB in the absence of Trx

The apparent K_m and k_{cat} values for wt and NTR mutants were determined using DTNB as substrate in the absence of Trx with saturating concentration of NADPH (Table 4.2). As we expected the reactivity of NTR towards DTNB was very slow, however, this assay allowed measurements of the activity of NTR independent of Trx. The k_{cat} value for wt HvNTR2 was calculated to 0.19 (s^{-1}). This value for both mutants R140A$_{HvNTR2}$ and R140M$_{HvNTR2}$ was 79% (0.15 s^{-1}) of that from wt HvNTR2. The K_m value of both mutants R140A$_{HvNTR2}$ and R140M$_{HvNTR2}$ was similar to that of wt.

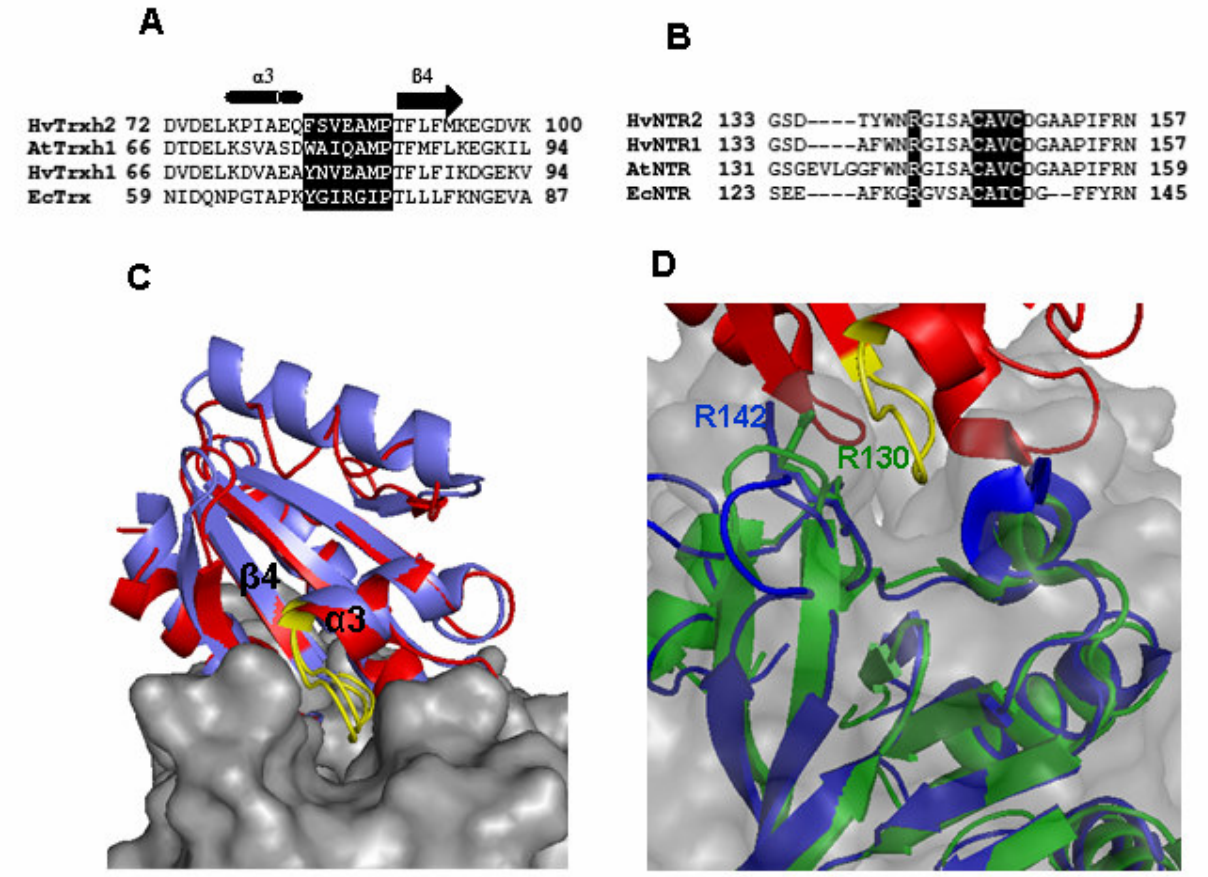

Figure 4.2. The possible role of $R142_{AtNTR}$ ($R140_{HvNTR2}$, $R130_{EcNTR}$) in HvNTR-HvTrxh interaction. A, Part of the multiple alignment between amino acid sequences of HvTrxh1, HvTrxh2, AtTrxh1, and EcTrx (the amino acids in Trx loop interacting with NTR between two indicated secondary structures are marked). B, Part of multiple alignment between amino acid sequences of HvNTR1, HvNTR2, AtNTR, and EcNTR (The residues corresponding to $R130_{EcNTR}$ and active sites are marked). C, The Close-up view of structural alignment of HvTrxh2 and EcTrx (from EcNTR-EcTrx complex) D, Close-up view of structural alignment between NADP-binding domains of AtNTR and EcNTR (from EcNTR-EcTrx complex). [In C and D: EcNTR is shown in the surface display and is colored gray. EcTrx, HvTrxh2, NADP-binding domain of EcNTR, and NADP-binding domain of AtNTR are shown in cartoon display and colored red, light blue, green and dark blue, respectively. The Trx loop involved in NTR interactions is positioned between the two indicated secondary structures and is colored yellow. The residues $R130_{EcNTR}$ and $R142_{AtNTR}$($R140_{HvNTR2}$) are shown in stick representation, labeled and colored green and dark blue, respectively].

Table 4.1. Kinetic parameters of wt and mutants HvNTR2 in reactions with wt and mutants HvTrxh1, HvTrxh2 and EcTrx

HvNTR2	**HvTrxh2**	K_m **(μM)**	k_{cat} **(s^{-1})**	K_{cat}/k_m **($s^{-1}M^{-1}$)**
Wt	Wt	1.04±0.31	3.39±0.69	3.25×10^6
R140A	Wt	4.3±0.98	1.21±0.11	0.28×10^6
R140M	Wt	4.5±1.28	1.16±0.25	0.25×10^6
Wt	M88G	4.46±0.70	5.54±1.22	1.24×10^6
Wt	M88A	4.3±0.16	4.47±1.03	1.02×10^6
Wt	M88L	3.5±0.32	4.54±1.10	1.20×10^6
Wt	M88P	2.9±0.12	0.10±.0.02	3.59×10^4
Wt	G105A	2.7±0.11	3.95±0.7	1.46×10^6
Wt	A106P	1.51±0.29	3.60±0.18	2.42×10^6
Wt	E86R	1.51±0.38	4.76±0.62	3.10×10^6
I154G	Wt	3.05±0.21	3.62±0.10	1.18×10^6
I154G	E86R	1.55±0.35	3.45±0.41	2.23×10^6
R140A	E86R	2.25±0.35	1.45±0.11	0.64×10^6
R140M	E86R	1.69±0.39	1.56±0.19	0.92×10^6
HvNTR2	**HvTrxh1**	K_m **(μM)**	k_{cat} **(s^{-1})**	K_{cat}/k_m **($s^{-1}M^{-1}$)**
Wt	Wt	0.7±0.12	3.25±0.19	4.60×10^6
R140A	Wt	3.1	1.08	0.34×10^6
R140M	Wt	3.6	1.08	0.30×10^6
Wt	M82G	9.05±1.34	3.2±0.35	0.35×10^6
HvNTR2	**EcTrxh**	K_m **(μM)**	k_{cat} **(s^{-1})**	K_{cat}/k_m **($s^{-1}M^{-1}$)**
Wt	Wt	117.6	3.10	2.69×10^4
I154G	Wt	42.98	0.42	0.99×10^4

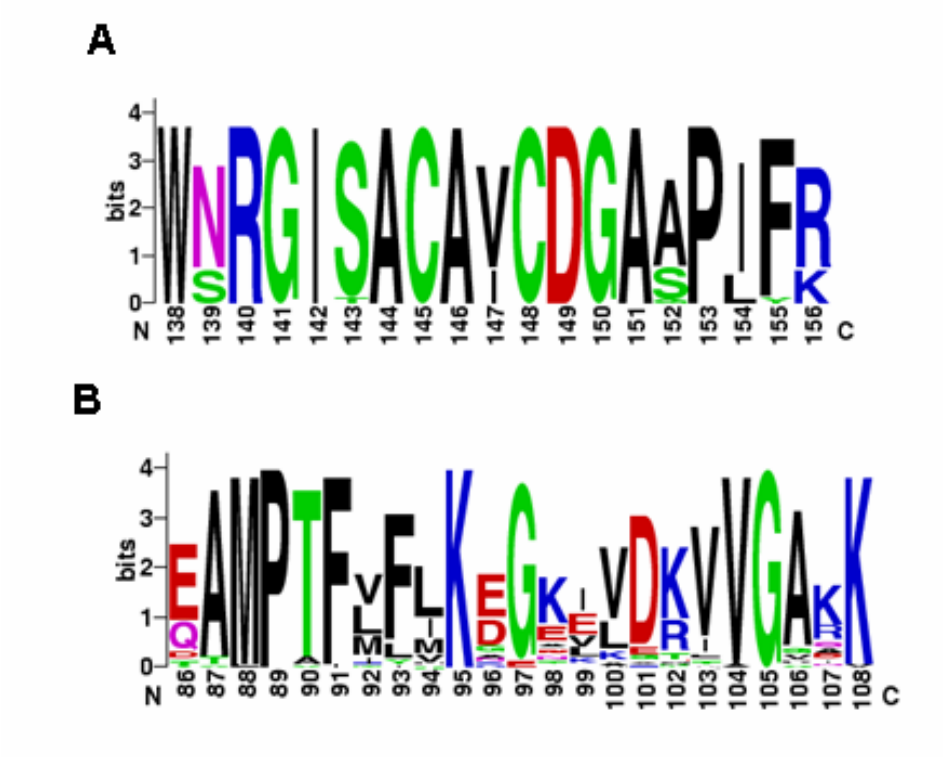

Figure 4.3. Sequence logos. A, Part of a sequence logo that was generated from 23 plant NTR amino acid sequences, which is showing the residues 138-156. The numbers are based on the HvNTR2 amino acid sequence. B, part of a sequence logo that was generated from 45 plant Trx h amino acid sequences showing the residues 86-108. The numbers are based on the HvTrxh2 amino acid sequence.

Table 4.2. Kinetic parameters of wt and mutants HvNTR2 with DTNB in the absence of HvTrx h.

HvNTR2	K_m **(mM)**	k_{cat} **(s^{-1})**	K_{cat}/k_m **($s^{-1}M^{-1}$)**
Wt	3.7	0.19	51.35
R140A	3.3	0.15	45.45
R140M	3.3	0.15	45.45
I154G	2.3	0.11	47.82

4.3.2. HvNTR-HvTrxh interaction specificity

The structural alignment of the NADP-binding domain of AtNTR with the NADP-binding domain of EcNTR (from EcNTR-EcTrx complex), suggests that part of the surface groove interacting with Trx loop (HvTrxh2 $loop_{83-89}$/EcTRx $loop_{70-76}$) in AtNTR is blocked by the side chain of $I156_{AtNTR}$ (corresponding to $I154_{HvNTR2/HvNTR1}$). Several amino acids in this region are not conserved between the NTRs from *E. coli* and plants (Fig. 4.4A). In the sequence alignment, the position of $I156_{AtNTR}$ is occupied by F142 in EcNTR. The 3D structure of EcNTR shows that the side chain of $F142_{EcNTR}$ does not interfere with the NTR surface groove (Fig. 4.4B). Therefore we speculated that the side chain of $I156_{AtNTR}$ ($I154_{HvNTR2, HvNTR1}$) might prevent the side chain of $R73_{EcTrx}$ (located in EcTrx $loop_{70-76}$) from fitting into the surface groove (Fig. 4.4C). This may explain the lower affinity of wt HvNTR2 or AtNTR towards EcTrx. Accordingly, the position of R73 in EcTrx is occupied by E86 in HvTrxh2 which has a smaller side chain, more likely to fit into the smaller groove on AtNTR or HvNTR (Fig 4.4D). As mentioned before the guanidine group of $R73_{EcTrx}$ forms two hydrogen bonds to the backbone CO group of $R130_{EcNTR}$ in EcNTR-EcTrx complex (Fig. 4.1). These hydrogen bonds are probably not present in HvNTR-HvTrxh interaction since $E86_{HvTrxh2}$ does not have a side chain guanidine group. $I156_{AtNTR}$ is highly conserved in plant NTRs or replaced by a leucine residue (Fig. 4.3A) and the position of $E86_{HvTrxh2}$ is occupied by glutamic acid, glutamine or aspartic acid in plant Trxhs (Fig. 4.3B), all of which have smaller side chains than arginine. Therefore, we hypothesized that the nature of amino acids present at the position of $E86_{HvTrxh2}$ and $I154_{HvNTR2}$ can be an important determinant for specificity of plant NTR-Trx h interaction. In other words, $I154_{HvNTR2}$ may cause incompatibility between plant NTR and EcTrx. Therefore to test this hypothesis $I154_{HvNTR2}$

was replaced by glycine ($I154G_{HvNTR2}$) to highly shorten the side chain and $E86_{HvTrxh2}$ was replaced by arginine ($E86R_{HvTrxh2}$) that is the corresponding residue in EcTrx.

4.3.2.1. Production of mutants, spectrophotometer and MS analysis

The recombinant His-tagged $I154G_{HvNTR2}$ was obtained in almost similar yield as wt HvNTR2. However, its solubility was found to be sensitive to pH, so that it was aggregated at pH 7.0 but it was soluble at pH 8.0. SDS-PAGE of $I154G_{HvNTR2}$ after purification showed the prominent bands with the expected molecular mass for HvNTR monomer and dimer (Fig. 4.5A). The mutant $I154G_{HvNTR2}$ was yellow and showed an absorbance spectrum (Fig. 4.5 B) similar to wt and other NTR mutants as explained above. The mutant $I154G_{HvNTR2}$ was verified at protein level by MS trypsin digestion peptide fingerprint. The peak of *m/z* 1664.782 Da which is assigned to $[M+H]^+$ of peptide $_{141}$GISACAVCDGAAPIFR$_{156}$ was replaced with the peak *m/z* 1608.726 (Fig. 4.6) corresponds to molecular mass of $_{141}$GISACAVCDGAAPGFR$_{156}$.

4.3.2.2. NTR assay with Trx

The kinetic parameters of wt HvNTR2 and NTR mutant $I154G_{HvNTR2}$ towards wt HvTrxh2, $E86R_{HvTrxh2}$ and EcTrx were determined (Table 4.1). The K_m value of wt HvNTR2 towards mutant $E86R_{HvTrxh2}$ was close to that of wt HvNTR2 towards wt HvTrxh2 with slightly higher k_{cat} value. Compared to wt HvNTR2, the k_{cat} value of $I154G_{HvNTR2}$ towards wt HvTrxh2 remained the same but the K_m value increased by 3-fold. However, the K_m of $I154G_{HvNTR2}$ was retained at the wt level when $E86R_{HvTrxh2}$ was used as a substrate. It is noticeable that the K_m value was also retained for $R140M_{HvNTR2}$ and $R140A_{HvNTR2}$ when $E86R_{HvTrxh2}$ was used as substrate. The K_m value of wt HvNTR2 towards EcTrx is more than 100-fold higher than that

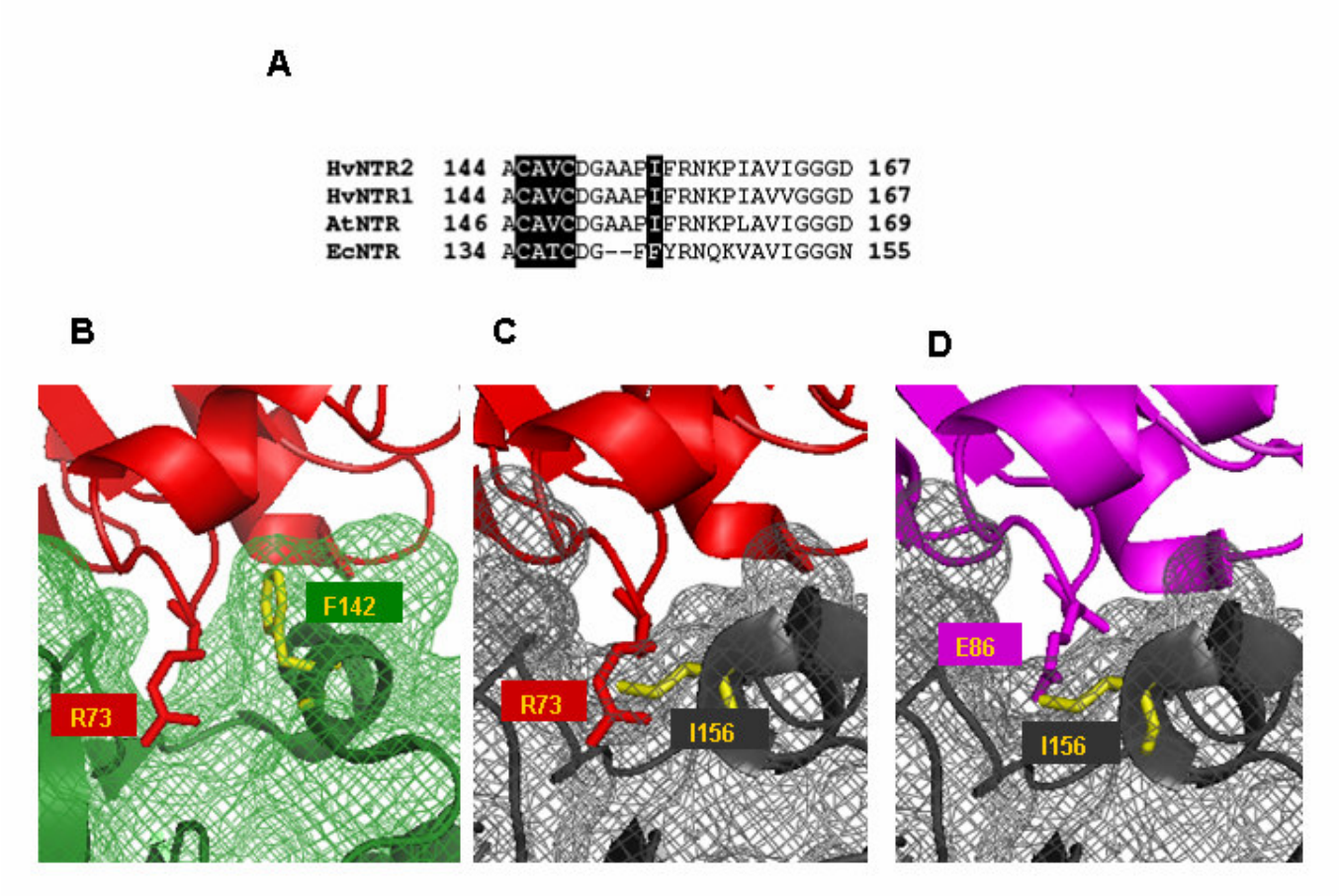

Figure 4.4. The possible role of $I154_{HvNTR2}$ and $E86_{HvTrxh2}$ in the specificity of the HvNTR-HvTrxh interaction . A, multiple alignment between HvNTR1, HvNTR2, AtNTR and EcNTR [The corresponding residues to $I156_{AtNTR}$ and NTR active site are marked]. The close-up view of 3D structure of B, EcNTR-EcTrx complex. C, EcTrx and NADP-binding domain of AtNTR after alignment with EcNTR-EcTrx complex. D, HvTrxh2 and NADP-binding domain of AtNTR after alignment with EcNTR-EcTrx complex. [In B, C, and D: NADP-binding domain of EcNTR and AtNTR are shown in both cartoon and mesh display, and are colored green and gray, respectively. EcTrx and HvTrxh2 are shown in cartoon display, and are colored red and pink, respectively. The residues $R73_{EcTrx}$, $E86_{HvTrxh2}$, $F142_{EcNTR}$, and $I156_{AtNTR}$ ($I154_{HvNTR2}$) are shown in stick representation, labeled, and colored red, pink, yellow, and yellow, respectively.]

of wt HvNTR2 towards HvTrxh2. The K_m value of $I154G_{HvNTR2}$ towards EcTrx was 3-fold less than that of wt HvNTR2 towards EcTrx, but the k_{cat} value decreased significantly by 7-fold.

4.3.2.3. NTR assay with DTNB in the absence of Trx

The apparent K_m and k_{cat} values for $I154G_{HvNTR2}$ were determined using DTNB as substrate (Table 4.2). The k_{cat} value for $I154G_{HvNTR2}$ was 57% of that from wt. The apparent K_m value for $I154G_{HvNTR2}$ decreased to 2.3 mM compared to 3.7 mM for wt HvNTR2. However, the catalytic efficiency (k_{cat}/K_m) of mutant $I154G_{HvNTR2}$ was very similar to that of wt HvNTR2.

4.3.3. The involvement of Trx target protein recognition motifs in HvNTR-HvTrx interaction

Structural motif composed of the $_{45}WCGP_{48}$, $_{87}AMP_{89}$ and $_{104}VGA_{106}$ loops (referred to as substrate recognition loop motifs) on the surface of HvTrxh2 has been demonstrated in the recognition of BASI as Trx target protein (Maeda et al., 2006a). The residue $M88_{HvTrxh2}$ ($M82_{HvTrxh1}$) which is located in Trx loop83-$89_{HvTrxh2}$ (Fig. 4.2 A) and $A106_{HvTrxh2}$ function to stabilize BASI binding by making two and one intermolecular backbone-backbone hydrogen bonds, respectively (Maeda et al., 2006a). Previously in our group in order to study of Trx-target protein (like BASI) interaction, the mutants $M82G_{HvTrxh1}$, $M88G_{HvTrxh2}$, and $M88A_{HvTrxh2}$ to shorten the side chain, and $M88L_{HvTrxh2}$ to retain a similar size hydrophobic side chain were constructed (Hägglund et al., unpublished data). In the same study to prevent of the formation of the backbone-backbone hydrogen bond between $M88_{HvTrxh2}$ or $A106P_{HvTrxh2}$ and residues in Trx-target protein (like BASI), mutants $M88P_{HvTrxh2}$ and $A106P_{HvTrxh2}$ were constructed because the backbone amino group of proline residues cannot

act as hydrogen donors for formation of backbone hydrogen bonds. In addition, $G105_{Hvtrxh2}$ which is strictly conserved in plant Trx h (Fig 4.3.B) was replaced with alanine. In the present work to examine whether $M88_{HvTrxh2}$, $M82_{HvTrxh1}$, $A106_{HvTrxh2}$ and $G105_{HvTrxh2}$ have also role in HvNTR-HvTrx interaction, the kinetic parameters of wt HvNTR2 towards these available mutants were compared to that of wt HvNTR2 towards wt HvTrxh isoforms. The study of the residue $M88_{HvTrxh2}$ ($M82_{HvTrxh1}$) was particularly interested because in the crystal structure of EcNTR-EcTrx complex a hydrogen bond is formed between the backbone NH group of $I75_{EcTrx}$ ($M88_{HvTrxh2}$/$M82_{HvTrxh1}$) and the side chain of $D139_{EcNTR}$ ($D149_{HvNTR2/HvNTR1}$).

4.3.3.1. NTR assay with Trx

The k_{cat} of wt HvNTR2 towards the mutants $M88G_{HvTrxh2}$, $M88A_{HvTrxh2}$ was slightly higher than that of wt HvNTR2 towards wt HvTrxh2 and the k_{cat} of wt HvNTR2 towards M82G was similar to that of HvNTR2 towards wt HvTrxh1 (Table 4.1). However, the K_m value of HvNTR2 increased by more than 4-fold towards the mutants $M88G_{HvTrxh2}$ and $M88A_{HvTrxh2}$ and by 9-fold towards mutant $M82G_{HvTrxh1}$. The K_m of wt HvNTR2 towards mutant $M88L_{HvTrxh2}$ increased by 3.5-fold with a similar k_{cat} as compared to that of wt HvNTR2 towards wt HvTrxh2. The wt HvNTR2 showed extremely weak k_{cat} towards the mutant $M88P_{HvTrxh2}$ as compared to that of wt HvNTR2 towards wt HvTrxh2. The kinetic parameters of HvNTR2 towards $A106P_{HvTrxh2}$ were similar to that of HvNTR2 towards wt HvTrxh2. The k_{cat} of wt HvNTR2 towards mutant $G105A_{HvTrxh2}$ was similar to that of wt HvNTR2 towards wt HvTrxh2 and the K_m value increased by 2.7-fold.

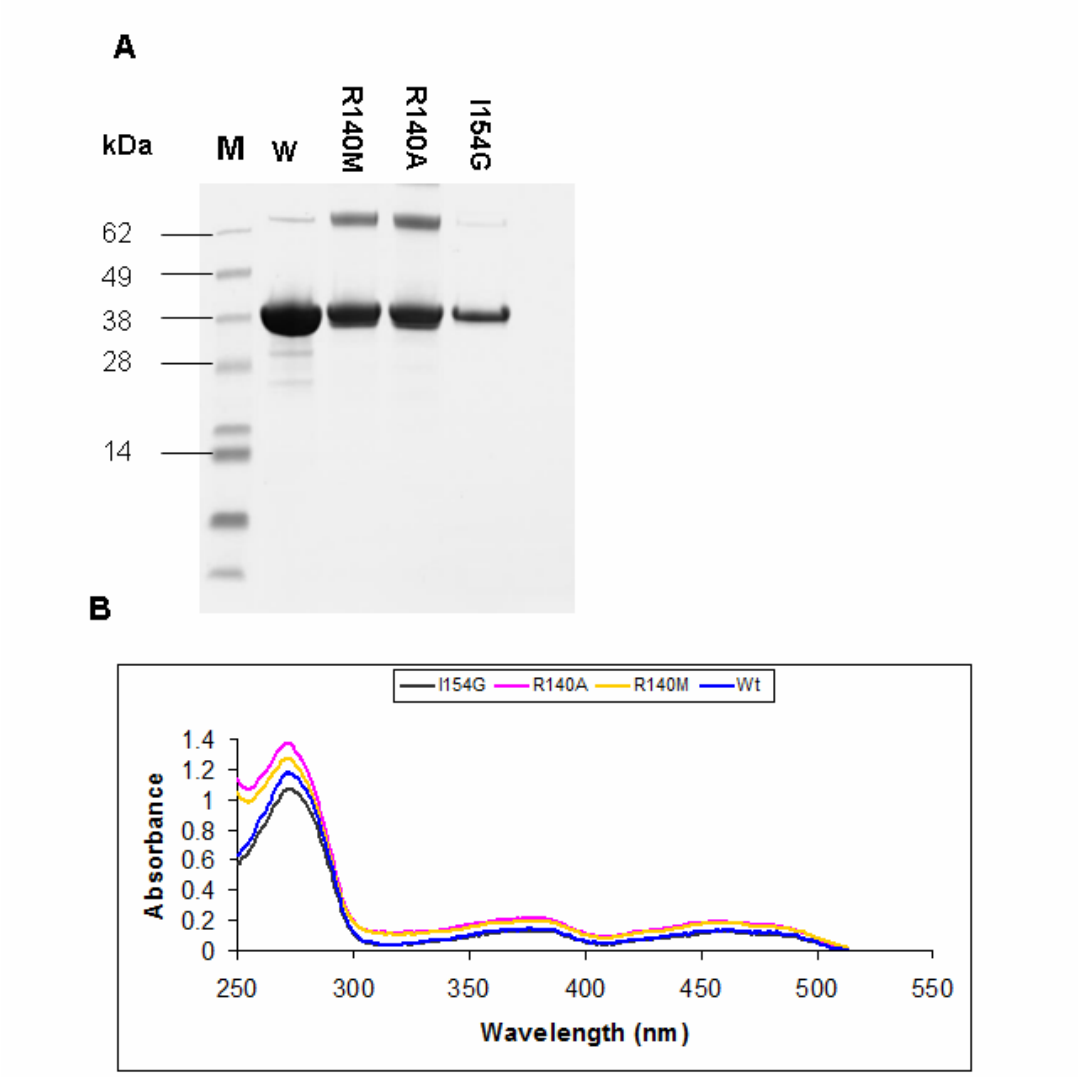

Figure 4.5. Heterologous expression of wt and mutants of His-HvNTR2 in *E. coli*. A, SDS-PAGE of wt and mutants after purification showing the bands corresponding to the molecular weight of dimer (top band) and monomer of HvNTR2 (bottom band). B, Absorption spectra of recombinant wt and mutants of HvNTR2.

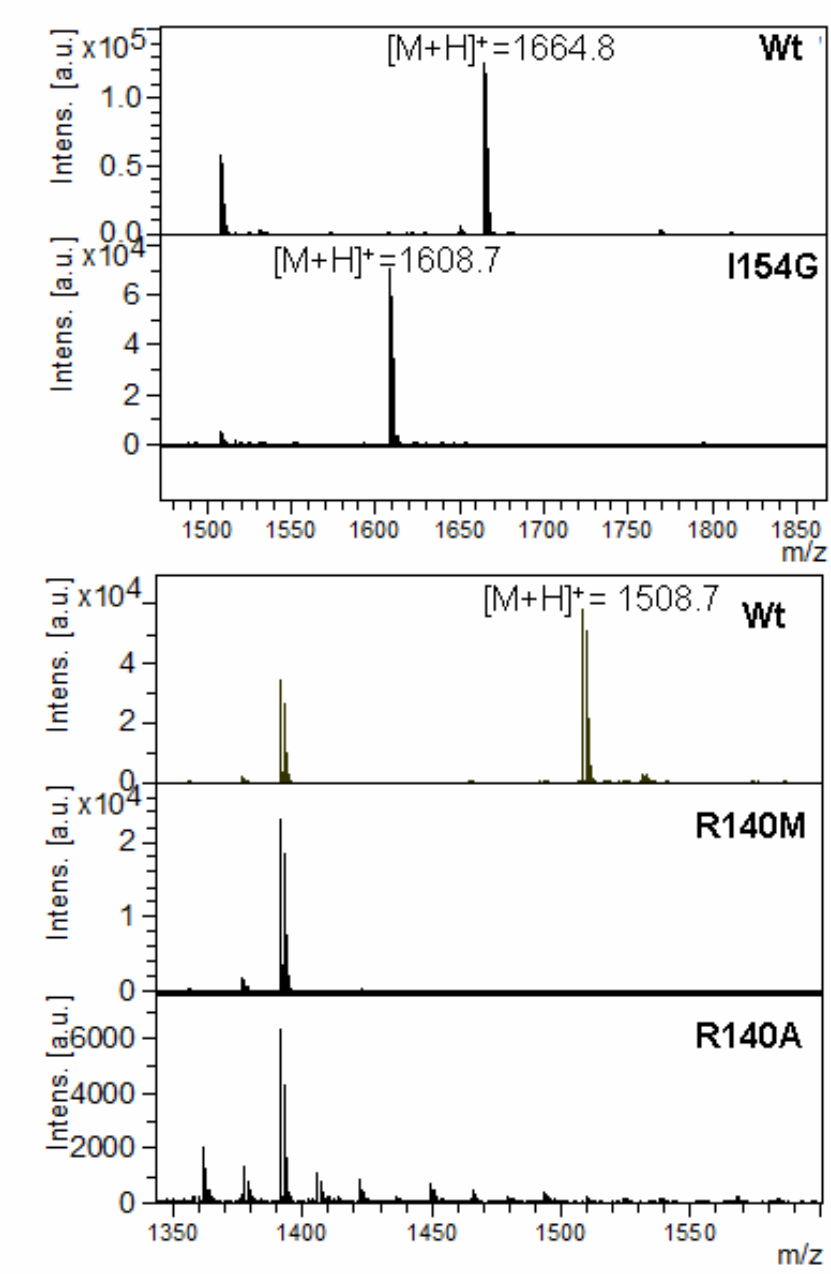

Figure 4.6. Trypsin digested peptide fingerprint of wt and mutants of HvNTR2 by MALDI-TOF MS.

4.4. Discussion

The wide range of physiological roles for Trxs in different organisms has provided strong purposes toward better understanding of the molecular mechanisms of reaction between Trx and other proteins involving the dithiol-disulfide interchange. The present work aimed to study the interaction between NTR and Trx h from barley using a 3D structure of EcNTR-EcTrx complex as a model to suggest mutagenesis targets in either HvNTR2 or HvTrxh isoforms.

4.4.1. The involvement of $R140_{HvNTR2}$ in HvNTR-HvTrxh interaction

The more than 10-fold decrease in the catalytic efficiency (k_{cat}/K_m) of HvNTR2 mutants $R140A_{HvNTR2}$ and $R140M_{HvNTR2}$ towards HvTrxh2 suggests that this residue has role in HvNTR-HvTrxh interaction. Since the replacement of $R140_{HvNTR2}$ by alanine or methionine removes the guanidine group, the results are in good agreement with the observation of the corresponding R130 guanidine group in EcNTR forming a hydrogen bond in EcNTR-EcTrx complex to the backbone CO group of $Y70_{EcTrx}$. This residue may be important for the general recognition mechanism of Trxs by NTR in many organisms since it is highly conserved. In addition, using DTNB as substrate in the absence of HvTrxh isoforms the kinetic parameters of mutants $R140A_{HvNTR2}$ and $R140M_{HvNTR2}$ was almost similar to that of wt HvNTR2. This may suggests that disulfide reductase activity of HvNTR2 is not affected by $R140_{HvNTR2}$ mutants. The decrease in activity of $R140A_{HvNTR2}$ and $R140M_{HvNTR2}$ is therefore dependent on Trx as substrate indicating the involvement of $R140_{HvNTR2}$ in HvNTR-HvTrxh interaction.

4.4.2 HvNTR-HvTrxh interaction specificity

Clearly, specificity exists for NTR and Trx interactions since the affinity of NTR is much higher towards the Trx from the same source (Juttner et al., 2000). Here we observed that wt HvNTR2 has much higher affinity (100-fold) towards wt HvTrxh isoforms than EcTrx. The replacement of $I154_{HvNTR2}$ by glycine enhanced the affinity of HvNTR2 by 3-fold towards EcTrx. However, a decrease (7-fold) in the catalytic activity (k_{cat}) resulted in a 2-fold decrease in catalytic efficiency (k_{cat}/K_m). Moreover, wt HvNTR2 showed similar affinity on both wt HvTrxh2 and $E86R_{HvTrxh2}$. These data does not support our hypothesis that $I154_{HvNTR2}$ causes incompatibility between plant NTRs and EcTrx.

A 3-fold decrease in affinity of $I154G_{HvNTR2}$ with similar catalytic activity towards wt HvTrxh2 compared to wt HvNTR2 may exclude the significant role of this residue in HvNTR-HvTrxh interaction. The affinity of mutants $I154G_{HvNTR2}$ and $R140M_{HvNTR2}$ towards $E86R_{HvTrxh2}$ were retained at the wt level. This may be due to backbone-side chain hydrogen bonds that can be formed with the guanidin group of arginine from $E86R_{HvTrxh2}$ in reaction with NTR as observed in EcNTR-EcTrx interaction (Fig. 4.1), but not with the E86 in wt HvTrxh2.

4.4.3. The involvement of Trx target protein recognition motifs in HvNTR-HvTrxh interaction

The catalytic activity of wt HvNTR2 towards the $M88_{HvTrxh2}$ and $M82_{HvTrxh1}$ mutants except $M88P_{HvTrxh2}$ was similar or slightly higher compared to that of wt HvNTR2 towards wt HvTrxh isoforms. However, decrease in affinity of wt HvNTR2 (4 to 9-fold) towards $M88G_{HvTrxh2}$, $M88A_{HvTrxh2}$, $M88L_{HvTrxh2}$ and $M82G_{HvTrxh1}$ compared to wt HvTrxh2 and wt HvTrxh1 indicates a role for $M88_{HvTrxh2}$ ($M82_{HvTrxh1}$) in HvNTR-HvTrxh interaction. This can

be extended to other plants since $M88_{HvTrxh2}$ ($M82_{HvTrxh2}$) is a highly conserved residue between plant Trx h (Fig 4.3B).

The catalytic activity of wt HvNTR2 towards $M88P_{HvTrxh2}$ dramatically decreased compared to wt HvTrxh2. Noticeably the mutant $M88P_{HvTrxh2}$ lost its activity (7% of wt) in an insulin assay (Holmgren, 1979) in which DTT was used as the electron donor for Trx and insulin was used as substrate (Hägglund et al., unpublished data). By contrast, $M88_{HvTrxh2}$ and $M82_{HvTrxh1}$ mutants showed a high level of activity (50-80% of wt) in the insulin assay (Hägglund et al., unpublished data). Therefore, the low k_{cat} of wt HvNTR2 towards $M88P_{HvTrxh2}$ may stem from an effect of this mutant on the disulfide reductase activity of HvTrxh2 independent of loosing of backbone-backbone hydrogen bond in interaction with NTR.

The role of $A106_{HvTrxh2}$ in the HvNTR-HvTrxh interaction can be excluded since the kinetic parameters of wt HvNTR2 towards $A106P_{HvTrxh2}$ was similar to that of wt HvNTR2 towards wt HvTrxh2. Although $G105A_{HvTrxh2}$ lost its activity in an insulin assay (Hägglund, unpublished data), the kinetic parameters of HvNTR2 towards G105A did not change significantly compared to the kinetic parameters of HvNTR2 towards wt HvTrxh2. This may suggests that $G105_{HvTrxh2}$ is involved mainly in Trx-target protein interactions and not in HvNTR-HvTrx interaction.

4.5. Conclusion

The present study attempts to use a protein-protein complex structure from *E. coli* as model to manipulate of NTR and Trx from barley as representative of plants to understand more about the plant NTR-Trx h interaction. The residues $R140_{HvNTR}$ and $M88_{HvTrxh2}$ ($M82_{HvTrxh1}$) found to be involved in the HvNTR-HvTrxh interaction which can be extended to NTR and Trx h from other plants. The importance of these residues which belong to the Trx loop83-$89_{HvTrxh2}$

and the NTR surface groove supports the involvement of these parts of the HvTrxh and HvNTR isoforms in the interaction as observed for the EcNTR-EcTrx interaction. Moreover the present study reveals the role of $M88_{HvTrxh2}$ in interaction with both Trx target proteins where Trx acts as electron donor and with NTR where Trx acts as electron acceptor. The effects of the mutants observed here in the most of the cases, however, are quite small and in no case, the mutants abolish or dramatically alter the interaction. Therefore, other residues or a combination of residues must have critical role in interaction. The crystal structure of HvNTR-HvTrxh remains to be solved and help to learn more about the plant NTR-Trx h interaction.

4.6. Materials and methods

4.6.1. Construction of HvNTR2 mutants

The replacement of the natural amino acids with the different ones was performed by using an *in vitro* site-directed mutagenesis method. The genes encoding HvNTR2 (Shahpiri et al., 2008), HvTrxh1 and HvTrxh2 (Maeda et al., 2003) inserted into plasmid pET15b containing a T7 promoter and N-terminal thrombin-cleavable His-tag (Novagen) were used as template. The polymerase chain reaction (PCR) was performed using Pfu Ultra High-fidelity DNA polymerase (Stratagene) and mutagenic primers (Table 4.3) in a reaction mixture containing template plasmid, deoxynucleotides and reaction buffer according to the manufacturer's instructions (Stratagene). The cycling parameters were 95 ^{o}C for 30 s, 55 ^{o}C for 1 min, and 69 ^{o}C for 7 min, 15 cycles. The PCR products were treated with restriction enzyme *Dpn*I (Stratagene) to digest methylated non-mutated parental DNA template and then transformed to either *E. coli* DH5α (home made competent cells) or NEB 5-alpha competent cells (New

England Biolabs). All mutations were confirmed by DNA sequencing at MWG Biotech (Ebserberg, Germany).

4.6.2. Heterologous expression of mutant proteins, purification, spectrophotometer and MS analysis

The *E. coli* strain Rosetta (DE3) cells were transformed using the plasmids carrying the mutations. Cells were grown at 37 ^{o}C in LB medium supplemented with ampicillin (100 µg/ml) and chloramphenicol (5 µg/ml) to an OD_{600} of 0.6. Cultures were induced with 100 µM isopropyl β-D-thiogalactopyranoside (IPTG) for 3.5 h. The soluble proteins were extracted from cells using bugbuster protein extraction reagent including benzonase nuclease (Novagen). After centrifugation supernatants were loaded onto His-Trap HP columns (Amersham Biosciences) preequilibrated with loading buffer (10 mM imidazole, 500 mM NaCl, 30 mM Tris-HCl, (pH 8.0) and eluted with gradient of 10-200 mM imidazole. Purified proteins were desalted using PD-10 columns (GE healthcare) against 10 mM Tris-HCl (pH 8.0). Protein concentration was determined by aid of amino acid analysis. The absorption spectrum was recorded for 8 µM NTR in 10 mM Tris-HCl (pH 8.0) at room temperature.

NTR mutants were also verified at the protein level using MS analysis. The purified proteins were loaded on SDS-PAGE and the gel was stained with colloidal Coomassie Brilliant Blue G-250 (Candiano et al., 2004). The bands cut out from the gel were in-gel digested with trypsin (Promega) as previously described (Finnie et al., 2002) and after micropurification (Gobom et al., 1999) directly loaded on MALDI target with 5 µg/µl α-cyano-hydroxy-cinnamic acid in 70% ACN and 0.1% TFA. An Ultraflex II MALDI-TOF-TOF mass spectrometer (Bruker-Daltonics, Bermen, Germany) was used in positive ion reflector mode

and spectra were analyzed using FlexAnalysis software (Bruker-Daltonics, Bermen, Germany).

4.6.3. NTR assay with Trx

The ability of NTR to catalyze the reduction of Trx by NADPH was examined in a NTR assay as described before (Krause and Holmgren, 1991) with slight modifications. The assay mixture contained 100 mM potassium phosphate (pH 7.5), 10 mM EDTA, 0.1 mg/ml bovine serum albumin (BSA), 200 µM DTNB [5,5´- dithio-bis (2-nitrobenzoic acid), Sigma-Aldrich], 200 µM NADPH (Sigma-Aldrich). The reaction containing of 1–7 µM HvTrxh1, HvTrxh2 or EcTrx (Sigma-Aldrich) was started with addition of 40 nM NTR. The reaction was monitored by measuring the rate of increase of absorbance at 412 nm reflecting the formation of TNB (2-nitro-5-thiobenzoic acid). Since 1 mol Trx-$(SH)_2$ reduces 1 mol DTNB to yield 2 mol of TNB with a molar extinction coefficient of 13,600 $M^{-1}cm^{-1}$ (Ellman, 1959), a molar extinction coefficient of 27,200$M^{-1}cm^{-1}$was applied for the quantification. The reaction velocity as a function of the Trx concentration was plotted and the Michaelis-Menton kinetic parameters were calculated by using Lineweaver-Burk plot.

4.6.4. NTR activity with DTNB in the absence of Trx

Activities of NTR mutants as well as wt NTR were determined using DTNB in the absence of Trx (Holmgren, 1977). The reaction mixture was prepared as described above but with much higher concentrations of DTNB (1-10 mM) and NTR (240 nM). A DTNB stock solution was prepared in 96% ethanol. The rate of reduction of DTNB was calculated from the absorbance in 412 nm as described above and the reaction velocity as a function of the DTNB

concentration was plotted and the Michaelis-Menton kinetic parameters were calculated by using Lineweaver-Burk plot.

4.6.5. Structure and sequence analysis

Multiple alignments were performed using ClustalW2 (http://www.ebi.ac.uk/Tools/clustalw2/index.html; Larkin et al., 2007). The sequence logo was created using WebLogo (http://weblogo.berkeley.edu/logo.cgi; Crooks et al., 2004). Figures of protein structures were made in PyMOL (http://pymol.sourceforge.net; Delano, 2002). The protein accession numbers in National Center for Biotechnology Information (NCBI) or Swiss-Prot databases: AtNTR (Q39243), HvNTR1 (ABY27300), HvNTR2 (ABX09990), EcNTR (P09625), AtTrxh1 (P29448), HvTrxh2 (AAP72290), HvTrxh2 (AAP72291), EcTrx (P0AA25).

Table 4.3. Sequence of the sense primers used for site-directed mutagenesis.

HvNTR2 mutants	
$R140A_{HvNTR2}$	5'-cacctactggaacgccggcatctccgcc-3'
$R140M_{HvNTR2}$	5'-cgacacctactggaacatgggcatctccgcctgcg-3'
$I154G_{HvNTR2}$	5'-gacggcgctgcgcccgggttccggaacaagccc-3'

Concluding remarks and perspectives

The barley aleurone layer is an ideal system for study of germination signaling. During the present Ph.D. study this system was well established in the lab and parallel profiles for gene expression, protein appearance in the aleurone layer and release of proteins to the culture supernatant responding to hormones gibberellic acid (GA) and abscisic acid (ABA) were demonstrated. Thus the aleurone layer culture system has been carefully characterized with respect to appearance of marker genes and proteins like α-amylase and limit dextrinase and has provided an excellent framework for study the role of hormones and other signals such as reactive oxygen species and reactive nitrogen species in regulation of seed germination. Moreover, the characterization of this system together with good resolution 2D-gel from soluble proteins extracted from aleurone layer has provided a basis for proteome analysis in aleurone layer and study of the changes in proteome responding to hormone signals. This may lead to identification of new proteins regulated with hormones in cereal seeds.

The present Ph.D. project describes the cloning, characterization and the first comparison of two NADPH-dependent thioredoxin reductase isoforms (HvNTR1 and HvNTR2) from barley. Their gene expression and protein profiles were analyzed in parallel with the two thioredoxin h isoforms (HvTrxh1 and HvTrxh2) in barley seed tissues. The data presented here indicate that the HvNTR2 and HvTrxh1 could be the dominant isoforms in aleurone layer of barley seeds. We provided evidence for differential regulation of NTR gene expression in seed tissues and demonstrated that the expression of HvNTR2 is affected by GA. Production of the recombinant proteins also allowed the first study of reciprocal interactions between NTR and Trx h isoforms from the same species. The present study suggests that Trx and NTR isoforms can function interchangeably. We demonstrated for the first time that the barley seed NTR/Trx system is active at the acidic pH expected to exist in the germinating starchy

endosperm. The HvNTR isoforms identified here have high homology with respect to both amino acid sequence and kinetic properties. Thus determination of intracellular localization of individual NTR isoforms and promoter structure, may clarify their possible *in vivo* functions. This also will help to explain their differential expression pattern in response to hormones. Furthermore the cloning of barley NTR genes and heterologous expression of NTR isoforms in considerable amounts (30 and 10 mg/ L HvNTR1 and HvNTR2, respectively) provided a basis for determining the 3D structure of a protein-protein complex of NTR-Trx for first time in plants. This study currently is going on by a Ph.D. student in our group. In parallel, the present Ph.D. project has attempted to use the structure of *E.coli* NTR-Trx complex as model for design and characterization of NTR and Trx h mutants to investigate the interaction between NTR and Trx h from barley. The present study suggests that $R140_{HvNTR2}$ and $M88_{HvTrxh2}$ ($M82_{HvTrxh1}$) may have role in barley HvNTR-HvTrxh interaction. However, the effects of mutants provided in this study did not change the kinetic parameters by a very big amounts compared to wild types, so these are not critical residues for interaction between these proteins. However, this study provides a new step forward to better understanding of HvNTR-HvTrxh interaction.

Finally, the knowledge achieved in the present Ph.D. project provides useful insights in understanding the molecular mechanisms influencing development, germination, and environment stress resistance of cereal seeds which can ultimately be applied for improvement of these important properties.

References

Alkhalfioui F, Renard M, Montrichard F (2007a) Unique properties of NADP-thioredoxin reductase C in legumes. J Exp Bot **58**: 969-978

Alkhalfioui F, **Renard M**, **Vensel WH**, **Wong J**, **Tanaka CK**, **Hurkman WJ**, **Buchanan BB**, **Montrichard F** (2007b) Thioredoxin-linked proteins are reduced during germination of *Medicago truncatula* seeds. Plant Physiol **144**: 1559-1579

Aman P, Hesselman K, Tilly AC (1985) The variation in chemical composition of Swedish barleys. J Cereals Sci **3**: 73-77

Arnér ES, Holmgren A (2000) Physiological functions of thioredoxin and thioredoxin reductase. Eur J Biochem. **267**: 6102-6109

Bailly C (2004) Active oxygen species and antioxidants in seed biology. Seed Sci Res **14**: 93-107

Bak-Jensen KS , Laugesen S, Roepstorff P , Svensson B (2004) Two-dimensional gel electrophoresis pattern (pH 6-11) and identification of water-soluble barley seed and malt proteins by mass spectrometry. Proteomics **4**: 728-742

Bak-Jensen KS, Laugesen S, Østergaard O, Finnie C, Roepstorff P, Svensson B (2007) Spatio-temporal profiling and degradation of α-amylase isozymes during barley seed germination. FEBS J **274**: 2552-2565

Baulcombe DC, Buffard D (1983) Gibberellic-acid-regulated expression of α-amylase and six other genes in wheat aleurone layer. Planta **157**: 493-501

Benjamin AM, Jones RL (1982) α-amylase secretion by single barley aleurone layer. Plant Physiol **70**: 1149-1155

Bertoft E, Andtfolk C, Kulp SE (1984) Effect of pH, temperature, and calcium-ions on barley malt α-amylase isoenzymes. J Inst Brew **90**: 298-302

Besse I, **Wong JH**, **Kobrehel K**, **Buchanan BB** (1996) Thiocalsin: a thioredoxin-linked, substrate-specific protease dependent on calcium. Proc Natl Acad Sci USA **93**: 3169-3175

Bethke PC, Schuurink R, Jones RL (1997) Hormonal signaling in cereal aleurone. J Exp Bot **48**: 1337-1356

Bethke PC, Lonsdale JE, Fath A, Jones RL (1999) Hormonally regulated programmed cell death in barley aleurone cells. Plant Cell **11**: 1033-1046

Bethke PC, Jones RL (2001) Cell death of barley aleurone layer protoplasts is mediated by reactive oxygen species. Plant J **25**: 19-29

Bethke PC, Fath A, Spiegel YN, Hwang YS, Jones RL (2002) Abscisic acid, gibberellin and cell viability in cereal aleurone. Euphytica **126**: 3-11

Bethke PC, Hwang YS, Tong Z, Russell LJ (2006) Global patterns of gene expression in the aleurone of wild type and *dwarf1* mutant rice. Plant Physiol **140**: 484-498

Bewley, JD, Black, M (1994) Seeds: Physiology of Development and Germination. New York, Plenum. PP. 1-33

Bewley JD (1997) Seed germination and dormancy. Plant Cell **9**: 1055-1066

Bower MS, Matias DD, Fernandes-Carvalho E, Mazzurco M, Gu TS et al. (1996) Two members of the thioredoxin h family interact with the kinase domain of a Brassica S locus receptor kinase. Plant Cell **8**: 1641-1650

Bowler C, Van Montague M, Inzé D (1992) Superoxide dismutase and stress tolerance. Annu Rev Plant Physiol Plant Mol Biol **43**: 83-116

Boyd R (1997) Electrospray ionization mass spectrometry: fundamentals, instrumentation, and applications. J Am Soc Mass Spectrom **8**:1191-1192

Bønsager BC, **Finnie C**, **Roepstorff P**, **Svensson B** (2007) Spatio-temporal changes in germination and radical elongation of barley seeds tracked by proteome analysis of dissected embryo, aleurone layer, and endosperm tissues. Proteomics **7**: 4528-4540

Brehelin C, Laloi C, Setterdahl AT, Knaff DB, Meyer Y (2004) Cytosol, mitochondrial thioredoxins and thioredoxin reducatses in *Arabidopsis thaliana*. Photosynth Res **79**: 295-304

Buchanan BB (1980) Role of the light in the regulation of chloroplast enzymes. Annu Rev Plant Physiol **31**: 341-374

Buchanan BB (1991) Regulation of CO_2 assimilation in oxygen photosynthesis: the ferredoxin/thioredoxin system: perspective on its discovery, present status, and future development. Arch Biochem Biophys **288**: 1-9

Buchanan BB, Balmer Y (2005) Redox regulation: A broading horizon. Annu Rev Plant Biol **56**: 187-220

Burton RA, Zhang XQ, Hrmova M, Fincher GB (1999) A single limit dextrinase gene is expressed both in the developing endosperm and in germinated grians of barley. Plant Physiol **119**: 859-871

Cabrillac D, Cock JM, Dumas C, Gaude T (2001) The S-locus receptor kinase is inhibited by thioredoxins and activated by pollen coat proteins. Nature **410**: 220-223

Candiano G, Bruschi M, Musante L, Santucci L, Ghiggeri GM, Carnemolla B, Orecchia P, Zardi L, Righetti PG (2004) Blue silver: a very sensitive colloidal Coomassie G-250 staining for proteome analysis. Electrophoresis **25**: 1327-1333

Casaretto J, Ho THD (2003) The transcription factors HvABI5 and HvVP1 are required for the abscisic acid induction of gene expression in barley aleurone cells. Plant Cell **15**: 271-284

Caspers MP, **Lok F**, **Sinjorgo KM**, **van Zeijl MJ**, **Nielsen KA**, **Cameron-Mills V** (2001) Synthesis, processing and export of cytoplasmic endo-beta-1,4-xylanase from barley aleurone during germination. Plant J **26**: 191-204

Cazalis R, Pulido P, Aussenac T, Pérez-Ruiz JM, Cejudo FJ (2006) Cloning and characterization of three thioredoxin h isoforms from wheat showing differential expression in seeds. J Exp Bot **57**: 2165-2172

Chandler PM, Marion-Poll A, Ellis M, Bubler F (2002) Mutants at the *Slender1* locus of barley cv himalaya. Molecular and physiological characterization. Plant Physiol **129**: 181-190

Chen K, An YQC (2006) Transcriptional responses to gibberellin and abscisic acid in barley aleurone. J Integr Plant Biol **48**: 591-612

Cho MJ, Wong JH, Marx C, Jiang W, Lemaux PG, Buchanan BB (1999) Overexpression of thioredoxin h leads to enhanced activity of starch debranching enzyme (pullulanase) in barley grain. Proc Natl Acad Sci USA **96**: 14641-14646

Cotter RJ (1999) The new time-of-flight mass spectrometry. Anal Chem. **71**: 445-451

Crooks GE, Hon G, Chandonia JM, Brenner SE (2004) WebLogo: A sequence logo generator. Genome Res **14**: 1188-1190

Dai S, Saarinen M, Ramaswamy S, Meyer Y, Jacquot JP, Eklund H (1996) Crystal structure of *Arabidopsis thaliana* NADPH dependent thioredoxin reductase at 2.5 Å resolution. J Mol Biol **264**: 1044-1057

DeLano WL (2002) The PyMOL molecular graphics system DeLano scientific, Palo Alto, CA, USA.

Dalle-Donne I, **Rossi R**, **Giustarini D**, **Colombo R**, **Milzani A** (2008) Molecular mechanisms and potential clinical significance of S-Glutathionylation. Antioxid Redox Signal **10**: 445-474

Danpure CJ (1995) How can the products of a single gene be localized to more than one intracellular compartment? Trends Cell Biol **5**: 230-238

Day DA, Tuite MF (1998) Post-transcriptional gene regulatory mechanisms in eukaryotes: an overview. J Endocrinol **157**: 361-371

de Hoog CL, Mann M (2004) Proteomics. Annu. Rev Genomics Hum Genet **5**: 267-293

Dominguez F, Cejudo FJ (1999) Patterns of starchy endosperm acidification and protease gene expression in wheat grains following germination. Plant Physiol **119**: 81-88

Ellman GL (1959) Tissue sulfhydryl groups. Arch Biochem Biophys **82**: 70-77

Fath A, Bethke PC, Jones RL (2001) Enzymes that scavenge reactive oxygen species are down-regulated prior to gibberellic acid-induced programmed cell death in barley aleurone. Plant Physiol **126**: 156-166

Finkelstein RR, Lynch TJ (2000) The Arabidopsis abscisic acid response gene ABI5 encodes a basic leucine zipper transcriptin factor. Plant Cell **12**: 599-609

Fincher GB (1992) Cell wall metabolism in barley. In: Shewry PR (Ed.) Barley: Genetics, Biochemistry, Molecular Biology and Biochemistry. Wallingford UK, CAB international, PP. 413-437

Finnie C, Melchior S, Roepstorff P, Svensson B (2002) Proteomics analysis of grain filling and seed maturation in barley. Plant Physiol **129**: 1308-1319

Finnie C, Svensson B (2003) Feasibility study of a tissue-specific approach to barley proteome analysis: aleurone layer, endosperm, embryo and single seeds. J Cereal Sci **38**: 217-227

Finnie C, Bak-Jensen KS, Laugesen S, Roepstorff P, Svensson B (2006) Differential appearance of isoforms and cultivar variation in protein temporal profiles revealed in the maturing barley grain proteome. Plant Sci **170**: 808-821

Fischbeck G (2002) Contributiion of barley to agriculture: A brief overview. In: Slafer GA, Molina-Cano JL, Savin R, Araus JL, Romagosa I (Eds.) Barley Science: Recent Advances from Molecular Biology to Agronomy of Yield and Quality. New York, Haworth. PP. 1-10

Frommer WB, Ninnemann O (1995) Heterologous expression of genes in bacteria, animal, and plant cells. Annu Rev Plant Physiol Plant Mol Biol **46**: 419-444

Furtado A, **Henry R**, **Scott K**, **Meech S** (2003) The promoter of the *asi* gene directs expression in the maternal tissues of the seed in transgenic barley. Plant Mol Biol **52**: 787-799

Gasdaska PY, Gasdaska JR, Cochran S, Powis G (1995) Cloning and sequencing of a human thioredoxin reductase. FEBS Let **373**: 5-9

Gautier MF, Lullien-Pellerin V, de Lamotte-Guéry F, Guirao A, Joudrier P (1998) Characterization of wheat thioredoxin h cDNA and production of an active *Triticum aestivum* protein in *Escherichia coli*. Eur J Biochem **252**: 314-324

Gelhaye E, Rouhier N, Jacquot JP (2003) Evidence for a subgroup of thioredoxin h that requires GSH/Grx for its reduction. FEBS Lett **555**: 443-448

Gelhaye E, Rouhier N, Jacquot JP (2004) The thioredoxin h system of higher plants. Plant Physiol Biochem **42**: 265-271

Gelhaye E, Rouhier N, Navrot N, Jacquot JP (2005) The plant thioredoxin system. Cell Mol Life Science **62**: 24-35

Gelhaye E, Navrot N, Macdonald IK, Rouhier N, Raven EL, Jacquot JP (2006) Ascorbate peroxidase-thioredoxin interaction. Photosynth Res **89**: 193-200

Gilroy S, Jones RL (1994) Perception of gibberellin and abscisic acid at the external face of the plasma membrane of barley (*Hordeum vulgare* L.) aleurone protoplasts. Plant Physiol **104**: 1185–1192

Girke T, Todd J, Ruuska S, White J, Benning C, Ohlrogge J (2000) Microarray analysis of developing arabidopsis seeds. Plant Physiol **124**: 1570-1581

Gladyshev VN, Jeang KT, Stadtman TC (1996) Selenocysteine, identified as the penultimate C-terminal residue in human T-cell thioredoxin reductase, corresponds to TGA in the human placental gene. Proc Natl Acad Sci USA **93**: 6146-6151

Gobom J, Nordhoff E, Mirgorodskaya E, Ekman R, Roepstorff P (1999) Sample purification and preparation technique based on nano-scale reversed-phase columns for the sensitive analysis of complex peptide mixtures by matrix-assisted laser desorption/ionization mass spectrometry. J Mass Spectrom **34**: 105 –116

Gomez-Cadenas A,Verhey SD, Holappa LD, Shen Q, Ho THD, Walker-Simmons MK (1999) An abscisic acid-suppressed gene expression in barley aleurone layer. Proc Natl Acad Sci USA **96**: 1767-1772

Gomez-Cadenas A, **Zentella R**, **Walker-Simmons MK**, **Ho TH** (2001) Gibberellin/abscisic acid antagonism in barley aleurone cells: site of action of the protein kinase PKABA1 in relation to gibberellin signaling molecules. Plant Cell **13**: 667-679

Gubler F, Ashford AE, Jacobsen JV (1987) The release of α-amylase through gibberellin-treated barley aleurone cell walls. Planta **172**: 155-161

Gubler F, **Chandler PM**, **White RG**, **Llewellyn DJ**, **Jacobsen JV** (2002) Gibberellin signaling in barley aleurone cells. Control of SLN1 and GAMYB expression. Plant Physiol **129**: 191-200

Gygi SP, Rochon Y, Franza BR, Aebersold R (1999) Correlation between protein and mRNA abundance in yeast. Mol Cell Biol **19**: 1720-1730

Hara S, Motohashi K, Arisaka F, Romano PGN, Hosoya-Matsuda N, Kikuchi N, Fusada N, Hisabori T (2006) Thioredoxin-h1 reduces and reactivates the oxidized cytosolic malate dehydrogenase dimmer in higher plants. J Biol Chem **281**: 32065-32071

Hara-Nishimura L, Nishimura M, Daussant J (1986) Conversion of free β-amylase to bound β-amylase on starch granules in the barley endosperm during desiccation phase of seed development. Protoplasma **134**: 149-153

Heukeshoven J, Dernick R (1985) Improved silver staining procedure for fast staining in PhastSystem Development Unit. I. Staining of sodium dodecyl sulfate gels. Electrophoresis **9**: 28-32

Hirasawa M, Schürmann P, Jacquot JP, Manieri W, Jacquot P, Keryer E, Hartman FC, Knaff DB (1999) Oxidation-reduction properties of chloroplast thioredoxins, ferredoxin:thioredoxin reductase, and thioredoxin f-regulated enzymes. Biochemistry **38**: 5200-5205

Ho THD, Gomez-Cadenas A, Zentella R, Casaretto J (2003) Crosstalk between gibberellin and abscisic acid in cereal aleurone layer. Plant Growth Regul **22**: 185-194

Holmgren A (1977) Bovine thioredoxin system. J Biol Chem **252**: 4600-4606

Holmgren A (1979) Thioredoxin catalyzes the reduction of insulin disulfides by dithiothreitol and dihydrolipoamide. J Biol Chem. **254**: 9627-9632

Holmgren A (1989) Thioredoxin and glutaredoxin system. J Biol Chem. **264**: 13963-13966

Holmgren A (2008) The thioredoxin system. In: Banerjee R, Becker D, Dickman M, Gladyshev V, Ragsdale S (Eds.) Redox Biochemistry. New Jersey, Wiley-Interscience, PP. 68-74

Hong B, Uknes SJ, Ho THD (1988) Cloning and characterization of a cDNA encoding a mRNA rapidly-induced by ABA in barley aleurone layers. Plant Mol Biol **11**: 495-506

Hobo T, Asada M, Kowyama Y, Hattori T (1999) ACGT-containing abscisic acid response element (ABRE) and coupling element 3 (CE3) are functionally equivalent. Plant J **19**: 679-689

Hooley R, Beale MH, Smith SJ (1991) Gibberellin perception at the plasma membrane of *Avena fatua* aleurone protoplasts. Planta **183**: 274–80

Huang, AHC, Trelease RN, Moore TS (1983) Plant peroxisomes. London, Academic Press.

Hynek R, **Svensson B**, **Jensen ON**, **Barkholt V**, **Finnie C** (2006) Enrichment and identification of integral membrane proteins from barley aleurone layers by reversed-phase chromatography, SDS-PAGE, and LC-MS/MS. J Proteome Res **5**: 3105-3113

Ikeda A, **Ueguchi-Tanaka M**, **Sonoda Y**, **Kitano H**, **Koshioka M**, **Futsuhara Y**, **Matsuoka M**, **Yamaguchi J** (2001) slender rice, a constitutive gibberellin response mutant, is caused by a null mutation of the *SLR1* gene, an ortholog of the height-regulating gene *GAI*/*RGA*/*RHT*/*D8*. Plant Cell **13**: 999-1010

Ishiwatari Y, Honda C, Kawashima I, Nakamura S, Hirano H, Mori S, Fujiwara T, Hayashi H, Chino M (1995) Thioredoxin h is one of the major proteins in rice phloem sap. Planta **195**: 456-463

Jacquot JP, Rivera-Madrid R, Marinho P, Kollarova M, Le Maréchal P, Miginiac-Maslow M, Meyer Y (1994) *Arabidopsis thaliana* NADPH thioredoxin reductase. cDNA characterization and expression of the recombinant protein in *Escherichia coli*. J Mol Biol **235**: 1357-1363

Jacquot JP, Lancelin JM, Meyer Y (1997) Thioredoxins: structure and function in plant cells. New physiol **136**: 543-570

Juge N,Andersen JS, Tull D, Roepstorff P, Svensson B (1996) Overexpression, purification and characterization of barley α-amylases 1 and 2 secreted by the Methylotrophic yeast *Pichia Pastoris.* Protein Expr Purif **8**: 204-214

Juttner J, **Olde D**, **Langridge P**, **Baumann U** (2000) Cloning and expression of a distinct subclass of plant thioredoxins. Eur J Biochem **267**: 7109-7117.

Kadokura H, Beckwith J, Gilbert HF (2008) Oxidative Folding. In: Banerjee R, Becker D, Dickman M, Gladyshev V, Ragsdale S (Eds.) Redox Biochemistry. New Jersey, Wiley-Interscience, PP. 113-120

Kallis GB, Holmgren A (1980) Differential reactivity of the functional sulfhydryl groups of cysteine-32 and cysteine-35 present in the reduced form of thioredoxin from *Escherichia coli*. J Biol Chem **255**: 10261-10265

Kobrehel K, Yee BC, Buchanan BB (1991) Role of the NADP/thioredoxin system in the reduction of alpha-amylase and trypsin inhibitor proteins. J Biol Chem **266**: 16135-16140

Kobrehel K, Wong JH, Balogh A, Kiss F, Yee BC, Buchanan BB (1992) Specific reduction of wheat storage proteins by thioredoxin h. Plant Physiol **99**: 919-924

Knochbin S, Gorka C, Lawrence JJ (1991) Multiple control level governing H10 mRNA and protein accumulation. FEBS Lett **283**: 65-67

Krause G, **Holmgren A** (1991) Substitution of the conserved tryptophan 31 in *Escherichia coli* thioredoxin by site-directed mutagenesis and structure-function analysis. J Biol Chem **266**: 4056-4066

Kristensen M, Planchot V, Abe J, Svensson B (1998) Large-scale purification and characterization of barley limit dextrinase, a member of the α-amylase structural family. Cereal Chem **75**: 473-479

Kristensen M, Lok F, Vèronique P, Svendsen I, Leah R, Svensson B (1999) Isolation and characterization of the gene encoding the starch debranching enzyme limit dextrinase from germinating barley. Biochem Biophys Acta **1431**: 538-546

Krnajski Z, Gilberger TW, Walter RD, Müller S (2001) The malaria parasite *Plasmodium falciparum* possesses a functional thioredoxin system. Mol Biochem Parasitol **112**: 219-228

Kulmar JK, Tabor S, Richardson CC (2004) Proteomic analysis of thioredoxin-target proteins in *Esherichia coli*. Proc Natl Acad Sci USA **101**: 3759-3764

Kurella M, **Hsiao LL**, **Yoshida T**, **Randall JD**, **Chow G**, **Sarang SS**, **Jensen RV**, **Gullans SR** (2001) DNA microarray analysis of complex biologic processes. J Am Soc Nephrol **12**: 1072-1078

Larkin MA, Blackshields G, Brown NP, Chenna R, McGettigan PA, McWilliam H, Valentin F, Wallace IM, Wilm A, Lopez R, Thompson JD, Gibson TJ, Higgins DG (2007) Clustalw2 and clustalX version 2. Bioinformatics **23**: 2947-2948

Lacey BM, Hondal RJ (2006) Characterization of mitochondrial thioredoxin reductase from *C. elegans*. Biochem Biophys Res Commun **346**: 629-636

Laloi C, Rayapuram N, Chartier Y, Grienenberger JM, Bonnard G, Meyer Y (2001) Identification and characterization of a mitochondrial thioredoxin system in plants. Proc Natl Acad Sci USA **98**: 14144-14149

Lauriere C, Lauriere M, Daussant J (1986) Immunohistochemical localization of β-amylase in resting barley seeds. Physiol Plant **67**: 383-388

Leipzig J, **Pevzner P**, **Heber S** (2004) The alternative splicing gallery (ASG): bridging the gap between genome and transcriptome. Nucleic Acids Res **32**:3977-3983

Lennon BW, Williams CH Jr, Ludwig ML (2000) Twists in catalysis: alternating conformations of *Escherichia coli* thioredoxin reductase. Science **289**: 1190-1194

Leung J, Giraudat J (1998) Abscisic acid signal transduction. Annu Rev Plant Physiol. Plant Mol. Biol **49**: 199-222

Longstaff MA, **Bryce JH** (1993) Development of limit dextrinase in germinated barley (*Hordeum vulgare* L.). Plant Physiol **101**: 881-889

Lou MF (2008) Antioxidant enzymes. In: Banerjee R, Becker D, Dickman M, Gladyshev V, Ragsdale S (Eds.) Redox Biochemistry. New Jersey, Wiley-Interscience, PP. 50-131

Lozano RM, Wong JH,Yee BC, Peters A, Kobrehel K, Buchanan BB (1996) New evidence for a role for thioredoxin h in germination and seedling development. Planta **200**: 100-106

MacGregor AW, Fincher GB (1993) Carbohydrates of the barley grain. In: MacGregor AW, Bhatty RS (Eds.) Barley: Chemistry and Technology. St. Paul, Minn. (USA), American Association of cereal chemists, PP. 73-130

MacGregor EA (2004) The proteinaceous inhibitor of limit dextrinase in barley and malt. Biochimica et Biophysica Acta **1696**: 165-170

Macheroux P (1999) UV-Visible spectroscopy as a tool to study flavoproteins. Methods Mol Biol **131**: 1-8

Maeda K, Finnie C, Østergaard O, Svensson B (2003) Identification, cloning and characterization of two thioredoxin h isoforms, HvTrxh1 and HvTrxh2, from the barley seed proteome. Eur J Biochem **270**: 2633-2643

Maeda K, Finnie C, Svensson B (2004) Cy5 maleimide labeling for sensitive detection of free thiols in native protein extracts: identification of seed proteins targeted by barley thioredoxin h isoforms. Biochem J **378**: 479-507

Maeda K, Hägglund P, Finnie C, Svensson B, Henriksen A (2006a) Structural basis for target protein recognition by the protein disulphide reductase thioredoxin. Structure **14**: 1701-1710

Maeda K, Hagglund P, Finnie C, Svensson B (2006b) Proteomics of disulfide and cysteine oxidoreduction. In: Finnie C (Ed.) Plant Proteomics, Annu Plant Rev, vol. 28.Oxford, Blackwell. PP. 71-97

Maeda K, **Hägglund P**, **Finnie C**, **Svensson B**, **Henriksen A** (2008) Crystal structures of barley thioredoxin h isoforms HvTrxh1 and HvTrxh2 reveal features involved in protein recognition and possibly in discriminating the isoform specificity. Protein Sci (in press)

Marx C, Wong JH, Buchanan BB (2003) Thioredoxin and germinating barley: targets and protein redox changes. Planta **216**: 454-460

Mewies M, McIntire WS, Scruton NS (1998) Covalent attachment of flavin adenine dinucleotide (FAD) and flavin mononucleotide (FMN) to enzymes: The current state of affairs. Protein Sci **7**: 7-20

Meyer Y, Vignols F, Reichheld JP (2002) Classification of plant thioredoxins by sequence similarity and intron position. Methods Enzymol **347**: 394-402

Meyer Y, Reichheld JP, Vignols F (2005) Thioredoxins in Arabidopsis and other plants. Photosynth Res **86:** 419-33

Minakuchi K, Yabushita T, Masumura T, Ichihara K, Tanaka K (1994) Cloning and sequence analysis of a cDNA encoding rice glutaredoxin. FEBS Lett **337**: 157-160

Miranda-Vizuete A, Damdimopoulos AE, Gustafsson J, Spyrou G (1997) Cloning, expression, and characterization of a novel *Escherichia coli* thioredoxin. J Biol Chem **272**: 30841-30847

Montrichard F, Renard M, Alkhalfioui F, Duval FD, Macherel D (2003) Identification and differential expression of two thioredoxin h isoforms in germinating seeds from pea. Plant Physiol **132**: 1707-1715

Morell S, Follmann H, Haberlein I (1995) Identification and localization of the first glutaredoxins in leaves of a higher plant. FEBS Lett **369**: 149-152

Møller IM (2001) Plant mitochondria and oxidative stress: electron transport, NADPH turnover, and metabolism of reactive oxygen species. Annu Rev Plant Physiol Plant Mol Biol **52**: 561-591

Mundy J, Svendsen I, Hejgaard J (1983) Barley α-amylase/subtilisin inhibitor I. Isolation and characterization. Carlsberg Res. Commun. **48**: 81-90

Mundy J, Rogers JC (1986) Selective expression of a probable amylase/protease inhibitor in barley (*Hordeum vulgare*) aleurone cells: comparison to the barley amylase/subtilisin inhibitor. Planta **169:** 51-63

Mustacich D, Powis G (2000) Thioredoxin reductase. Biochem J **346**: 1-8

Næsted H, Kramhøft B, Lok F, Bojsen K, Yu S, Svensson B (2006) Production of enzymatically active recombinant full-length barley high pI α-glucosidase of glycoside family 31 by high cell-density fermentation of *Pichia pastoris* and affinity purification. Protein Exp Purif **46**: 56-63

Nakai H, Ito T, Tanizawa S, Matsubara K, Yamamoto T, Okuyama M, Mori H, Chiba S, Sano Y, Kimura A (2006) Plant α-glucosidase: molecular analysis of rice α-glucosidase and degradation mechanism of starch granules in germination stage. J Appl Glycosci **53**: 137-242

Nilan RA (1974) Barley (*Hordeum vulgare*) In: King RC (Ed.) Handbook of genetics. New York, Plenum Press, PP. 93-110

Noctor G, Foyer CH (1998) Ascorbate and glutathione: keeping active oxygen under control. Annu Rev Plant Physiol Plant Mol Biol **49**: 249-279

Ogawa M, Hanada A,Yamauchi Y, Kuwahara A, Kamiya Y, Yamaguchi S (2003) Gibberellin Biosynthesis and Response during Arabidopsis Seed Germination. Plant Cell **15**: 1591-1604

Oztur ZN, **Talamé V**, **Deyholos M**, **Michalowski CB**, **Galbraith DW**, **Gozukirmizi N**, **Tuberosa R**, **Bohnert HJ** (2002) Monitoring large-scale changes in transcript abundance in drought- and salt-stressed barley. Plant Mol Biol **48**: 551-573

Østergaard O, Melchior S, Roepstorff P, Svensson B (2002) Initial proteome analysis of mature barley seeds and malt. Proteomics **2**: 733-739

Østergaard O, Finnie C, Laugesen S, Roepstorff P, Svennson B (2004) Proteome analysis of barley seeds: Identification of major proteins from two-dimensional gels (pI 4-7). Proteomics **4**: 2437-2447

Paleg LG (1960) Physiological effects of gibberellic acid: I. On carbohydrate metabolism and amylase activity of barley endosperm. Plant Physiol **35**: 293-309

Palzkill T (2002) Proteomics. New York, Kluwer Academic Publisher.

Patton WF (2002) Detection technologies in proteome analysis. J Chromatogr B Analyt Technol Biomed Life Sci **771**: 3-31

Popov N, Schmitt M, Schulzeck S, Matthies H (1975) Eine störungsfreie mikromethode zur Bestimmung des proteingehaltes in gewebehomogenaten. Acta Biol Med Ger **34**: 1441-1446

Potokina E, **Sreenivasulu N**, **Altschmied L**, **Michalek W**, **Graner A** (2002) Differential gene expression during seed germination in barley (*Hordeum vulgare L.*). Funct Integr Genomics **2**: 28-39

Rabbani MA, Maruyama K, Abe H, Khan MA, Katsura K, Ito Y, Yoshiwara K, Seki M, Shinozaki K, Yamaguchi-Shinozaki K (2003) Monitoring expression profiles of rice genes under cold, drought, and high-salinity stresses and abscisic acid application using cDNA microarray and RNA gel-blot analyses. Plant Physiol **133**: 1755-1767

Rai M, Padh H (2001) Expression systems for production of heterologous proteins. Curr Sci **80**: 1121-1128

Raina S, Missiakas D (1997) Making and breaking disulfide bonds. Annu Rev Microbial **51**: 179-202

Ranki H, Sopanen T (1984) Secretion of α-amylase by the aleurone layer and the scutellum of germination barley grain. Plant Physiol **75**: 710-715

Reichheld JP, Meyer E, Khafif M, Bonnard G, Meyer Y (2005) AtNTRB is the major mitochondrial thioredoxin reductase in *Arabidopsis thaliana*. FEBS Lett **579**: 337-342

Reichheld JP, Khafif M, Riondet C, Droux M, Bonnard G, Meyer Y (2007) Inactivation of thioredoxin reductases reveals a complex interplay between thioredoxin and glutathione pathway in arabidopsis. Plant Cell **19**: 1851-1865

Ritchie S, Swanson SJ, Gilory S (2000) Physiology of the aleurone layer and starchy endosperm during grain development and early seedling growth: new insights from cell and molecular biology. Seed Sci Res **10**: 193-212

Rivera-Madrid R, Mestres D, Marinho P, Jacquot JP, Decotignies P et al. (1995) Evidences for five divergent thioredoxin h sequences in *Arabidopsis thaliana*. Proc Natl Acad Sci USA **92**: 5620-5624

Rodenburg KW, Juge N,Guo XJ, Søgaard M, Chaix AG, Svensson B (1994) Domain B protruding at the third β strand of the α/β barrel in barley α-amylase confers distinct isozyme-specific properties. Eur J Biochem. **221**: 277-284

Rodenburg KW, Várallyay E, Svendsen I, Svensson B (1995) Arg-27, Arg-127 and Arg-155 in the β-trefoil protein barley α-amylase/subtilisin inhibitor are interface residues in the complex with barley α-amylase 2. Biochem J **309**: 969-976

Rogers JC, Milliman C (1983) Isolation and sequence analysis of a barley α-amylase cDNA clone. J Biol Chem **258**: 8169-8174

Rogers JC (1985) Two barley α-amylase gene families are regulated differently in aleurone cells. J Biol Chem **260**: 3731-3738

Rousseau D, Knochbin S, Gorka C, Lawrence JJ (1992) Induction of H1(0)-gene expression in B16 murine melanoma cells. Eur J Biochem **208**: 775-779

Schürmann P, Jacquot JP (2000) Plant thioredoxin system revisted. Annu Rev Plant Physiol Plant Mol Biol **51**: 371-400

Serrato AJ, Crespo JL, Florencio FJ, Cejudo FJ (2001) Characterization of two thioredoxins h with predominant localization in the nucleus of aleurone and scutellum cells of germinating wheat seeds. Plant Mol Biol **46**: 361-371

Serrato AJ, Pérez-Ruiz JM, Cejudo FJ (2002) Cloning of thioredoxin h reductase and characterization of the thioredoxin reductase-thioredoxin h system from wheat. Biochem J **367**: 491-497

Serrato AJ, Cejudo FJ (2003) Type-h thioredoxins accumulate in the nucleus of developing wheat seed tissues suffering oxidative stress. Planta **217**: 392-399

Serrato AJ, Pe´rez-Ruiz JM, Spı´nola MC, Cejudo FJ (2004) A novel NADPH thioredoxin reductase, localized in the chloroplast, which deficiency causes hypersensitivity to abiotic stress in *Arabidopsis thaliana.* J Biol Chem **279**: 43821-43827

Setterdahl AT, Chivers PT, Hirasawa M, Lemaire SD, Keryer E, Miginiac-Maslow M, Kim SK, Mason J, Jacquot JP, Longbine CC, de Lamotte-Guery F, Knaff DB (2003) Effect of pH on the oxidation-reduction properties of thioredoxins. Biochemistry **42**: 14877-14884

Shahpiri A, Svensson B, Finnie C (2008) The NADPH-dependent thioredoxin reductase/thioredoxin system in germinating barley seeds: gene expression, protein profiles and interactions between isoforms of thioredoxin h and thioredoxin reductase. Plant Physiol **146**: 789-799

Shen Q, **Zhang P**, **Ho THD** (1996) Modular nature of abscisic acid (ABA) response complexes: composite promoter units that are necessary and sufficient for ABA induction of gene expression in barley. Plant Cell **8**: 1107-1119

Shewry PR, Halford NG (2002) Cereal seed storage proteins: structures, properties and role in grain utilization. J Exp Bot **53**: 947–958

Shewry PR (2007) Improving the protein content and composition of cereal grain. J Cereal Sci **46**: 239-250

Singh DP, **Jermakow AM**, **Swain SM** (2002) Gibberellins are Required for seed development and pollen tube growth in arabidopsis. Plant Cell **14**: 3133-3147

Sissons MJ, Lancer RCM, Sparrow DHB (1993) Studies on limit dextrinase in barley. 3. Limit dextrinase in developing kernels. J Cereal Sci **17**: 19-24

Sharova EI (2002) Protein transport in plant cells. Russ. J. Plant Physiol **49**: 286-301

Shewry PR, Parmar S, Buxton B, Gale MD, Liu CJ, Hejgaard J, Kreis M (1988) Multiple molecular forms of β-amylase in seeds and vegetative tissue of barley. Planta **176**: 127-134

Sun Zhuotao, Henson CA (1991) A quantitative assessment of the importance of barley seed α-amylase, β-amylase, debranching enzyme, α-glucosidase in starch degradation. Arch Biochem Biophys **284**: 298-305

Steinberg TH, Haugland RP, Singer VL (1996) Applications of SYPRO orange and SYPRO red protein gel stains. Anal Biochem **239**: 238-245

Tamura T, Stadtman TC (1996) A new selenoprotein from human lung adenocarcinoma cells: purification, properties, and thioredoxin reductase activity. Proc Natl Acad Sci USA **93**: 1006-1011

Teresa A, Wolpert S, Wolpert TJ (2007) Thioredoxin H5 is required for victorin sensitivity mediated by CC-NBS-LRR gene in Arabidopsis. Plant Cell **19**: 673-687

Thön M, Al-Abdallah Q, Hortschansky P, Brakhage AA (2007) The thioredoxin system of the filamentous fungus *Aspergillus nidulans*: impact on development and oxidative stress response. J Biol Chem **282**: 27259-27269

Thorpe GH, Kricka LJ (1986) Enhanced chemiluminescent reactions catalyzed by horseradish peroxidase. Methods Enzymol **133**: 331-353

Tibbot BK, **Henson CA**, **Skadsen RW** (1998) Expression of enzymatically active, recombinant barley α-glucosidase in yeast and immunological detection of α-glucosidase from seed tissue. Plant Mol Biol **38**: 379-391

Ueguchi-Tanaka M, **Nakajima M**, **Motoyuki A**, **Matsuoka M** (2007) Gibberellin receptor and its role in gibberellin signaling in plants. Annu Rev Plant Biol **58**: 183-198

Varner JE, **Mense RM** (1972) Characteristics of the process of enzyme release from secretory plant cells. Plant Physiol **49**: 187-189

Vensel WH, Tanaka CK, Cai N, Wong JH, Buchanan BB, Hurkman WJ (2005) Developmental changes in the metabolic protein profiles of wheat endosperm. Proteomics **5**: 1594-1611

Verdoucq L, **Vignols F**, **Jacquot JP**, **Chartier Y**, **Meyer Y** (1999) In vivo characterization of a thioredoxin h target protein defines a new peroxiredoxin family. J Biol Chem **274**: 19714-19722

Waksman G, Krishna TS, Williams CH Jr, Kuriyan J (1994) Crystal structure of *Escherichia coli* thioredoxin reductase refined at 2 Å resolution. Implications for a large conformational change during catalysis. J Mol Biol **236**: 800-816

Wang PF, **Veine DM**, **Ahn SH**, **Williams CH Jr** (1996) A stable mixed disulfide between thioredoxin reductase and its substrate, thioredoxin: preparation and characterization. Biochemistry **35**: 4812-4819

Weselake RJ, MacGregor AW, Hill RD (1983) An endogenous α-amylase inhibitor in barley kernels. Plant Physiol **72**: 809-812

Willekens H, Inzé D, Van Montagu M, Van Camp W (1995) Catalases in plants. Mol Breed **1**: 207-228

Williams CH Jr (1995) Mechanism and structure of thioredoxin reductase from *Escherichia coli*. FASEB J **9**: 1267-1276

Wong JH, Kim YB, Ren PH, Cai N, Cho MJ, Hedden P, Lemaux PG, Buchanan BB (2002) Transgenic barley grain overexpressing thioredoxin shows evidence that the starchy endosperm communicates with the embryo and the aleurone. Proc Natl Acad Sci USA **99**: 16325-16330

Wong JH, Cai N, Tanaka CK, Vensel WH, Hurkman WJ, Buchanan BB (2004) Thioredoxin reduction alters the solubility of proteins of wheat starchy endosperm: an early event in cereal germination. Plant Cell Physiol **45**: 407-415

Yamauchi D, **Zentella R**, **Ho THD** (2002) Molecular analysis of the barley (*Hordeum vulgare* L.) gene encoding the protein kinase PKABA1 capable of suppressing gibberellin action in aleurone layers. Planta **215**: 319-326

Yano H, Wong JH, Lee YM, Cho MJ, and Buchanan BB (2002) A strategy for the identification of proteins targeted by thioredoxin. Proc Natl Acad Sci USA **98**: 4794-4799

Yamazaki D, Motohashi K, Kasama T, Hara Y, Hisabori T (2004) Target proteins of the cytosolic thioredoxins in *Arabidopsis thaliana.* Plant Cell Physiol **45**: 18-27

Yomo H (1960) Studies on the α-amylase activating substance. IV. On the amylase activating action of gibberellin. Hakko Kyokai Shi **18**: 600-602

You L, Yin J (2000) Patterns of regulation from mRNA and protein time series. Metab Eng **2**: 210-217

Ziegler DM (1985) Role of reversible oxidation-reduction of enzyme thiols-disulfides in metabolic regulation. Annu Rev Biochem **54**: 305-329

Appendix 1

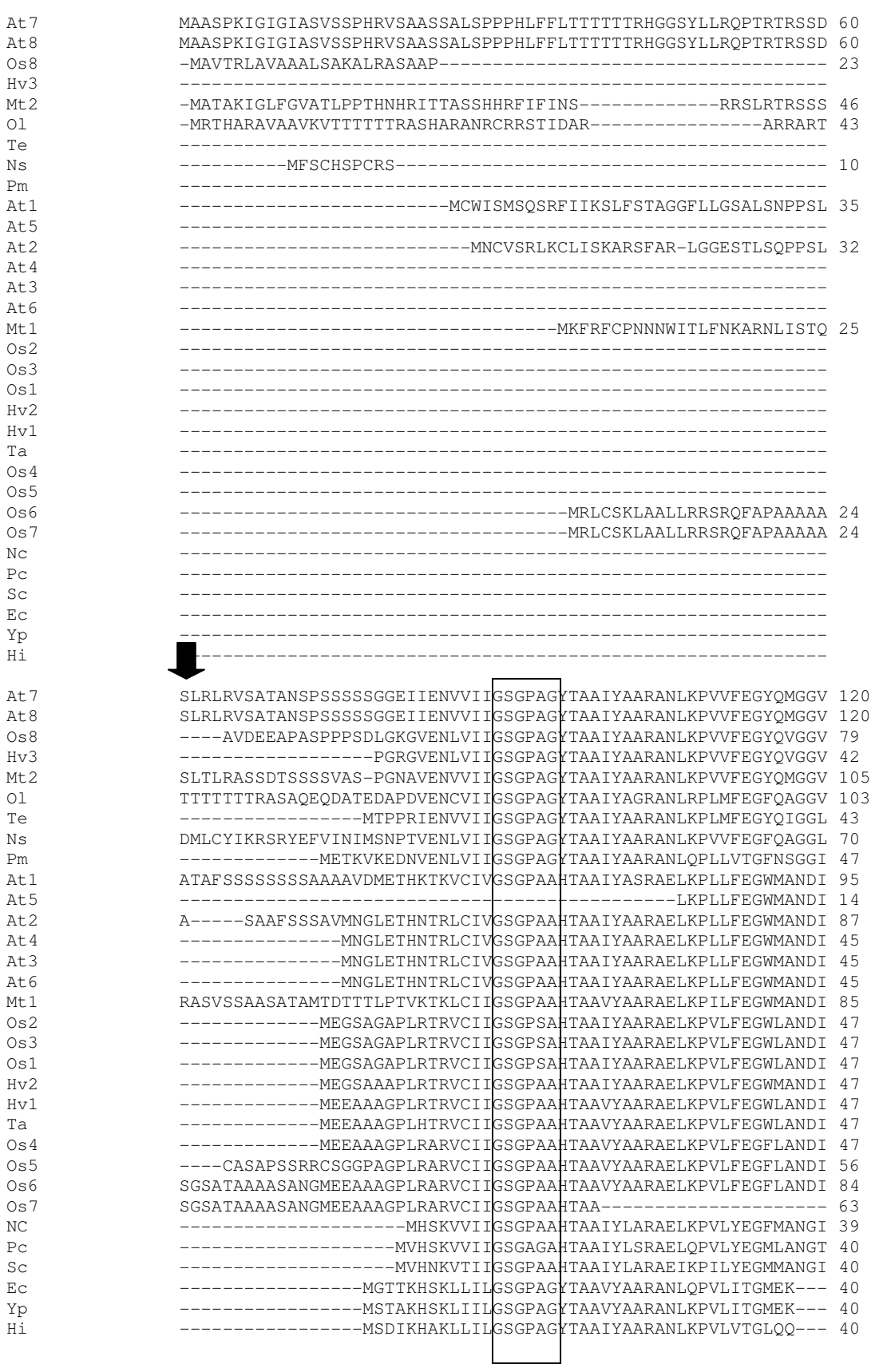
At7 MAASPKIGIGIASVSSPHRVSAASSALSPPPHLFFLTTTTTTRHGGSYLLRQPTRTRSSD 60
At8 MAASPKIGIGIASVSSPHRVSAASSALSPPPHLFFLTTTTTTRHGGSYLLRQPTRTRSSD 60
Os8 -MAVTRLAVAAALSAKALRASAAP---------- 23
Hv3 ----------
Mt2 -MATAKIGLFGVATLPPTHNHRITTASSHHRFIFINS----------RRSLRTRSSS 46
Ol -MRTHARAVAAVKVTTTTTTRASHARANRCRRSTIDAR----------ARRART 43
Te ----------
Ns ----------MFSCHSPCRS---------- 10
Pm ----------
At1 ----------MCWISMSQSRFIIKSLFSTAGGFLLGSALSNPPSL 35
At5 ----------
At2 ----------MNCVSRLKCLISKARSFAR-LGGESTLSQPPSL 32
At4 ----------
At3 ----------
At6 ----------
Mt1 ----------MKFRFCPNNNWITLFNKARNLISTQ 25
Os2 ----------
Os3 ----------
Os1 ----------
Hv2 ----------
Hv1 ----------
Ta ----------
Os4 ----------
Os5 ----------
Os6 ----------MRLCSKLAALLRRSRQFAPAAAAA 24
Os7 ----------MRLCSKLAALLRRSRQFAPAAAAA 24
Nc ----------
Pc ----------
Sc ----------
Ec ----------
Yp ----------
Hi ----------
At7 SLRLRVSATANSPSSSSSGGEIIENVVIIGSGPAGYTAAIYAARANLKPVVFEGYQMGGV 120
At8 SLRLRVSATANSPSSSSSGGEIIENVVIIGSGPAGYTAAIYAARANLKPVVFEGYQMGGV 120
Os8 ----AVDEEAPASPPPSDLGKGVENLVIIGSGPAGYTAAIYAARANLKPVVFEGYQVGGV 79
Hv3 ----------PGRGVENLVIIGSGPAGYTAAIYAARANLKPVVFEGYQVGGV 42
Mt2 SLTLRASSDTSSSSVAS-PGNAVENVVIIGSGPAGYTAAIYAARANLKPVVFEGYQMGGV 105
Ol TTTTTTTRASAQEQDATEDAPDVENCVIIGSGPAGYTAAIYAGRANLRPLMFEGFQAGGV 103
Te ----------MTPPRIENVVIIGSGPAGYTAAIYAARANLKPLMFEGYQIGGL 43
Ns DMLCYIKRSRYEFVINIMSNPTVENLVIIGSGPAGYTAAIYAARANLKPVVFEGFQAGGL 70
Pm ----------METKVKEDNVENLVIIGSGPAGYTAAIYAARANLQPLLVTGFNSGGI 47
At1 ATAFSSSSSSSSAAAAVDMETHKTKVCIVGSGPAAHTAAIYASRAELKPLLFEGWMANDI 95
At5 ----------LKPLLFEGWMANDI 14
At2 A-----SAAFSSSAVMNGLETHNTRLCIVGSGPAAHTAAIYAARAELKPLLFEGWMANDI 87
At4 ----------MNGLETHNTRLCIVGSGPAAHTAAIYAARAELKPLLFEGWMANDI 45
At3 ----------MNGLETHNTRLCIVGSGPAAHTAAIYAARAELKPLLFEGWMANDI 45
At6 ----------MNGLETHNTRLCIVGSGPAAHTAAIYAARAELKPLLFEGWMANDI 45
Mt1 RASVSSAASATAMTDTTTLPTVKTKLCIIGSGPAAHTAAVYAARAELKPILFEGWMANDI 85
Os2 ----------MEGSAGAPLRTRVCIIGSGPSAHTAAIYAARAELKPVLFEGWLANDI 47
Os3 ----------MEGSAGAPLRTRVCIIGSGPSAHTAAIYAARAELKPVLFEGWLANDI 47
Os1 ----------MEGSAGAPLRTRVCIIGSGPSAHTAAIYAARAELKPVLFEGWLANDI 47
Hv2 ----------MEGSAAAPLRTRVCIIGSGPAAHTAAIYAARAELKPVLFEGWMANDI 47
Hv1 ----------MEEAAAGPLRTRVCIIGSGPAAHTAAVYAARAELKPVLFEGWLANDI 47
Ta ----------MEEAAAGPLHTRVCIIGSGPAAHTAAVYAARAELKPVLFEGWLANDI 47
Os4 ----------MEEAAAGPLRARVCIIGSGPAAHTAAVYAARAELKPVLFEGFLANDI 47
Os5 ----CASAPSSRRCSGGPAGPLRARVCIIGSGPAAHTAAVYAARAELKPVLFEGFLANDI 56
Os6 SGSATAAAASANGMEEAAAGPLRARVCIIGSGPAAHTAAVYAARAELKPVLFEGFLANDI 84
Os7 SGSATAAAASANGMEEAAAGPLRARVCIIGSGPAAHTAA---------- 63
NC ----------MHSKVVIIGSGPAAHTAAIYLARAELKPVLYEGFMANGI 39
Pc ----------MVHSKVVIIGSGAGAHTAAIYLSRAELQPVLYEGMLANGT 40
Sc ----------MVHNKVTIIGSGPAAHTAAIYLARAEIKPILYEGMMANGI 40
Ec ----------MGTTKHSKLLILGSGPAGYTAAVYAARANLQPVLITGMEK--- 40
Yp ----------MSTAKHSKLIILGSGPAGYTAAVYAARANLKPVLITGMEK--- 40
Hi ----------MSDIKHAKLLILGSGPAGYTAAIYAARANLKPVLVTGLQQ--- 40

```
At7             P-GGQLMTTTEVENFPGFPDGITGPDLMEKMRKQAERWGAELYPEDVESLSVTTAPFTVQ 179
At8             P-GGQLMTTTEVENFPGFPDGITGPDLMEKMRKQAERWGAELYPEDVESLSVTTAPFTVQ 179
Os8             P-GGQLMTTTEVENFPGFPDGVTGPDLMDKMRKQAERWGAELHQEDVEFVNVKSRPFVIR 138
Hv3             P-GGQLMTTTEVENFPGFPDGITGPDLMDKMRKQAERWGAELHQEDVEFVDVKSRPFVIR 101
Mt2             P-GGQLMTTTEVENFPGFPDGITGPDLMDRMRRQAERWGAELHHEDVEAIDVKTSPFTVQ 164
Ol              P-GGQLMTTTEVENFPGFPEGVTGPDLMDKMRKQAERWGAVMHTEDVVTVDFTSRPFTVS 162
Te              P-GGQLMTTTEVENFPGFPEGIQGPQLMARMKAQAERWGTEMVTEDVIQVDFSQRPFLIS 102
Ns              P-GGQLMTTTEVENFPGFPQGITGPELMDRMKAQAERWGAELYTEDVISVDLSQRPFTVR 129
Pm              P-GGQLMTTTFVENYPGFPDGVLGPELMDLMKAQAERWGTNLYESDVISIDTSKSPFELK 106
At1             APGGQLTTTTDVENFPGFPEGILGIDIVEKFRKQSERFGTTIFTETVNKVDFSSKPFKLF 155
At5             APGGQLTTTTDVENFPGFPEGILGIDIVEKFRKQSERFGTTIFTETVNKVDFSSKPFKLF 74
At2             APGGQLTTTTDVENFPGFPEGILGVELTDKFRKQSERFGTTIFTETVTKVDFSSKPFKLF 147
At4             APGGQLTTTTDVENFPGFPEGILGVELTDKFRKQSERFGTTIFTETVTKVDFSSKPFKLF 105
At3             APGGQLTTTTDVENFPGFPEGILGVELTDKFRKQSERFGTTIFTETVTKVDFSSKPFKLF 105
At6             APGGQLNQPP-RENFPGFPEGILGVELTDKFRKQSERFGTTIFTETVTKVDFSSKPFKLF 104
Mt1             APGGQLTTTTDVENFPGFPDGILGGELMERCRQQSAKFGTEIFTETVSKVDFSARPFRVF 145
Os2             AAGGQLTTTTDVENFPGFPEGILGGELMDRCRAQSLRFGTSIISETVTAVDFSARPFRVA 107
Os3             AAGGQLTTTTDVENFPGFPEGILGGELMDRCRAQSLRFGTSIISETVTAVDFSARPFRVA 107
Os1             AAGGQLTTTTDVENFPGFPEGILGGELMDRCRAQSLRFGTSIISETVTAVDFSARPFRVA 107
Hv2             AAGGQLTTTTDVENFPGFPTGIMGIDLMDNCRAQSVRFGTNILSETVTEVDFSARPFRVT 107
Hv1             AAGGQLTTTTDVENFPGFPDGILGIDLMDRCRAQSVRFGTKIFSETVTSVDFSSRPFRVA 107
Ta              AAGGQLTTTTDVENFPGFPDGILGIDLMDRCRAQSVRFGTKIFSETVTSVDFSSRPFRVS 107
Os4             AAGGQLTTTTDVENFPGFPDGILGADLMDRCRAQSVRFGTRILTETVTAVDLSSRPFRVA 107
Os5             AAGGQLTTTTDVENFPGFPDGILGADLMDRCRAQSVRFGTRILTETVTAVDLSSRPFRVA 116
Os6             AAGGQLTTTTDVENFPGFPDGILGADLMDRCRAQSVRFGTRILTETVTAVDLSSRPFRVA 144
Os7             -----LTTTTDVENFPGFPDGILGADLMDRCRAQSVRFGTRILTETVTAVDLSSRPFRVA 118
NC              AAGGQLTTTTEIENFPGFPDGIMGQELMDKMKAQSERFGTQIISETVAKVDLSARPFKYA 99
Pc              AAGGQLTTTTDVENFPGFPSGIGGAELMDNMRAQSERFGTEIITETISKLDLSSRPFKMW 100
Sc              AAGGQLTTTTEIENFPGFPDGLTGSELMDRMREQSTKFGTEIITETVSKVDLSSKPFKLW 100
Ec              --GGQLTTTTEVENWPGDPNDLTGPLLMERMHEHATKFETEIIFDHINKVDLQNRPFRLN 98
Yp              --GGQLTTTTEVENWPGDPEGLTGPALMERMHEHAEKFQTEIIFDHISSVDLQNRPFRLF 98
Hi              --GGQLTTTDEIENWPGDFEMTTGSGLMQRMLQHAEKFETEIVFDHINRVDLSSRPFKLF 98
                     *  .   **:**      *  :      :: :: : :  . :  :.    **

At7             TSE-------RKVKCHSIIYATGATARRLRLPRE----EEFWSRGISACAICDGASPLFK 228
At8             TSE-------RKVKCHSIIYATGATARRLRLPRE----EEFWSRGISACAICDGASPLFK 228
Os8             SSD-------REVKCHSVIIATGAAAKRLRLPRE----DEFWSRGISACAICDGASPLFK 187
Hv3             SSD-------REVKCHSVIIATGATAKRLRLPRE----EEFWSRGISACAICDGASPLYK 150
Mt2             SSE-------RKVKSHTVIIATGATAKRLRLPRE----DEFWSRGISACAICDGASPLFK 213
Ol              SSD-------RTVKANSVIVATGATAKRLGIPAE----ATLWSRGISACAICDGASPIFK 211
Te              SAE-------RQVYAHSVIICTGATAKRLHLPGE----EQYWTKGVSACAICDGATPIFK 151
Ns              SEE-------REVKAHTIIIATGATAKRLGLPSE----HEFWSRGISACAICDGATPIFH 178
Pm              TLE-------GSIKSNSIIIATGASANRLGVINE----DKFWSKGISACAICDGATPQFR 155
At1             TDS-------RTVLADSVIISTGAVAKRLSFTGSGEGNGGFWNRGISACAVCDGAAPIFR 208
At5             TDS-------RTVLADSVIISTGAVAKRLSFTGSGEGNGGFWNRGISACAVCDGAAPIFR 127
At2             TDS-------KAILADAVILATGAVAKRLSFVGSGEASGGFWNRGISACAVCDGAAPIFR 200
At4             TDS-------KAILADAVILATGAVAKRLSFVGSGEASGGFWNRGISACAVCDGAAPIFR 158
At3             TDS-------KAILADAVILAIGAVAKRLSFVGSGEVLGGFWNRGISACAVCDGAAPIFR 158
At6             TDS-------KAILADAVILAIGAVAKWLSFVGSGEVLGGLWNRGISACAVCDGAAPIFR 157
Mt1             TDS-------RTVEADSVIVATGAVAKRLPFTGSGDGPNGYWNRGISACAVCDGAAPIFR 198
Os2             SDS-------TTVLADAVVVATGAVARRLHFAGS----DAYWNRGISACAVCDGAAPIFR 156
Os3             SDS-------TTVLADAVVVATGAVARRLHFAGS----DAYWNRGISACAVCDGAAPIFR 156
Os1             SDS-------TTVLADAVVVATGAVARRLHFAGS----DAYWNRGISACAVCDGAAPIFR 156
Hv2             SDS-------TTVLADTVVVATGAVARRLYFSGS----DTYWNRGISACAVCDGAAPIFR 156
Hv1             SDD-------TVVHADSVVVATGAVARRLHFAGS----DAFWNRGISACAVCDGAAPIFR 156
Ta              SDD-------TVVHADSVVVATGAVARRLHFAGS----DAFWNRGITACAVCDGAAPIFR 156
Os4             SGD-------TVVHADAVVVATGAVARRLHFAGS----DAFWNRGISACAVCDGAAPIFR 156
Os5             SGD-------TVVHADAVVVATGAVARRLHFAGS----DAFWNRGISACAVCDGAAPIFR 165
Os6             SGD-------TVVHADAVVVATGAVARRLHFAGS----DAFWNRGISACAVCDGAAPIFR 193
Os7             SGD-------TVVHADAVVVATGAVARRLHFAGS----DAFWNRGISACAVCDGAGPIFR 167
NC              TEWSPEE----YHTADSIILATGASARRLHLPGE----EKYWQNGISACAVCDGAVPIFR 151
Pc              TEWNDDEGSEPVRTADAVIIATGANARRLNLPGE----ETYWQNGISACAVCDGAVPIFR 156
Sc              TEFNEDAEP---VTTDAIILATGASAKRMHLPGE----ETYWQKGISACAVCDGAVPIFR 153
Ec              GDN-------GEYTCDALIIATGASARYLGLPSE----EAFKGRGVSACATCDG--FFYR 145
```

```
Yp              GDG-------AEYTCDALIIATGASARYLGMASE----EAFKGKGVSACATCDG--FFYR 145
Hi              GDV-------QNFTCDALIIATGASARYIGLPSE----ENYKGRGVSACATCDG--FFYR 145
                             .::: . ** *. : .  .         .*::*** ***    ::

At7             GQVLAVVGGGDTATEEALYLTKYARHVHLLVRRDQLRASKAMQDRVINNP---NITVHYN 285
At8             GQVLAVVGGGDTATEEALYLTKYARHVHLLVRRDQLRASKAMQDRVINNP---NITVHYN 285
Os8             GQVLAVVGGGDTATEEAIYLTKYARHVHLLVRKDQLRASKAMQDRVLNNP---NITVHFN 244
Hv3             GQVLAVVGGGDTATEEAIYLTKYACHVHLLVRRDQLRASKAMQDRVLNNP---NITVHFN 207
Mt2             GQILAVVGGGDTATEEALYLTKYARHVHLLVRRDQLRASKAMQDRVYDNP---NVTVHFN 270
Ol              GEEVAVVGGGDTATEEAVYLTKYAKHVHLLVRGSTMRASKAMQDRVLQHK---AITVHYN 268
Te              DVELAVIGGGDSAAEEAVYLTKYGSHVHLLVRSDKMRASKAMQDRVFANP---KITVHWQ 208
Ns              GAELAVIGAGDSAAEESIYLTKYGSKVNLLVRSEKMRASKAMQDRVLSNP---KIQVHWN 235
Pm              NEELAVIGGGDSACEEAAYLTKYGSKVHLLVRSEKLRASAAMIDRVKANS---KIEIHWN 212
At1             NKPLVVIGGGDSAMEEANFLTKYGSKVYIIHRRDTFRASKIMQQRALSNP---KIEVIWN 265
At5             NKPLVVIGGGDSAMEEANFLTKYGSKVYIIHRRDTFRASKIMQQRALSNP---KIEVIWN 184
At2             NKPLAVIGGGDSAMEEANFLTKYGSKVYIIHRRDAFRASKIMQQRALSNP---KIDVIWN 257
At4             NKPLAVIGGGDSAMEEANFLTKYGSKVYIIHRRDAFRASKIMQQRALSNP---KIDVFWN 215
At3             NKPLAVIGGGDSAMEEANFLTKYGSKVYIIHRRDAFRASKIMQQRALSNP---KIDVIWN 215
At6             NKPLAVIGGGDSAMEEANFLTKYGSKVYIIDRRDAFRASKIMQQRALSNP---KIDVIWN 214
Mt1             NKPLAVIGGGDSAMEEATFLTKYGSEVYIIHRRDTFRASKIMQSKALSNE---KIKVIWN 255
Os2             NKPIAVIGGGDSAMEESNFLTKYGSHVYIIHRRNTFRASKIMQARALSNP---KIQVFWD 213
Os3             NKPIAVIGGGDSAMEESNFLTKYGSHVYIIHRRNTFRASKIMQARALSNP---KIQVFWD 213
Os1             NKPIAVIGGGDSAMEESNFLTKYGSHVYIIHRRNTFRASKIMQARALSNP---KIQVFWD 213
Hv2             NKPIAVIGGGDSAMEEGNFLTKYGSQVYIIHRRNTFRASKIMQARALSNP---KIQVVWD 213
Hv1             NKPIAVVGGGDSAMEEANFLTKYGSRVYIIHRRDAFRASKIMQARALSNP---KIQVVWD 213
Ta              NKPIAVVGGGDSAMEEANFLTKYGSRVYIIHRRDAFRASKIMQARALSNP---KIQVVWD 213
Os4             NKPIAVVGGGDSAMEEANFLTKYGSRVYIIHRRNAFRASKIMQARALSNP---KIQVVWD 213
Os5             NKPIAVVGGGDSAMEEANFLTKYGSRVYIIHRRNAFRASKIMQARALSNP---KIQVVWD 222
Os6             NKPIAVVGGGDSAMEEANFLTKYGSRVYIIHRRNAFRASKIMQARALSNP---KIQVVWD 250
Os7             NKPIAVVGGGDSAMEEANFLTKYGSRVYIIHRRNAFRASKIMQARALSNP---KIQVVWD 224
NC              NKHLVVIGGGDSAAEEAMYLTKYGSHVTVLVRKDKLRASSIMAHRLLNHE---KVTVRFN 208
Pc              NKPLYVIGGGDSAAEEAMFLAKYGSSVTVLVRKDKLRASNIMADRLLAHP---KCKVRFN 213
Sc              NKPLAVIGGGDSACEEAQFLTKYGSKVFMLVRKDHLRASTIMQKRAEKNE---KIEILYN 210
Ec              NQKVAVIGGGNTAVEEALYLSNIASEVHLIHRRDGFRAEKILIKRLMDKVENGNIILHTN 205
Yp              NQKVAVVGGGNTAVEEALYLANIAAEVHLIHRRDTFRSEKILIDRLMEKVKNGNIVLHTD 205
Hi              NKPVGVIGGGNTAVEEALYLANIASTVHLIHRRDSFRAEKILIDRLYKKVEEGKIVLHTD 205
                .  : *:*.*::* **. :*:: .  * :: * . :*:.  :  :   :       :  :

At7             TETVDVLSNTK--GQMSGILLRRL-DTGEETELEAKGLFYGIGHSPNSQLLEGQVELDSS 342
At8             TETVDVLSNTK--GQMSGILLRRL-DTGEETELEAKGLFYGIGHSPNSQLLEGQVELDSS 342
Os8             TEAVDVVSNPK--GQMSGIQLKRT-DTGEESVLEVKGLFYGIGHTPNSQLLQGQIDLDDA 301
Hv3             TEAVDVVGNTK--GQMSGIQLRRI-DTGEEKVLEVKGLFYGIGHTPNSQLLEGQIELDSS 264
Mt2             TETVDIVSNTK--GQMSGILVRKL-DSGEESVLEAKGLFYGIGHSPNTQLLKGQVELDQS 327
Ol              TECVDGSPNSK--GNLGALKLRDT-NNGDERQLKVKGLFYGIGHTPNSKIFGNQIELDEA 325
Te              TEAREILGDGN---LMTGLRIINK-ATGEESLLPVRGLFYAIGHTPNTQLFKDFLELDSV 264
Ns              TEVVDVFGNG----HMDGVKVRNN-QTGEETNVHAKGLFYAIGHKPNTSLFQGQLELDEI 290
Pm              TKVEK--ANGT--DWLENVETINS-HKGN-VEIKVKGLFYAIGHTPNTKFLNNKIELDKK 266
At1             SAVVEAYGDEN-GRVLGGLKVKNV-VTGDVSDLKVSGLFFAIGHEPATKFLDGQLELDED 323
At5             SAVVEAYGDEN-GRVLGGLKVKNV-VTGDVSDLKVSGLFFAIGHQPATKFLDGQLELDED 242
At2             SSVVEAYGDGE-RDVLGGLKVKNV-VTGDVSDLKVSGLFFAIGHEPATKFLDGGVELDSD 315
At4             SSVVEAYGDGE-RDVLGGLKVKNV-VTGDVSDLKVSGLFFAIGHEPATKFLDGGVELDSD 273
At3             SSVVEAYGDGE-RDVLGGLKVKNV-VTGDVSDLKVSGLFFAIGHEPATKFLDGGVELDSD 273
At6             SSVVEAYGDGE-RDVLGGLKVKNV-VTGDVSDLKVSGLFFAIGHEPATKFLDGGVELDSD 272
Mt1             SMVVEAFGDGE-NKKLGGLKVENV-VTKEVTDLKVSGLFFAIGHEPATKFLDGQLELDSD 313
Os2             SEVVEAYGGEG-GGPLAGVKVKNL-VTGKISDLQVSGLFFAIGHEPATKFLGGQLELDAD 271
Os3             SEVVEAYGGEG-GGPLAGVKVKNL-VTGKISDLQVSGLFFAIGHEPATKFLGGQLELDAD 271
Os1             SEVVEAYGGEG-GGPLAGVKVKNL-VTGKISDLQVSGLFFAIGHEPATKFLGGQLELDAD 271
Hv2             SEVVEAYGGAG-GGPLAGVKVKNL-VTGEVSDLQVSGLFFAIGHEPATKFLNGQLELHAD 271
Hv1             SEVVEAYGGSD-GGPLAGVKVKNL-VSGEVSDVQVAGLFFAIGHEPATKFLAGQLELDSE 271
Ta              SEVVEAYGGSD-GGPLGGVKVKNL-VTGEVSDFRVAGLFFAIGHEPATKFLAGQLELDSE 271
Os4             SEVVEAYGGAD-GGPLAGVKVKNV-VSGEVSDLQVAGLFFAIGHEPATKFLGGQLELDSD 271
Os5             SEVVEAYGGAD-GGPLAGVKVKNV-VSGEVSDLQVAGLFFAIGHEPATKFLGGQLELDSD 280
Os6             SEVVEAYGGAD-GGPLAGVKVKNV-VSGEVSDLQVAGLFFAIGHEPATKFLGGQLELDSD 308
Os7             SEVVEAYGGAD-GGPLAGVKVKNV-VSGEVSDLQVAGLFFAIGHEPATKFLGGQLELDSD 282
NC              TVGVEVKGDDK--GLMSHLVVKDV-TTGKEETLEANGLFYAIGHDPATALVKGQLETDAD 265
```

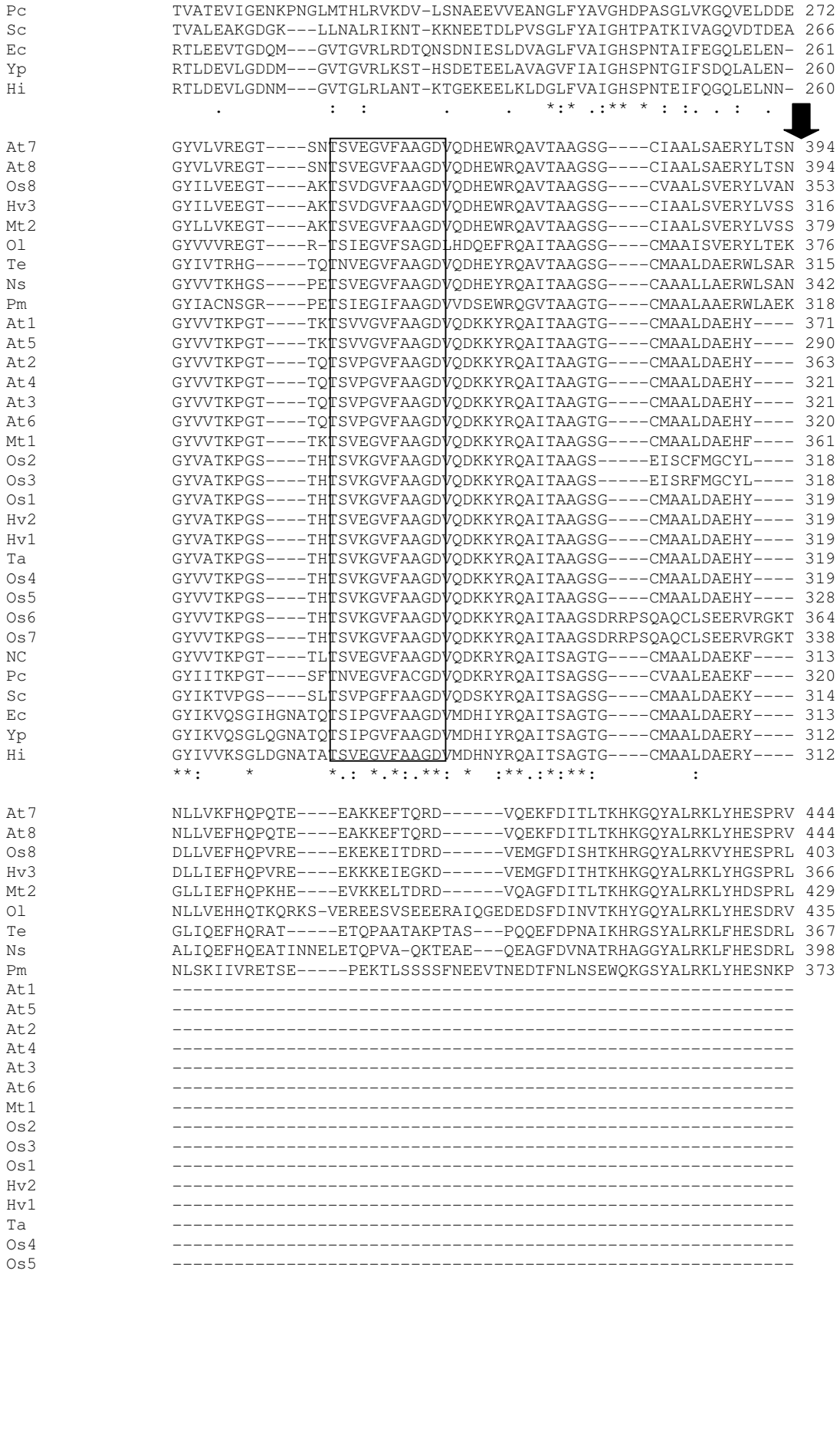
Pc TVATEVIGENKPNGLMTHLRVKDV-LSNAEEVVEANGLFYAVGHDPASGLVKGQVELDDE 272
Sc TVALEAKGDGK---LLNALRIKNT-KKNEETDLPVSGLFYAIGHTPATKIVAGQVDTDEA 266
Ec RTLEEVTGDQM---GVTGVRLRDTQNSDNIESLDVAGLFVAIGHSPNTAIFEGQLELEN- 261
Yp RTLDEVLGDDM---GVTGVRLKST-HSDETEELAVAGVFIAIGHSPNTGIFSDQLALEN- 260
Hi RTLDEVLGDNM---GVTGLRLANT-KTGEKEELKLDGLFVAIGHSPNTEIFQGQLELNN- 260
At7 GYVLVREGT----SNTSVEGVFAAGDVQDHEWRQAVTAAGSG----CIAALSAERYLTSN 394
At8 GYVLVREGT----SNTSVEGVFAAGDVQDHEWRQAVTAAGSG----CIAALSAERYLTSN 394
Os8 GYILVEEGT----AKTSVDGVFAAGDVQDHEWRQAVTAAGSG----CVAALSVERYLVAN 353
Hv3 GYILVEEGT----AKTSVDGVFAAGDVQDHEWRQAVTAAGSG----CIAALSVERYLVSS 316
Mt2 GYLLVKEGT----AKTSVEGVFAAGDVQDHEWRQAVTAAGSG----CIAALSVERYLVSS 379
Ol GYVVVREGT----R-TSIEGVFSAGDLHDQEFRQAITAAGSG----CMAAISVERYLTEK 376
Te GYIVTRHG-----TQTNVEGVFAAGDVQDHEYRQAVTAAGSG----CMAALDAERWLSAR 315
Ns GYVVTKHGS----PETSVEGVFAAGDVQDHEYRQAITAAGSG----CAAALLAERWLSAN 342
Pm GYIACNSGR----PETSIEGIFAAGDVVDSEWRQGVTAAGTG----CMAALAAERWLAEK 318
At1 GYVVTKPGT----TKTSVVGVFAAGDVQDKKYRQAITAAGTG----CMAALDAEHY---- 371
At5 GYVVTKPGT----TKTSVVGVFAAGDVQDKKYRQAITAAGTG----CMAALDAEHY---- 290
At2 GYVVTKPGT----TQTSVPGVFAAGDVQDKKYRQAITAAGTG----CMAALDAEHY---- 363
At4 GYVVTKPGT----TQTSVPGVFAAGDVQDKKYRQAITAAGTG----CMAALDAEHY---- 321
At3 GYVVTKPGT----TQTSVPGVFAAGDVQDKKYRQAITAAGTG----CMAALDAEHY---- 321
At6 GYVVTKPGT----TQTSVPGVFAAGDVQDKKYRQAITAAGTG----CMAALDAEHY---- 320
Mt1 GYVVTKPGT----TKTSVEGVFAAGDVQDKKYRQAITAAGSG----CMAALDAEHF---- 361
Os2 GYVATKPGS----THTSVKGVFAAGDVQDKKYRQAITAAGS-----EISCFMGCYL---- 318
Os3 GYVATKPGS----THTSVKGVFAAGDVQDKKYRQAITAAGS-----EISRFMGCYL---- 318
Os1 GYVATKPGS----THTSVKGVFAAGDVQDKKYRQAITAAGSG----CMAALDAEHY---- 319
Hv2 GYVATKPGS----THTSVEGVFAAGDVQDKKYRQAITAAGSG----CMAALDAEHY---- 319
Hv1 GYVATKPGS----THTSVKGVFAAGDVQDKKYRQAITAAGSG----CMAALDAEHY---- 319
Ta GYVATKPGS----THTSVKGVFAAGDVQDKKYRQAITAAGSG----CMAALDAEHY---- 319
Os4 GYVVTKPGS----THTSVKGVFAAGDVQDKKYRQAITAAGSG----CMAALDAEHY---- 319
Os5 GYVVTKPGS----THTSVKGVFAAGDVQDKKYRQAITAAGSG----CMAALDAEHY---- 328
Os6 GYVVTKPGS----THTSVKGVFAAGDVQDKKYRQAITAAGSDRRPSQAQCLSEERVRGKT 364
Os7 GYVVTKPGS----THTSVKGVFAAGDVQDKKYRQAITAAGSDRRPSQAQCLSEERVRGKT 338
NC GYVVTKPGT----TLTSVEGVFAAGDVQDKRYRQAITSAGTG----CMAALDAEKF---- 313
Pc GYIITKPGT----SFTNVEGVFACGDVQDKRYRQAITSAGSG----CVAALEAEKF---- 320
Sc GYIKTVPGS----SLTSVPGFFAAGDVQDSKYRQAITSAGSG----CMAALDAEKY---- 314
Ec GYIKVQSGIHGNATQTSIPGVFAAGDVMDHIYRQAITSAGTG----CMAALDAERY---- 313
Yp GYIKVQSGLQGNATQTSIPGVFAAGDVMDHIYRQAITSAGTG----CMAALDAERY---- 312
Hi GYIVVKSGLDGNATATSVEGVFAAGDVMDHNYRQAITSAGTG----CMAALDAERY---- 312
At7 NLLVKFHQPQTE----EAKKEFTQRD------VQEKFDITLTKHKGQYALRKLYHESPRV 444
At8 NLLVEFHQPQTE----EAKKEFTQRD------VQEKFDITLTKHKGQYALRKLYHESPRV 444
Os8 DLLVEFHQPVRE----EKEKEITDRD------VEMGFDISHTKHRGQYALRKVYHESPRL 403
Hv3 DLLIEFHQPVRE----EKKKEIEGKD------VEMGFDITHTKHKGQYALRKLYHGSPRL 366
Mt2 GLLIEFHQPKHE----EVKKELTDRD------VQAGFDITLTKHKGQYALRKLYHDSPRL 429
Ol NLLVEHHQTKQRKS-VEREESVSEEERAIQGEDEDSFDINVTKHYGQYALRKLYHESDRV 435
Te GLIQEFHQRAT-----ETQPAATAKPTAS---PQQEFDPNAIKHRGSYALRKLFHESDRL 367
Ns ALIQEFHQEATINNELETQPVA-QKTEAE---QEAGFDVNATRHAGGYALRKLFHESDRL 398
Pm NLSKIIVRETSE-----PEKTLSSSSFNEEVTNEDTFNLNSEWQKGSYALRKLYHESNKP 373
At1 ----------
At5 ----------
At2 ----------
At4 ----------
At3 ----------
At6 ----------
Mt1 ----------
Os2 ----------
Os3 ----------
Os1 ----------
Hv2 ----------
Hv1 ----------
Ta ----------
Os4 ----------
Os5 ----------

```
Os6             ------------------------------------------------------------
Os7             ------------------------------------------------------------
NC              ------------------------------------------------------------
Pc              ------------------------------------------------------------
Sc              ------------------------------------------------------------
Ec              ------------------------------------------------------------
Yp              ------------------------------------------------------------
Hi              ------------------------------------------------------------

At7             ILVLYTSPTCGPCRTLKPILNKVVDEYNHDVHFVEIDIEEDQEIAEAAGIMGTPCVQFFK 504
At8             ILVLYTSPTCGPCRTLKPILNKVVDEYNHDVHFVEIDIEEDQEIAEAAGIMGTPCVQFFK 504
Os8             VCVLYTSPTCGPCRTLKPILSKVIDEYNEHVHFVEIDIEEDPEIAEAAGIMGTPCVQFFK 463
Hv3             ILVLYTSPTCGPCRTLKPILNKVIDEYDEYVHFVEIDIEEDPEIAEAAGIMGTPCVQFFK 426
Mt2             ICVLYTSPTCGPCRTLKPILSKVIDEYDQSVHFVEIDIEEDPEIAEAAGIMGTPCVQFFK 489
Ol              VMVMYSAPTCGPCRRLKPMLDKVIAEYGDKVHYVEIDIAADPEIAEAAGVTGTPMTQIFY 495
Te              LLVKYVSPTCGPCHTLKPILDRLVEEFDGKVQLIEIDITEDSAIAEQAGVTSTPTIQLFK 427
Ns              LIVKYVSPGCGPCHTLKPILNKVVDEFDSKIHFVEIDIDQDRDIAENAGVTGTPTVQFFK 458
Pm              ILVIFSSPSCGPCHVLKPQLKRVIKEFDGAVQGIEIDIDKDQEIAKQAGINGTPTIQLFK 433
At1             -------------------------------LQEIGSQEGKSD------------------ 383
At5             -------------------------------LQEIGSQEGKSD------------------ 302
At2             -------------------------------LQEIGSQQGKSD------------------ 375
At4             -------------------------------LQEIGSQQGKSD------------------ 333
At3             -------------------------------LQEIGSQEGKSD------------------ 333
At6             -------------------------------LQEIGSQQGKSD------------------ 332
Mt1             -------------------------------LQGVGLQQDKSD------------------ 373
Os2             -------------------------------LVRIAIEIVQGLSM----------------- 332
Os3             -------------------------------LVRIAIEIVQGLSM----------------- 332
Os1             -------------------------------LQEVGAQEGKAD------------------ 331
Hv2             -------------------------------LQEVGAQVGKSD------------------ 331
Hv1             -------------------------------LQEVGAQEGKTD------------------ 331
Ta              -------------------------------LQEVGAQEGKTD------------------ 331
Os4             -------------------------------LQEIGAQEDKTD------------------ 331
Os5             -------------------------------LQEIGAQEDKTD------------------ 340
Os6             -------------------------------ITEYLSFSGDTS------------------ 376
Os7             -------------------------------ITEYLSFSGDTS------------------ 350
NC              -------------------------------LSEHEETPAEHRDTSAVQGNL--------- 334
Pc              -------------------------------IAETET----HQEAKPVL------------ 334
Sc              -------------------------------LTSLE--------------------------- 319
Ec              -------------------------------LDGLADAK----------------------- 321
Yp              -------------------------------LDGLANDK----------------------- 320
Hi              -------------------------------LDAQEA------------------------- 318
                                               :

At7             NKEMLRTISGVKMKKEYREFIE------ANK---------------------- 529
At8             NKEMLRTISGVKMKKEYREFIE------ANK---------------------- 529
Os8             NKEMLRTVSGVKMKKEYREFIE------SNK---------------------- 488
Hv3             NKEMIRTFSGVKMKKEYREFIE------SNK---------------------- 451
Mt2             NKENLKTVSGVKMKREYREFIE------ANI---------------------- 514
Ol              QKERIEVLSGVKMKSEYRRVIDGALGASATKEVTMPAAQAGEKKESPVETSR 547
Te              NKELLEVIVGMKPKSQYRETLQR------YLS---------------------- 453
Ns              DKELVKEVKGVKQKSEYRLLIEG------NL---------------------- 483
Pm              DKLLKKQWQGVKQRSEFKEAIQN------II---------------------- 458
At1             ------------------------------------------------------
At5             ------------------------------------------------------
At2             ------------------------------------------------------
At4             ------------------------------------------------------
At3             ------------------------------------------------------
At6             ------------------------------------------------------
Mt1             ------------------------------------------------------
Os2             ------------------------------------------------------
Os3             ------------------------------------------------------
Os1             ------------------------------------------------------
Hv2             ------------------------------------------------------
Hv1             ------------------------------------------------------
```

```
Ta              --------------------------------------------------
Os4             --------------------------------------------------
Os5             --------------------------------------------------
Os6             --------------------------------------------------
Os7             --------------------------------------------------
NC              --------------------------------------------------
Pc              --------------------------------------------------
Sc              --------------------------------------------------
Ec              --------------------------------------------------
Yp              --------------------------------------------------
Hi              --------------------------------------------------
```

Multiple alignment of primary sequences of NTRs from different sources using ClustalW:

Active site and the motifs in NADP- and FAD-binding domains are marked with boxes. The region used for phylogenetic analysis is enclosed between arrows. Accession numbers in NCBI protein database are: Os, *Oryza sativa*, Os1 (NP_001047911), Os2 (EAY87270), Os3 (EAZ24372), Os4 (BAD33510), Os5 (NP_001057531), Os6 (EAZ00754), Os7 (EAZ36842), Os8 (NP_001060515); At, *Arabidopsis thaliana,* At1 (Q39242), At2 (NP_195271), At3 (1VDC), At4 (AAO42318), At5 (AAO42318), At6 (CAA80656), At7 (AAL08250), At8 (NP_565954); Hv, *Hordeum vulgare*, Hv1 (EU314717), Hv2 (ABX09990), Hv3 (TC132362); Ta, *Triticum aestivum* (CAD19162); Mt, *Medicago truncatula*, Mt1 (ABH10138), Mt2 (ABH10139); Ol, *Ostreococcus lucimarinus* (XP_001422184); Te, *Thermosynechococcus elongates* (NP_682714); Ns, *Nostoc sp*. (NP_484780); Pm, *Prochlorococcus marinus* (NP_893267) ; Nc, *Neurospora crassa* (P51978); Pc, *Penicillium chrysogenum* (P43496); Sc, *Saccharomyces cerevisiae* (P29509); Ec, *Escherichia coli* (P09625); Yp, *Yersinia pestis* (NP_404967); Hi, *Haemophilus influenzae* (P43788).

Appendix 2

Appendix 3

Monitoring enzymes of the ascorbate-glutathione cycle of the barley seed embryo during seedling growth

Birgit C. Bønsager, Azar Shahpiri, Christine Finnie, and Birte Svensson*

Enzyme and Protein Chemistry, Department of System Biology, Technical University of Denmark, Søltofts Plads, Bldg 224, DK-2800 Kgs. Lyngby, Denmark

*Corresponding Author: Birte Svensson, Enzyme and Protein Chemistry, BioCentrum-DTU, Søltofts Plads, Building 224, Technical University of Denmark, DK-2800 Kgs. Lyngby, Denmark. bis@biocentrum.dtu.dk, Fax: +45 4588 6307

Abbreviations: APX: ascorbate peroxidase, AsA: ascorbic acid, DHA: dehydroascorbate. DHAR: dehydroascorbate reductase, GSH; glutathione, GSSG: oxidized glutatione, GR: glutathione reductase, MDHA: monodehydroascorbate, MDHAR: monodehydroascorbate reductase, MS: mass spectrometry; PI: post imibibition,

Abstract

Imbibition of dry mature barley seeds provokes changes in metabolic activity including *de novo* synthesis of proteins presumably from already existing mRNA. Enzymes involved in redox control especially in the embryo seem to play important functional roles during germination and seedling growth. This is described for enzymes involved in the ascorbate-glutathione cycle (ascorbate peroxidase, dehydroascorbate reductase, glutathione reductase and monodehydroascorbate reductase) by monitoring the time-course of relative increase or decrease in activity 4-144 h post imbibition (PI). Three of these enzymes were previously identified 0-72 h PI in 2D gels spot patterns and compared with the respective enzyme activities, some showing deviating and some matching behavior. The deviation most probably reflects post-translational regulation of the activity of dehydroascorbate reductase, while for ascorbate peroxidase (APX) and glutathione reductase the two analyses agreed. mRNA analysis and 2D western blotting indicated the same appearance profiles of two APX isoforms (APX1 and APX2). Ten forms of APX1 with varying pI and molecular weight and one form of APX2 were identified by mass spectrometry. This indicated post-translational modification of APX1; however, there was no indication that the modifications influenced the APX activity.

Introduction

Upon imbibition of the dry mature barley seed, oxygen uptake and oxidative phosphorylation are required to support the high energy cost of germination and rapidly resumed. Oxidative phosphorylation and mobilization of storage compounds generate reactive oxygen spieces (ROS), which cause considerable structural and functional damage to proteins and other molecules. It is well documented in the literature that ROS production after imbibition appears to be a negative event that has to be counteracted, but ROS could also be involved in cell-wall loosening processes underlying cell expansion (Schweikert et al., 2000; 2002) or take part in protecting the embryo against pathogens (Schopfer et al., 2001). ROS moreover function in signaling. H_2O_2 thus signals programmed cell death of the aleurone layer (Jabs, 1999; Amor et al., 2000; Fath et al., 2001). Redox homeostasis is governed by large pools of antioxidants, which scavenge and buffer reductants, and oxidants including ascorbate (AsA) and glutathione (GSH). Oxidation of AsA leads to monodehydroascorbate (MDHA), which

disproportionates to dehydroascorbate (DHA) and AsA, while oxidized glutathione (GSSG) is formed from GSH.

Enzymes of the ascorbate-glutathione cycle are involved in protection against ROS (Fig. 1). H_2O_2 is thus broken down to H_2O and molecular oxygen (O_2) by ascorbate peroxidase (APX) in the oxidation of AsA to MDHA. The three other enzymes in the ascorbate-glutathione cycle participate in regeneration of AsA; monodehydroascorbate reductase (MDHAR) and dehydroascorbate reductase (DHAR) reduce MDHA and DHA to AsA, respectively, and glutathione reductase (GR) reduces GSSG to GSH, which acts as electron donor for DHAR. MDHAR and GR use NADPH as an electron donor.

The enzymes of the ascorbate-glutathione cycle are present in plants and occur as different isoforms specific to various compartments (cytoplasma, chloroplasts, mitchondria, peroxisomes and apoplast) (Mittler, 2002). The ascorbate-glutathione cycle was studied under different physiological conditions of seeds. During seed development of wheat and broad bean levels of AsA and DHA, MDHA and GSH increase, but they decrease again during desiccation where AsA completely disappears (Arrigoni et al., 1992; De Gara et al., 2003). Accordingly, enzyme activities involved in the ascorbate-glutathione cycle decrease at desiccation. At germination of wheat and pine seeds the AsA content increases significantly and DHA increases slightly 24 h PI (De Gara et al., 1997; Tommasi et al., 2001). This is in agreement with the biosynthesis increasing of the last precursor (galactono-γ-lactone) for AsA in germinating wheat seeds (De Gara et al., 1997). The absence of APX in 2D gels of mature barley embryo extracts (Bønsager et al., 2007) and of APX activity in mature wheat and pine seeds (Asada, 1997; Tommasi, 2001; De Gara, 2003) indicate that the ascorbate-glutathione cycle is not important in desiccation (Bailly, 2004). Residual levels of DHAR and MDHAR in the dry seed may be needed for immediate generation of AsA upon imbibition, as new AsA biosynthesis only starts 10-20 h PI (De Gara et al., 1997). DHAR activity decreases, while MDHAR and GR activities slightly increase PI.

APX, DHAR and GR, have been tracked in a thorough spatiotemporal 2D gel-based analysis 0-72 h PI of dissected barley seed tissues, *i.e*. embryo, aleurone layer, and endosperm (Bønsager et al., 2007; Østergaard et al. 2004). DHAR appeared in two forms of the same gene product in all three tissues, GR was found in embryo and aleurone layer, and APX increased in abundance from 24 h PI and was found only in the embryo. This indicated that

the ascorbate-glutathione cycle plays a distinct role in the embryo during seedling growth (24-144 h PI).

To improve insight of the functional roles of APX, DHAR, GR and MDHAR during germination (0-24 h PI) and seedling growth (24-144 h PI), enzyme activities were measured in embryos of barley seeds germinated for 0-144 h PI. The progress of the different enzyme activities was compared to 2D gel spot patterns and intensities of the same enzymes (Bønsager et al. 2007). In case of APX, enzyme activity and 2D gel patterns were also compared to the mRNA levels and 2D western blotting. The results underline the importance of these various enzymes during seedling growth and indicate that the activity can be regulated at both the translational and the post-translational level.

Results

Protein extracts and enzyme activities: Efficient small scale extraction of water soluble proteins from barley seed embryos was based on the method used for samples in 2D gel analysis of dissected seed tissues (Finnie et al., 2003; Bønsager et al., 2007). The enzyme activities of APX, DHAR, GR, and MDHAR were monitored spectrophotometrically of formation or consumption of either AsA (for APX and DHAR) or NADPH (for MDHAR and GR). The activities were measured in triplicates using freshly prepared extract for each replicate and activity units were calculated based on the total protein content, which appeared to be approximately the same for all samples (4-144 h PI) as determined for individual replicates by using the Popov method (Popov et al., 1975). The enzyme activities were corrected for non-enzymatic side-reactions as previously described (Nakano and Asada, 1981). The 4 h PI sample was used to indicate the background activity level instead of 0 h PI, as dissection with reliable removal of remaining endosperm was much easier in 4 h imbibed seeds compared to dry seeds. It was assumed that the change in enzyme activity of APX, DHAR, MDHAR and GR to be insignificant during the first 4 h PI according to similarity of the 2D gel patterns of embryo extracts at 0 and 4 h PI (Bønsager et al., 2007). However it cannot be excluded that important activity regulation is induced immediately after imbibition. The activity assays were carried out only on embryo extracts (4-144 h PI) where the ascorbate-glutathione cycle is expected to play an important role.

Activities of APX, MDHAR, DHAR and GR: In embryos of mature dry barley seeds activity was found for DHAR, MDHAR and GR as opposed to APX (Table1), for which activity was detected 36 h PI and increased up to 144 h PI. DHAR activity rapidly decreased until 72 h PI and a small recovery in activity was observed 144 h PI which may represent response to increased generation of ROS during the late radicle elongation. The DHAR activity has not previously been measured in this time frame. GR and MDHAR showed small 1.8 and 2.7 fold increases in activity over the 144 h.

Comparison of enzyme activities with 2D gel spot patterns: APX, DHAR and GR were identified in 2D gels of dry, mature barley seed embryos and followed during germination and seedling growth until 72 h PI (Bønsager et al., 2007). Since the protein extracts were prepared almost the same way (5 or 7 embryos used, pH 7.5 or 8.0), the enzyme activities can be compared with the 2D gel spot patterns. GR was identified in one spot (Fig. 2b, # 409) that slightly decreased in intensity during 0-72 h PI; the enzymatic activity remained constant within the same timespan (Table 1). This visual change in spot intensity might stem from increased amounts of other proteins in the total protein extract and thus dominating the GR spot intensity. Therefore the activity profile and the 2D gel spot patterns of GR are in relatively good agreement. DHAR was identified in two spots differing in regards to molecular weight in the 2D gel (# 142 and 294; Fig. 2c); one remained constant 0-72 h PI and one decreased rapidly. According to mass spectrometry data, active site residues are found in both of these forms, but we do not know if both forms are active. The total amount of DHAR in the 2D gels disagrees with the disappearance of DHAR activity and this may indicate post-translational regulation of DHAR activity. Such a regulatory mechanism could turn off the activity during seedling growth, while at 144 h PI the DHAR may be re-activated due to an increase in ROS at the late period of seedling growth.

APX was previously identified in two different cytosolic isoforms (APX1, accession number AJ006358 and APX2, accession number AF411228) in 2D gels of developing barley seeds (Finnie et al., 2003). One of these (APX1) was identified in one clear spot in embryos from germinating barley seeds and increased from 24 h PI (# 79; Fig. 2d), whereas no APX was identified from mature dry seeds. The increase in APX activity from 24 h PI is in excellent agreement with 2D gel spot pattern of APX1 (Table 1). RT-PCR analysis and 2D western blotting (described below) indicated the presence of APX2 at mRNA and protein level as described below. This was confirmed by MS-MS on trypsin digests of gel pieces excised from

the area of the gel, where APX2 was expected to be present based the identification in developing endosperm. A few weak peaks specific to APX2 was identified by MS and a single peptide was subjected to MS/MS (1309.646; LPDATQGSDHLR). This sequence contain a lysine instead of a glutamine in position 6 in APX1, which would therefore be cleaved by trypsin and has not been observed in any of the APX1 spectra. Finally, MDHAR was not identified in germinating barley seeds, possible explanations can be low abundance or poor solubility in the extraction buffer, or both.

APX isoforms: The amount of APX2 seemed to be much lower than the amount of APX in the germinated embryo, however, APX2 may still play an important function and may contribute to the measured APX activity. The presence was examined using RT-PCR or specific antibodies. RT-PCR found both APX genes to be expressed in embryo of the dry seed. Since two genes have and the APX transcripts increase up to 72 h and then remained constant until 144 h (Fig. 3). It was previously reported that many mRNAs have survived the desiccation and are present in the dry, mature seed where they may serve in initial protein synthesis PI (Rajjou et al. 2004). This mRNA is probably replaced during seedling growth. A zymogram indicated that two active APX forms increase in activity in parallel (Fig. 4), which may represent APX1 and APX2. Noticeably, however, it cannot be excluded that these forms are of the same isoform at monomer and a dimmer states.

Identification of APX spots using antibodies and mass spectrometry: Using specific antibodies allowed test for appearance of APX by western blotting of 2D gels in embryos from non-germinated and germinated seeds. The antibodies most probable recognizing both APX isoforms which share 83.6% sequence identity. Two APX spots became visible at 24 h PI by western blotting and these increased in abundance up to 72 h PI (not shown). Size and pI for the basic spot corresponded to APX1 in embryo from germinated seeds (# 79; Fig. 5) while the more acidic spot most probable contain APX2, as this isoform was identified in this area of the gel. Approximately 15 additional APX spots were observed at 48 h PI and 35 at 72 h PI of varying intensity, pI, and Mw (Fig. 5). Spots were excised based on western blots, and from a corresponding Coomassie stained 2D gel, some very weak spots and some not visible, were analyzed by MS. APX1 was identified in a total of 10 different spots (Table 2). The identified 10 APX spots differed slightly in molecular mass and pI indicating that

truncation removing a short segment from some forms as well as post-translational modifications give rise to pI differences. This can include different states of oxidation of cysteine, deamidation of aspargine or glutamine, or glycosylation. There is a potential glycosylation site at Asn31, however, there is no clear evidence that it actually is glycosylated. Three different endoproteolytic enzymes (trypsin, AspN and LysC) were employed prior to MS in order to obtain high sequence coverage to aid identification of possible post-translational modifications. A sequence coverage of 92.4% was reached for spot 79 and between 29.2-83.2% was reached for the rest of APX1 spots probably depending on the abundance of the different forms. Despite of this high sequence coverage, it was not possible to identify any post-translational modifications.

Discussion

Enzyme activity analysis was compared with 2D gels analysis of spots containing the enzymes in question. In case of APX, mRNA analysis and western blotting of 2D gels were performed to understand functionality and regulation of APX isozymes from the ascorbate-glutathione cycle. While 2D gel analysis is an excellent multi-window method for monitoring proteins in complex extracts, the function of such enzyme need to be determined by analyzing enzyme activities. Generally enzyme activities in protein extracts are difficult to determine as influence of other proteins and compounds on the activity can be difficult to elucidate. However, active site-directed chemical probes for enzymatic activity profiling in complex mixtures known as activity-based proteomics has accelerated functional annotation of proteins (reviewed in Schmidinger et al., 2006). This employs probe design for different enzyme classes. Moreover, a platform for measuring 23 different plant enzyme activities has been developed (Gibon et al., 2004). Indeed comparison between 2D gel patterns with enzyme activities represents a rarely applied strategy. Several studies actually compare 2D gel analysis with cDNA microarray data, cases are reported; however, where these two types of analysis display poor correlation (Kollipara et al., 2002; Gygi et al. 1999; Tian et al., 2004), which stresses the importance of using more than one approach to study a process.

Enzyme activity assay- Using small scale protein extractions of barley embryos (Finnie and Svensson, 2003) with 20-24 h intervals at 4-144 h PI, activity profiles of enzymes involved in the ascorbate-glutathione could be followed reliably during seedling growth. Such activity

profiles agreed with published data previously for 48 h germinated wheat seeds (De Gara et al., 1997) and the present findings support the hypothesis that the ascorbate-glutathione cycle is not functioning during desiccation due to lack of APX activity. Most other major redox-related enzymes, e.g. superoxide dismutase, glutathione reductase, glutathione *S*-transferase, peroxiredoxin, thioredoxin h, GSH dependent dehyroascorbate reductase, seem to exist in the embryo and aleurone layer from non-germinated barley seeds and some even in the non-living endosperm tissue (Bønsager et al., 2007). However APX was only identified in germinated embryos (Bønsager et al., 2007) and therefore may exert a specific and important function in embryo during seedling growth in accordance with high metabolic activity in this active and dividing tissue. The ascorbate-glutathione cycle may be less important in the aleurone layer where many enzymes are degraded in connection with cell death and in the endosperm, which is dead tissue where protection against ROS has little importance.

The rather high activity of DHAR during germination may be critical for immediate formation upon imbibition of AsA to control ROS prior to AsA biosynthesis being adequately restored (Tommasi et al., 2001). Removal of DHA by reduction to AsA in chloroplasts is essential, since a low concentration of 50 μM DHA inhibits the regulatory functions of Trx in chloroplasts metabolism (Morell et al., 1997). This may however, not represent a problem as DHA ever accumulates to any significant extent due to high activities of MDHAR and the presence of reduced ferredoxin that reduces MDHA to AsA. During radicle elongation MDHAR may be more important than DHAR in generation of AsA, since activity of MDHAR increased slightly as opposed to the activity of DHAR (Arrigoni et al., 1981; Mittova et al., 2000). The relative impact of these two enzymes remains to be understood, the specific activity of MDHAR, however, is 10 fold higher than of DHAR in both mitochondria and chloroplasts of tomato (Mittova et al., 2000).

The GR and MDHAR activities both slightly increase 4-144 h PI and both use NADPH as a proton donor in catalysis. This was correlated with an increase in available NADPH during germination, where the pentose phosphate cycle responsible for generation of NADPH in non-green tissue was activated by imbibition (Mayer and Poljakoff-Mayber, 1982; Tommasi, 2001). A slightly elevated GR activity indicates constant utilization of GSH in germination and seedling growth and the activities of GR and DHAR that are tightly linked in the ascorbate-glutathione cycle, change in an opposite manner over the time spend on the analysis. This relation is expected since GSH is involved also in other processes, *i.e.* the

sulphur metabolism (Noctor et al., 1998; De Kok and Stulen, 1993) and for maintaining the redox potential.

Comparison with 2D gel spot patterns-The enzyme activity profiles were compared with 2D gel spot appearance patterns of APX, DHAR and GR. APX and GR showed agreement between these two types of analysis, but for DHAR the results deviated indicating regulation of the activity at a post-translational level. We cannot exclude that more than one form and/or isoform of individual proteins contribute to enzyme activities, but have not identified in the 2D gel spot pattern. A clear example was confirmed in case of APX, where 2D gel western blotting, approximately two orders of magnitude superior in sensitivity than Coomassie staining (and silver staining), revealed 35 different APX forms 72 h PI. Some of these forms displayed very low abundance, while others may be inactive forms. In case of DHAR, it is known that many other proteins have DHA reduction activity *in vitro* similarly to glutaredoxin, PDI, thioredoxin m and f, and Kunitz type trypsin inhibitor (Ahn and Moss, 1992; Park and Levine, 1996; Trümper et al., 1994; Wells et al., 1990). These proteins all have a tetrapeptide domain with a redox active cystine (disulphide- bonded form) group or a cysteine-serine site. It remains to be known, however, if the DHA reducing activity has any physiological role. DHAR may be regulated by the intracellular redox state and interaction with thioredoxin h was suggested (Wong et al., 2003; Gelhaye et al., 2006), however, a specific mechanism of interaction has not been identified.

APX isoforms- The present study confirms that mRNA of both APX1 and APX2 are found in the dry mature seed and the levels increase during radical elongation. It is not proven if this mRNA survived desiccation and is then used as a template for translation. The timeframe for synthesis of new mRNA is 30-90 min (Potokina et al., 2002) and newly synthesized mRNA may replace mRNA left over from the seed maturation. Translation of APX apparently starts at the end of germination and beginning of radicle elongation (24-36 h PI) and 10 APX1 forms and one APX2 form were identified by MS at 72 h PI. However, it has not yet been possible to identify the differences between these forms. The high molecular weight forms of APX1 may be glycosylated on Asn31 but this remains to be confirmed.

Concluding remarks

In the present study enzymes of the ascorbate-glutathione were detected during seed development and growth at the transcript level, the translated level, and the activity level. The unusual approach of comparing activity profiles with 2D gel patterns was allowed as very similar protein extraction procedures were applied for the preparation of protein samples. Both of these types, however, have limitations, and a combined methodology is needed therefore to give clues that enable concrete regulatory points to be addressed.

This study shows the intensity and activity of APX isoforms increase during seed germination and seedling growth. However, the enzymes which are involved on recycling APX substrate (AsA) was found to decrease in intensity and activity between 0-72 h. This suggest that maybe AsA are more synthesised during germination instead of recycling. In agreement the activity of GLDH, the enzyme that synthesizes AsA increased in embryo of *Pinus pinea* during germination (Tommasi et al., 2001).

APX1 seems to be dominant isoform in embryo whereas both isoforms are present in endosperm during development.This may suggest the specific role for APX2 in endosperm. Differential pattern of DHAR isoforms suggest that they may have different roles in germination. MDHR may have marginal role in recycling of AsA during germination since it is absent on 2D gel and it shows weak activity.

Materials and Methods

Preparation of plant material: Germination of barley seeds (cv. Barke), isolation of embryos, protein extraction and 2DE analysis were performed as previously described (Bønsager et al., 2007). Protein extracts for enzyme activity assays were made on 7 embryos. Embryos were ground to a fine powder using a plastic pestle in an eppendorf tube on ice with 350 µL ice cold extraction buffer (100 mL Tris pH 8.0, 0.5 mM ascorbate, mini-complete protease inhibitors (Roche, Basel, Switzerland), transferred using another 350 µL extraction buffer to a 2 mL tube, added one glass bead, and shaked in and eppendorf shaker for 30 min at top speed and 4^{o}C. Samples were centrifuged 30 min (14000 × g, 4^{o}C) and supernatants (500 µL) containing soluble proteins were desalted on NAP5 columns (GE-healthcare, Stockhom, Sweden) eluted in 1 mL extraction buffer, stored at -20^{o}C and used within a week. Protein concentrations in extracts were determined by the Popov method (Popov et al., 1975) with bovine serum albumin as a standard.

Enzyme assays: APX activity was assayed from AsA oxidation monitored by decrease in absorbance at 290 nm (Nakano and Asada, 1981) using 50 µL embryo extract (30 µg protein) in 50 mM potassium phosphate pH 7.0, 0.1 mM EDTA, 1 mM AsA, and 1 mM H_2O_2 in a final volume of 1 mL. The reaction was initiated by addition of H_2O_2 and followed at 290 nm for 9 min. Correction was made for a low, non-enzymatic oxidation of AsA by H_2O_2. Usually correction for oxidation of AsA in the absence of H_2O_2 was not required, showing absence even of very low activity of ascorbate oxidase in the barley seeds. The DHAR activity was measured from the increase in absorbance at 265 nm as DHA was reduced to AsA (Nakano and Asada, 1981). Activity of DHAR was analyzed in 20 µL embryo extract (12 µg protein) in 50 mM potassium phosphate pH 7.0, 0.1 mM EDTA, 2.5 mM GSH, 0.2 mM DHA (freshly preprared) in a final volume of 1 mL (Dalton et al., 1986). The reaction was initiated by addition of DHA and followed at 265 nm for 9 min. Correction was made for non-enzymatic reduction of DHA. GSSG has low absorbance at 265 nm and GR activity was assayed using the decrease in absorbance at 340 nm due to NADPH oxidation (Foster and Hess 1982). The Activity of GR was determined in 50 µL embryo extract (30 µg protein) 100 mM HEPES pH 7.8, 0.3 mM NADPH, 1 mM GSSG, initating the reaction by addition of GSSG and followed the absorbance at 340 nm for 9 min. MDHAR activity was measured from decrease in absorbance at 340 nm due to NADPH oxidation (de Pinto et al., 2000). The activity of MDHAR was measured in 350 µL embryo extract (220 µg protein) in 100 mM Tris-HCL pH 8.0, 0.2 mM NADPH, 1 U ascorbate oxidase (Sigma, St. Louis, MO, USA), 2.5 mM AsA in a volume of 1 mL. The reaction was started by adding AsA and followed at 340 nm for 9 min. All enzyme activities were measured at room temperature.

Calculation of enzyme activity: The change in absorbance per min per mg total protein was used to calculate the activity in extracts by dividing with the extinction coefficients for AsA at either 265 (14 $M^{-1}cm^{-1}$) or 290 nm (2.8 $M^{-1}cm^{-1}$) or for NADPH at 340 nm (6.22 $M^{-1}cm^{-1}$) (Hiner 2000).

Detection of APX activity in gels: Embryo extracts were concentrated (microcon spin column, cut off 3000 kDa; Millipore, Billerica, MA) to a concentration of ~2.5 mg/mL. A native tris glycine 12-14% acrylamide gel system (Novex system, Invitrogen) was pre-equilibrated 20 min with 2 mM AsA in the cathode buffer prior to sample application (10 µL; 25 µg protein). The gel was run according to the manufacture's recommendation on ice. Activity detection (Mittler and Zilinskas, 1993) was performed at room temperature.

Subsequent to the electrophoretic protein separation, the gel was equilibrated with 50 mM sodium phosphate pH 7, 2 mM AsA for 3 × 10 min and then incubated with 50 mM sodium phosphate pH 7.0, 4 mM AsA, 2 mM H_2O_2 for 20 min. H_2O_2 was added to start the reaction. The gel was subsequently washed with 50 mM sodium phosphate pH 7.0 for 1 min and submerged in 50 mM sodium phosphate pH 7.8, 28 mM TEMED, 2.45 mM nitroblue tetrazolium (NBT). APX activity was seen as an achromatic band on a purple background.

Immuno-detection of APX: 2D gels after 2nd dimension (Bønsager et al., 2007) were equilibrated in transfer buffer (Invitrogen, Groningen, Netherlands) containing 15% methanol for 30 min. Proteins were electroblotted onto a nitrocellulose membrane (equilibrated 10 min in Milli-Q H_2O and 15 min in transfer buffer) for 5 h (60 V, 120 mA, 20W; 0.3 mA/cm^2) in a semidry blotting apparatus (Multiphor II system; GE Healthcare) according to the manufacturer's recommendations.

The membrane with electroblotted proteins (Section 2.5.4) was soaked in TBST buffer (25 mM Tris-HCl pH 8, 150 mM NaCl, 0.1% Tween-20) for non-specific blocking followed by 1 h incubation with primary antibody (dilution 1:1000-3000) in TBST buffer. The membrane was washed 3 × 5 min in TBS and blocked again for 30 min in TBST. Secondary antibody (goat anti-rabbit/alkaline phosphatase conjugated; 1:2000) was added followed by incubation for 30 min. The membrane was washed 3 × 5 min and immunoreactive proteins were stained in 100 mM Tris Base pH 9.5, 100 mM NaCl, 5 mM $MgCl_2$ containing 0.33 mg/mL NBT and 0.17 mg/mL 5-bromo 4-chloro indolyl phosphate (BCIP) for 5 min. The reaction was stopped by change to Milli-Q H_2O.

Mass spectrometry: Trypsin, AspN or LysC digestion of the excised spots were analyzed by MALDI-TOF or MALDI-TOF/TOF MS (Bruker Reflex III). The peptide maps were subjected to a Mascot search in the NCBI database or in the EST-database for green plants. If the peptide map resulted in unsuccessful or uncertain identification, the peptides were analyzed by MALDI-TOF/TOF in order to obtain sequence information. Proteins were identified using peptide mass mapping and searching the National Center for Biotechnology Information non-redundant database (NCBInr) using the search engine MASCOT (Perkins et al., 1999). Identifications were considered positive identifications when at least 5-9 peptides were matching with an accuracy of 0.1 Da and a significant MASCOT score.

Gene expression analysis: Total RNA for RT-PCR analysis was isolated from embryo by the RNeasy Plant Mini Kit (Qiagen, city, states) and treated with RNase-Free DNase set (Qiagen)

to remove contaminating genomic DNA. RT-PCR analysis was performed using One-Step RT-PCR Kit (Qiagen) Barley 18S rRNA showing invariable expression across the samples was amplified in parallel. A 25 µL standard RT-PCR mixture contained 1 × reaction buffer, 1 × Q solution, 0.4 mM deoxynucleotide triphosphates, 0.6 µM primers, 2 units RNase inhibitor and 1 µL reverse transcriptase-DNA Taq polymerase enzyme mix. A total of 50 and 100 ng of RNA was used for analysis of APX and 18SrRNA, respectively. The optimal number of amplification cycles for each set of primers was determined at the exponential phase range of amplification. The thermal cycling consisted of 50ºC (30 min) to synthesize the first-strand cDNA; 95ºC (15 min) to inactivate reverse transcriptase and activate Taq DNA polymerase; 15 (18SrRNA) or 30 cycles (APX1 and APX2) of 94ºC (1 min), 63ºC (1 min), and 72ºC (1 min) for PCR amplification; and a final elongation at 72ºC (10 min). Reactions were performed in duplicate. Amplification products were separated on ethidium bromide agarose gel. Primers were 5´-CTACGTCCCTGCCCTTTGTACA-3´ and 5´-ACACTTCACCGGAC-CATTCAA-3´ for 18SrRNA. primers 5´-GCAAGTCTTTGGGAAGCAGA-3´ and 5´-AGTTTTGTCACTTGGA AGCTGAAG-3´ for APX1 (AJ006358) and Primers 5´-CAGGCAGGTGTTTTCCACTC-3´ and 5´-CCTTGTCGGTCGGCAACT-3´ for analysis of APX1 (AF411228) and. Due to high similarity between APX genes and possibility of recognition of each gene by another gene primer set RT-PCR products were cloned in pDrive cloning vector (Qiagen) and confirmed by sequencing (MWG, Biotech AG).

References

1. Bønsager, B.C., Finnie, C., Roepstorff, P., Svensson, B. (2007) Spatio-temporal changes in germination and radical elongation of barley seeds tracked by proteome analysis of dissected embryo, aleurone layer and endosperm tissues. Proteomics 7, 4528-4540
2. Mittova, V., Vanderauwera, S., Gollery, M., van Breusegem, F. (2000) Activities of SOD and the ascorbate-glutatione cycle enzymes in subcellular compartments in leaves and roots of the cultivated tomato and its wild salt-tolerant relative *Lycopersicon pennilli*. *Plant Physiol.* 110, 42-51.
3. Arrigoni, O., De Gara, L., Tommasi, F., Liso, R. (1992) Changes in the ascorbate system during seed development of *Vivia faba* L. *Plant Physiol*. 99, 235-238.
4. De Gara, L., de Pinto, M.C., Moliterni, V.M.C., D'Egidio, M.G. (2003) Redox regulation and storage processes during maturation in kernels of *Triticum durum. J. Exp. Bot*. 54, 249-381.

5. De Gara, L., Pinto, M.C., Arrigoni, O. (1997) Ascorbate synthesis and ascorbate peroxidase activity during the early stage of wheat germination. *Physiol. Plant.* 100, 894-900.
6. Tommasi, F., Paciolla, C., de Pinto, M.C., De Gara, L. (2001) A comparative study of glutathione and ascorbate metabolism during germination of *Pinus pinea* L. seeds. *J. Exp. Bot*. 52, 1647-1654.
7. Asada, K. (1997) The role of ascorbate peroxidase and monodehydroascorbate reductase in H_2O_2 scavenging in plants. In: Scandalios, J.D. Ed. *Oxidative stress and molecular biology of antioxidant defences*. New York: Cold Spring Habour Laboratory Press, 527-568.
8. Finnie, C., Svensson, B. (2003) Feasibility study of a tissue-specific approach to barley proteome analysis: aleurone layer, endosperm, embryo and single seeds. *J. Cereal Sci.* 38, 217-227.
9. Popov, N., Schmitt, M., Schulzeck, S., Matthies, H. (1975) Eine Störungsfreie Mikromethode zur Bestimmung des Proteingehaltes in Gewebehomogenaten. *Acta Biol. Med. Ger*. 34, 1441-1446.
10. Rajjou, L., Gallardo, K., Debeaujon, I., Vandekerckhove, J., Job, C., Job, D. (2004) The effect of α-amanitin on the Arabidopsis seed proteome highlights the distinct roles of stored and neosynthesized mRNAs during germination. *Plant Physiol.* 134, 1598-1613.
11. Wilhelmson, A., Laitila, A., Vilpola, A., Olkku, J., Kotaviita, E., Fagerstedt, K., Home, S. (2006) Oxygen deficiency in barley (*Hordeum vulgare*) grain during malting. *J. Agric. Food Chem*. 54, 409-416.
12. Morell, S., Follmann, H., De Tullio, M., Häberlein, I. (1997) Dehydroascorbate and dehydroascorbate reductase are phantom indicators of oxidative stress in plants. *FEBS Lett*. 414, 567-570.
13. Arrigoni, O., Dipierro, S., Borraccino, G. (1981) Ascorbate free radical reductase, a key enzyme of the ascorbic acid system. *FEBS Lett*. 120, 242-244.
14. Mayer, A., Poljakoff-Mayber, A. (1982) Metabolism of germinating seeds. In: Wareing, P.F., Galston, A.Y., (Eds.) *The germination of seeds*. New York. Pergamon Press, 85-139.
15. Nakano, Y., Asada, K. (1981) Hydrogen peroxide is scavenged by ascorbate-specific peroxidase in spinach chloroplasts. *Plant Cell Physiol*. 22, 867-880.
16. Jabs, T. (1999) Reactive oxygen intermediates as mediators of programmed cell death in plant and animals. *Biochem. Pharmacol*. 57, 231-245.
17. Amor, Y., Chevion, M., Levine, A. (2000) Anoxia pretreatment protects soybean cells against H_2O_2-induced cell death: possible involvement of peroxidases and of alternative oxidase. *FEBS Lett*. 477, 175-180.
18. Fath, A., Bethke, P.C., Jones, R.L. (2001) Enzymes that scavange reactive oxygen species are down-regulated prior to gibberellic acid-induced programmed cell death in barley aleurone. *Plant Physiol.* 126, 156-166.
19. Østergaard, O., Finnie, C., Laugesen, S., Roeostorff, P., Svensson, B. (2004) Proteome analysis of barley seeds: Identification of major proteins from two-dimensional gels (pI 4-7). *Proteomics* 4, 2437-2447.

20. Kollipara, K.P.K., Saab, I.N., Wych, R.D., Lauer, M.J., Singletary, G.W. (2002) Expression profiling of reciprocal maize hybrids divergent for cold germination and desiccation tolerance. *Plant Physiol*. 129, 974-992.
21. Gygi, S.P., Rochon, Y., Franza, R., Aebersold, R. (1999) Correlation between protein and mRNA abundance in yeast. *Mol. Cell. Biol.* 19, 1720-1730.
22. Tian, Q., Stepaniants, S.B., Mao, M., Weng, L., Feetham, M.C., Doyle, M.J., Yi, E.C., Dai, H.,Thorsson, V., Eng, J., Goodlett, D., Berger, J.P., Gunter, B., Linseley, P.S., Stoughton, R.B., Aebersold, R., Collins, S.J., Hanlon, W.A., Hood, L.E. (2004) Integrated genomics and proteomics analysis of gene expression in mammalian cells. *Mol. Cell. Proteomics* 3, 960-968.
23. Noctor, G., Foyer, C.H. (1998) ASCORBATE AND GLUTATHIONE: Keeping Active Oxygen Under Control. *Annu. Rev. Plant Physiol. Plant Mol. Biol.* 49, 249-279.
24. De Kok, L.J., Stulen, I. (1993) Role of glutathione under oxidative stress. In: De Kok, L.J. et al., (Eds.). *Sulphur nutrition and assimilation in higher plants*. The Hague, The Netherlands: SPB Acadmic Publishing, 125-152.
25. Wells, W.W., Xu, D.P., Yang, Y., Rocque, P.A. (1990) Mammalian thiotransferase (glutaredoxin) and protein disulfide isomerase have dehydroascorbate reductase activity. *J. Biol. Chem*. 265, 15361-15364.
26. Ahn, B.Y., Moss, B. (1992) Glutaredoxin homologue encoded by vaccinia virus is a virion-associated enzyme with thioltransferase and dehydroascorbate reductase activities. *Proc. Natl. Acad. Sci. USA* 89, 7060-7065.
27. Trümper, S., Follmann, H., Häberlein, I. (1994) A novel dehydroascorbate reductase from spinach chloroplasts homologous to plant trypsin inhibitor. *FEBS Lett*. 352, 159-162.
28. Park, J.B., Levine, M. (1996) Purification, cloning and expression of dehydroascorbic acid-reducing activity from human neutrophils: identification as glutaredoxin, *Biochem. J.* 315, 931-938.
29. May, J.M., Mendiratta, S., Hill, K.E., Burk, R.F. (1997) Reduction of dehydroascorbate to ascorbate by the selenoenzyme thioredoxin reductase*. J. Biol. Chem*. 272, 22607-22610.
30. Mittler, R. (2002) Oxidative stress, antioxidants and stress tolerance. *Trends Plant Sci*. 7, 405-410.
31. Schopfer, P. Plachy, C., Frahry, G. (2001) Release of ractive oxygen intermediates (superoxide radicals, hydrogen peroxide,, and hydroxyl radicals) and peroxidase in germinating radish seeds controlled by light, gibberellin, and abscisic acid. Plant Phys. 125, 1591-1602.
32. Schweikert, C., Liszkay, A., and Schopfer, P. (2000) Scission of polysaccharides by peroxidase-generated hydroxyl radicals. Phytochemistry 53, 565-570.
33. Schweikert, C., Liszkay, A., Schopfer, P. (2002) Polysaccharide degradation by Fenton reaction- or peroxidase-generated hydroxyl radicals in isolated plant cell walls. Phytochemistry 61. 31-35.
34. Wong, W.H., Balmer, Y., Cai, N., Tanaka, C.K., Vensel, W.H. Hurkman, W.J., Buchanan, B.B. (2003) Unraveling thioredoxin-linked metabolic processes of cereal starchy endosperm using proteomics. *FEBS Lett*. 547, 151-156.
35. Gelhaye, E., Navrot, N., Macdonald, I.K., Rouhier, N., Raven, E.L., Jacquot, J.-P. (2006) Ascorbate peroxidase-thioredoxin interaction. *Photosynth. Res*. 89, 193-200.

36. Potokina, E., Sreenivasulu, N., Altschmie, L., Michalek, W., Graner, A. (2002) Differential gene expression during seed germination in barley (*Hordeum vulgare* L.). *Funct. Integr. Genomics* 2, 28-39.
37. Chen, G-X., Asada, K. (1989) Ascorbate peroxidase in tea leaves: occurrence of two isozymes and differences in their enzymatic and molecular properties. *Plant Cell Physiol*. 30, 987-998.
38. Schmidinger H., Hermetter, A., Birner-Gruenberger, R. (2006) Activity-based proteomics: enzymatic activity profiling in complex proteomes. Amino acids 30, 333-350.
39. Gibon, Y., Blaesing, O.E., Hannemann, J., Carillo, P., Höhne, M., Hendriks, J.H.M., Palacios, N., Cross, J., Selbig, J., Stitt, M. (2004) A robot-based platform to measure multiple enzyme activities in Arabidopsis using a set of cycling assays: comparisons of changes of enzyme activities and transcript levels during cycles and in prolonged darkness. *Plant Cell.* 16, 3304-3325

Table 1. Enzyme activities of APX, DHAR, GR and MDHAR measured in embryo extracts.

	Units/microgram protein			
h PI	**APX**	**DHAR**	**GR**	**MDHAR**
4	0.023 (+/-0.006)	3.232 (+/-0.315)	0.189 (+/-0.031)	0.036 (+/-0.004)
24	0.064 (+/-0.002)	2.710 (+/-0.139)	0.202 (+/-0.027)	0.037 (+/-0.003)
48	0.203 (+/-0.055)	1.514 (+/-0.117)	0.240 (+/-0.053)	0.053 (+/-0.006)
72	0.439 (+/-0.117)	0.355 (+/-0.135)	0.197 (+/-0.051)	0.057 (+/-0.010)
96	0.666 (+/-0.056)	0.388 (+/-0.131)	0.282 (+/-0.068)	0.074 (+/-0.014)
120	0.898 (+/-0.092)	0.224 (+/-0.195)	0.317 (+/-0.045)	0.074 (+/-0.018)
144	0.900 (+/-0.135)	1.640 (+/-0.677)	0.337 (+/-0.067)	0.082 (+/-0.015)

The numbers are mean values of three replicates.

Table 2. Sequence coverage of identified forms of APX1. ID numbers refer to Fig. 5

Spot ID	Trypsin digest (%)	AspN digest (%)	LysC digest (%)	Total (%)
79	38.0		48.8	52.0
92.4				
4	38.0	31.2	34.0	74.0
5	26.4	30.8	20.0	51.2
8	32.0	30.0	46.4	70.0
12	32.0	48.4	48.8	83.2
13	10.0	38.0	20.8	60.8
15	6.0	38.0	nd	38.0
16	32.0	12.4	30.0	29.2
17	÷	48.4	48.8	83.2
25	nd	48.4	39.2	80.0

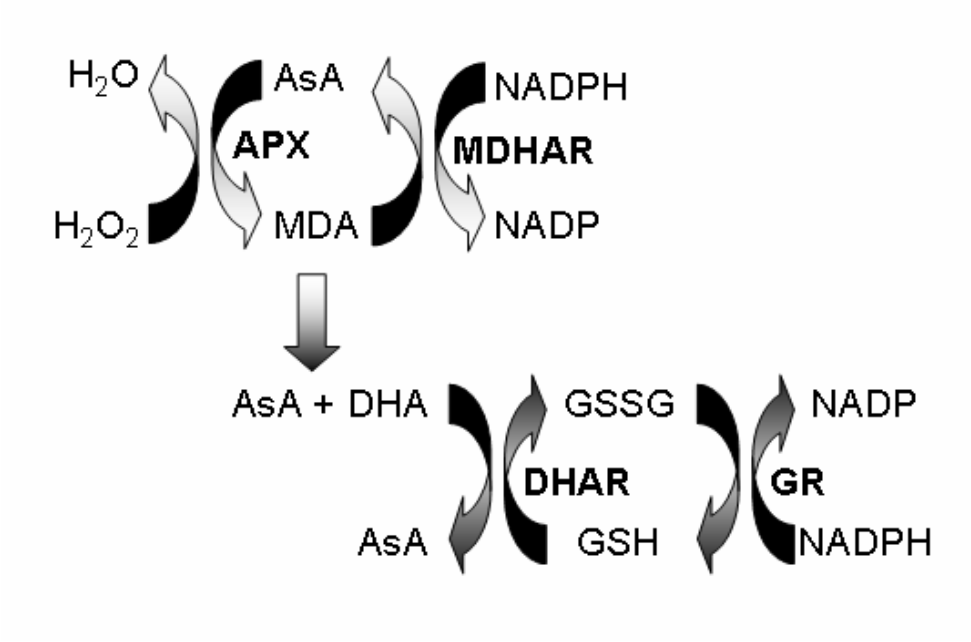

Figure 1: The ascorbate-glutathione cycle.

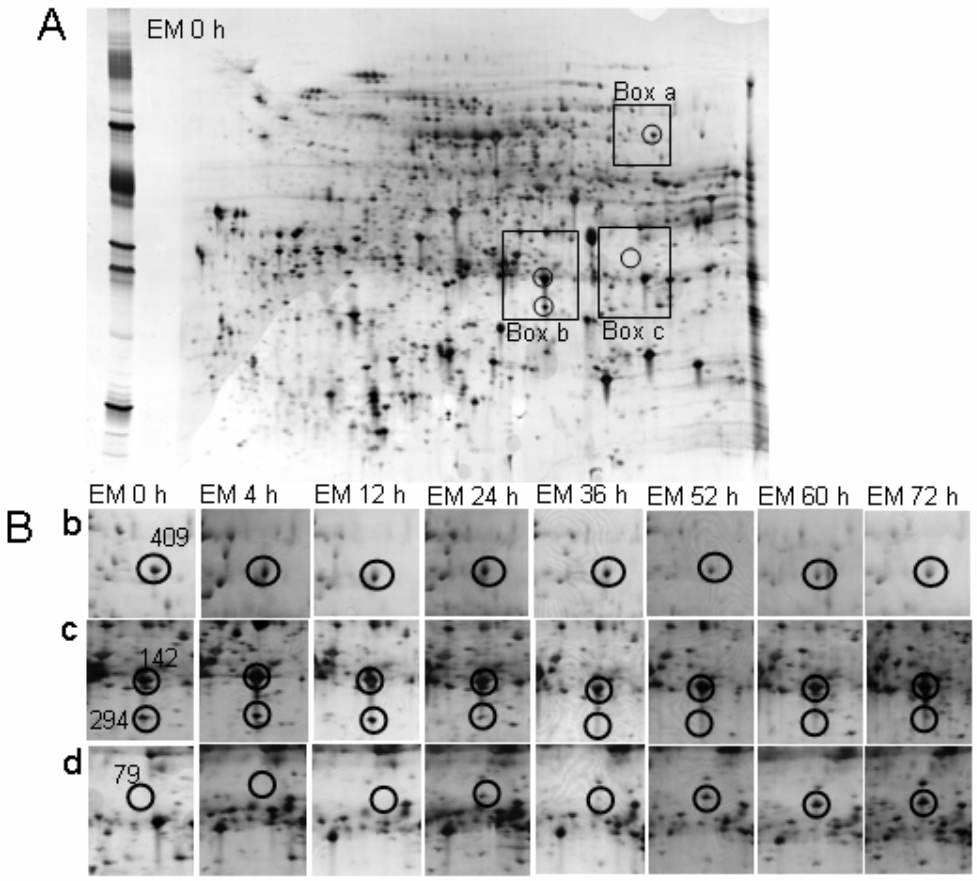

Figure 2: A) 2D gel pattern of soluble non-germinated embryo proteins, pH 4-7. Fifty microgram protein was loaded and silver stained (Bønsager et al. 2007). Boxes 1, 2 and 3 indicate regions where GR (# 409), DHAR (# 142 and 294) and APX (# 79) were identified, respectively. B) The regions are shown in b) box 1, c) box 2, and d) box 3 during 7 time points 0-72 h PI to follow appearance of GR, DHAR and APX.

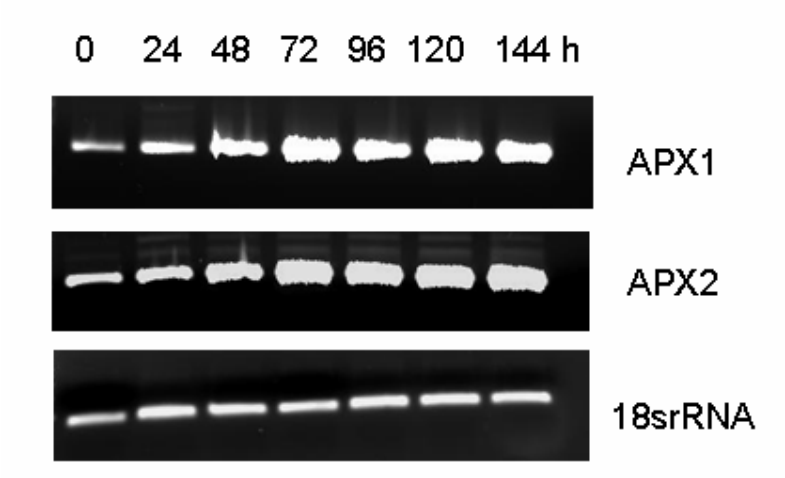

Figure 3: Gene expression analysis of APX isoforms and 18srRNAin embryo during 0-144 h PI. C). One representive gel is shown from two independent replicates.

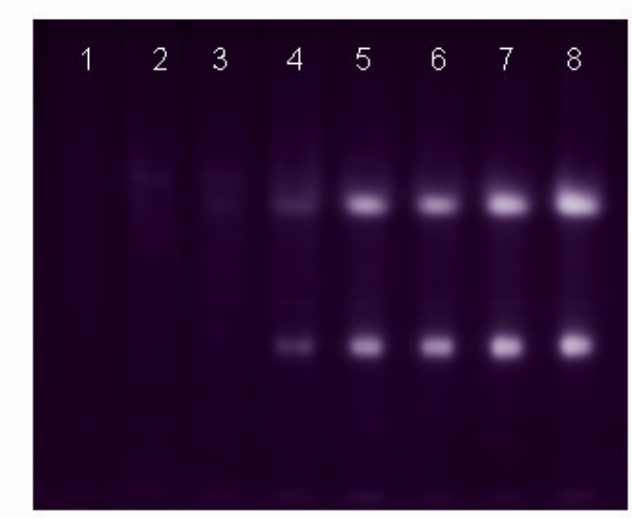

Figure 4: Zymogram of APX activity in embryo extracts 0-72 h PI. Approximately 25 µg protein was applied for each time point. APX activity was detected in a 4-12% Tris-glycine gel at pH 9.0 (see Materials and Methods).

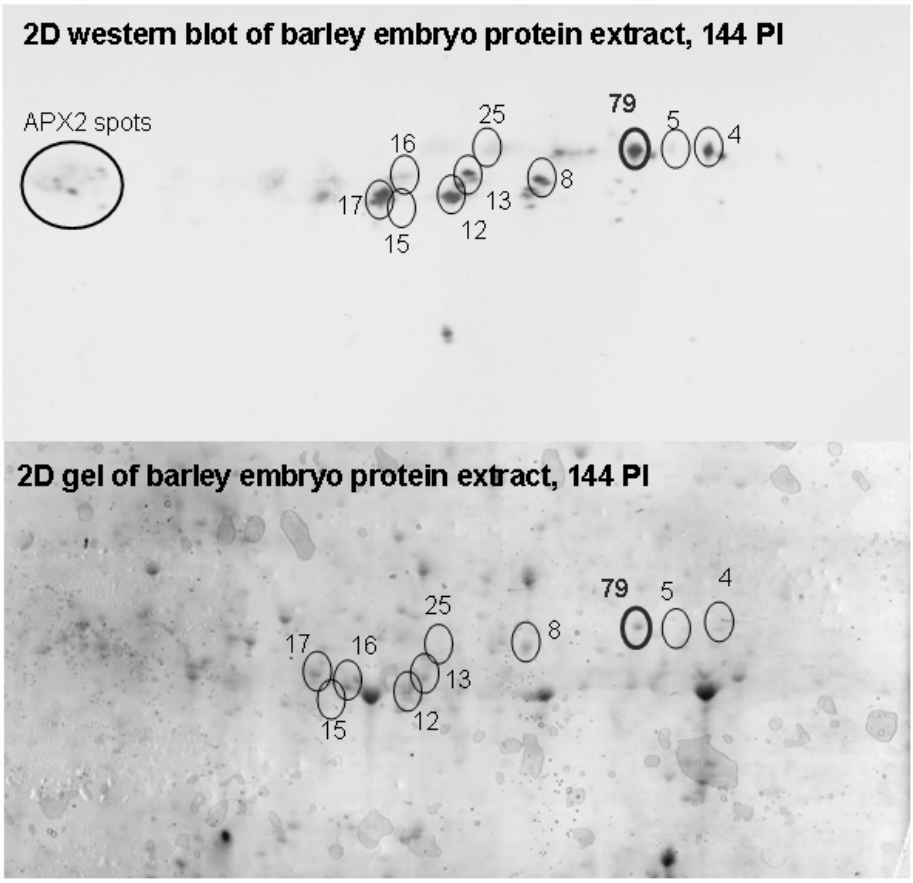

Figure 5: Identification of APX forms from A) 2D western blot and B) cCBB stained 2D gel of barley embryo extract. APX1 was identified in all encircled spot. The big circle indicates the region where APX2 was identified.